TABLE OF CONTENTS

NASA Contractor Report 2909

Dynamic Response of Some Tentative Compliant Wall Structures to Convected Turbulence Fields

H. H. Nijim and Y. K. Lin

CONTRACT NSG-1233
NOVEMBER 1977

NASA

NASA Contractor Report 2909

Dynamic Response of Some Tentative Compliant Wall Structures to Convected Turbulence Fields

H. H. Nijim and Y. K. Lin
University of Illinois at Urbana-Champaign
Urbana, Illinois

Prepared for
Langley Research Center
under Contract NSG-1233

National Aeronautics
and Space Administration

Scientific and Technical
Information Office

1977

BLANK PAGE

FOREWARD

The report is based essentially on a Ph.D thesis prepared by H. H. Nijim under the supervision of Y. K. Lin. The research grant is administered by the Fluid Mechanics Branch, High Speed Aerodynamics Division, NASA at Langley Research Center.

BLANK PAGE

INTRODUCTION

Boundary layer skin-friction drag on an aircraft accounts for approximately 40% of the total vehicle drag. Therefore, any substantial reduction in skin-friction drag would lead to great saving in fuel. Skin-friction drag is induced at both laminar and turbulent conditions. Laminar flow (low skin-friction) is limited to surfaces near the leading edge, while turbulent flow (high skin-friction) is dominant on the rest of the vehicle. Thus, any effective reduction in skin-friction drag should come from that part due to turbulent flow, and it has been suggested that this may be accomplished by use of compliant surfaces.

Skin-friction drag reduction using compliant surface is a unique concept. Its main advantage is simplicity; no slots, ducts, or internal equipment of any nature are used. It requires only a surface with certain characteristics which would interact favorably with the flow. Kramer [1] is credited with the original idea of drag reduction by using compliant surfaces, based on his observations of dolphins swimming in water.

Numerous experimental and theoretical studies have been undertaken to explain the phenomenon of drag reduction by compliant surfaces. A list of references and discussion of such results are given by Ash, et al. [2,3,4]. So far, there is no theory which can explain satisfactorily such a phenomenon. However, some mechanisms have been postulated as possible explanations. One postulate states that the motion of the compliant surface delays the transition from laminar to turbulent boundary layer. Another assumes that the motion of the compliant surface alters the structure of the fully turbulent layer. The latter postulate appears to be more likely. Accordingly, Ash, et al. [3] have proposed two models for the alteration

SUMMARY

Some tentative compliant wall structures designed for possible skin friction drag reduction are investigated. Among the structural models considered is a ribbed membrane backed by polyurethane or PVS plastisol. This model is simplified as a beam placed on a viscoelastic foundation as well as on a set of evenly spaced supports. The total length of the beam may be either finite or infinite, and the supports may be either rigid or elastic. Another structural model considered is a membrane mounted over a series of pre-tensioned wires, also evenly spaced, and the entire membrane is backed by an air cavity. All these structural models belong to the general class of periodic structures for which a simple mathematical analysis is possible. The forcing pressure field is idealized as a frozen random pattern convected downstream at a characteristic velocity. The results are given in terms of the frequency response functions of the system, the spectral density of the structural motion, and the spectral density of the boundary-layer pressure including the effect of structural motion. These results are used in a parametric study of structural configurations capable of generating favorable wave lengths, wave amplitudes and wave speeds in the structural motion for potential drag reduction.

of the structure of the boundary layer. In the first model, the change of boundary-layer structure is attributed to the direct coupling interaction at the fluid-wall interface, and in the second model it is assumed that the surface radiates acoustical disturbances which alter the distribution of turbulent energy from the large-scale eddies to the smaller ones.

In both models proposed in [3], desirable interactions of the surface with a turbulence field can be induced in one of three possible ways; using an active wall, a passive resonant wall, or a flow-triggered wall.

The first type is one that is mechanically or electrically driven at prescribed frequency, amplitude, wave speed and shape. The objective is to obtain a forced narrow-band surface motion at a predetermined frequency and amplitude.

The second type, a passive resonant compliant wall, has been the most commonly-used experimental configuration in the past. In this case, the compliant wall is excited by the pressure field to establish a resonant mode. A favorable interaction would occur if this resonant mode would vibrate in a frequency that falls within the energy-containing spectral range of the turbulence.

The flow-triggered wall (or in the true sence of the word, an ideal compliant wall) is one that responds to all the turbulence "bursts", not only to a few "bursts" as in the other two types. Although this kind of a compliant surface may be the most effective in drag reduction, it is extremely difficult or even impossible to design such an ideal surface.

Several possible structural configurations have been suggested for passive compliant surfaces: membrane surfaces, rigidly backed slabs, laminated structures, and periodic structures (structures which are composed of identical units repeated at equal distances). Of all these

configurations, periodic structures have received the least attention. In this investigation, therefore, the design of periodic structures as tentative compliant surfaces will be emphasized. In particular, two models of periodic structures will be investigated: a ribbed membrane backed by a soft material such as polyurethane or PVS plastisol, and a membrane backed by an air cavity. In the first model, the structure is assumed to be resting on a viscoelastic foundation which would approximate the behavior of polyurethane or PVS plastisol mentioned above. Also, in this analysis, the ribbed two-dimensional membrane is replaced by a one-dimensional periodic beam on equi-spaced supports. The supports, which are simplified versions of ribs, provide rotational and transversal elastic restraints to the beam.

In the second model, a number of circular solid wires are attached (glued) to a two-dimensional membrane. In the analysis, the wires are treated as pre-tensioned strings.

In either model the structure can be of finite or infinite length. For the first model, both cases will be considered while only an infinitely long structure will be considered for the second one.

In order to achieve drag reduction, the proposed design should possess certain dynamic characteristics which will interact favorably with the flow. In other words, the motion of the compliant surface when excited by a turbulence field should have the wave shape, propagation speed, wave length, and amplitude which would make such interaction possible. In the absence of a theory which can predict such characteristics, wind tunnel measurements have been the only available source of information. Historically, experimental investigations have been carried out at low subsonic speeds. This is probably because of the fact that it

is easier to control the experiment at such speeds. Accordingly, Ash, et al. [3,4] have done some experimental investigations at a speed range of 50-150 ft/sec to verify some of the previous experiments on one hand, and to try to establish a compliant drag reduction theory on the other hand. Based on their wind tunnel measurements, they have suggested that the desired motion of a possibly-successful compliant surface should have the following characteristics. (Private communication from R. L. Ash)

(1) the maximum amplitude of the vibration should be (1-3) x 10^{-3} inches

(2) the resonant frequency should not exceed 1500 Hz

(3) the wave length of the surface motion should not exceed .1 inches.

In this analysis, the above characteristics will act as criteria for the design of a tentative compliant surface. However, one should keep in mind that the actual goal of compliant drag reduction is to reduce drag not only at such low speeds, but most importantly at high subsonic and supersonic speeds which represent a range within which most vehicles fly.

The response of finite beams to a convected pressure field has been analyzed in the past by calculating the principle modes of the system, and by studying the forced motion in each significant mode [5-8]. Alternatively, transfer matrix techniques have been developed by Lin, et al. [9-12] to calculate the response directly without determination of normal modes. In the case of periodic structures, accurate computation of normal modes is extremely difficult. Mead and associates [13-17] have used another approach, namely the wave propagation approach which is originally due to Brillouin [18]. This approach works well and with

great simplicity for periodic structures of infinite length. It can also be applied to finite periodic structures but the procedure becomes more involved.

In this investigation, the wave propagation approach also will be used to obtain a closed-form solution for the structural response. However, the analysis differs from that of Mead in two respects: first, it takes into consideration the effect of the foundation (or the air gap) on the structural response, and secondly it incorporates the effect of the interaction between the fluid and the motion of the structure. Finally, the result of a parametric study aiming at an optimal design which has the desired surface motion will be presented.

I. THE EXCITING PRESSURE FIELD

The structure is assumed to be excited by a turbulent pressure field stemming from a fully turbulent boundary layer. The pressure field is random in nature and can be described only by statistical quantities. From the standpoint of the structural response, the simplest mathematical model for such a field is one that is statistically homogeneous in space and convected in a given direction as a frozen pattern. The frozen pattern assumption is known as Taylor's hypothesis. Since experimental measurements of the cross-correlation or cross-spectrum of a boundary layer turbulence generally show some degree of decay in addition to convection, Lin and Maekawa [19] recently have proposed a superposition scheme where a decaying turbulence can be constructed from infinitely many frozen-pattern components. Although the new model might represent a real turbulence more accurately, Taylor's hypothesis will be used in this investigation for computational savings.

Therefore, the turbulent pressure field will be treated as a random function of $x - U_c t$ and y where U_c is the convection speed, t is time, and the flow is assumed to be convected in the positive x-direction. Under this assumption, the pressure over a panel of width b can be expressed as a Fourier-Stieljes integral

$$P(x - U_c t, y) = \int_{-\infty}^{\infty} e^{i(\omega t - kx)} \, dF(k,y) \qquad (1.1)$$

where

ω = frequency in radians per second

k = wave number, $\left(k = \frac{\omega}{U_c}\right)$.

It can be shown that since P is statistically homogeneous

$$E\{dF(k_1,y_1)\ dF^*(k_2,y_2)\} = \bar{S}_p(k_1,\eta)\ \delta(k_1 - k_2)\ dk_1 dk_2$$

where $\eta = y_1 - y_2$, $E\{\cdot\}$ represents the ensemble average, an asterisk denotes the complex conjugate and $\bar{S}_p(k,\eta)$ is the wave-number cross-spectrum referred to a coordinate frame moving with velocity U_c. To simplify further our analysis, we assume that $\bar{S}_p$ can be expressed in a separable form as

$$\bar{S}_p(k_1,\eta) = \bar{S}_p(k_1)\ g(\eta)$$

where $g(\eta)$ is the cross-correlation of turbulence in the y-direction. In some cases the functional form of g can be determined analytically. For instance, in the case of homogeneous and isotropic turbulence, $g(\eta)$ is given by Lin [20]

$$g(\eta) = k_1^2 \left[\frac{\eta^2}{a^2} K_2\left(\frac{a\eta}{L}\right)\right] + \frac{1}{a^2}\left[3K_1\left(\frac{a\eta}{L}\right) - \frac{a\eta}{L} K_2\left(\frac{a\eta}{L}\right)\right]$$

where L is the scale of turbulence, $a = [1 + (Lk_1)^2]^{\frac{1}{4}}$, and $K_m(\cdot)$ is the Bessel function of the second kind (Although the above expression for $g(\eta)$ is derived for the cross-spectrum of turbulence velocity, it is reasonable to use the same form for the pressure using a different value for L). However, based on experimental data for homogeneous boundary layer turbulence, Mastrello [21] expresses $g(\eta)$ as

$$g(\eta) = e^{-|\eta|/\beta} \qquad (1.2)$$

where β is a characteristic length proportional to the boundary layer thickens δ. In what follows we will use Mastrello's expression, Eq. (1.2). Expanding Eq. (1.2) in a Fourier series,

$$g(\eta) = \sum_{n=-\infty}^{\infty} e^{in\pi\eta/b} f_n \tag{1.3}$$

The Fourier coefficients f_n's are computed from

$$f_n = \frac{1}{2b} \int_{-b}^{b} e^{-|\eta|/\beta} \; e^{-in\pi y/b} \, d\eta$$

$$= \frac{1}{b} \int_{0}^{b} e^{-\eta/\beta} \cos\left(\frac{n\pi}{b}\eta\right) d\eta$$

$$= \frac{1}{b} \frac{(1/\beta)}{(1/\beta)^2 + (\frac{n\pi}{b})^2} \{1 - (-1)^n e^{-b/\beta}\} \tag{1.4}$$

Now, the separability assumption of $\overline{S}_p$ is equivalent to replacing Eq. (1.1) by

$$P(x - U_c t, y) = G(y) \int_{-\infty}^{\infty} e^{i(\omega t - kx)} \, dF(k) \tag{1.5}$$

with

$$E\{G(y_1) \, G^*(y_2)\} = g(\eta)$$

If G(y) is also expressed as a Fourier series

$$G(y) = \sum_{n=-\infty}^{\infty} \tilde{f}_n \, e^{in\pi y/b} \tag{1.6}$$

then by use of the orthogonality of Fourier coefficients we can show that

$$|\tilde{f}_n|^2 = f_n$$

In the case of a one-dimensional structure, the variation of a pressure field in the y-direction becomes immaterial. Therefore, the pressure P may be expressed as

$$P(x - U_c t) = \int_{-\infty}^{\infty} e^{i(\omega t - kx)} \, dF(k) \qquad (1.7)$$

It can be seen from Eq. (1.5) or Eq. (1.7) that if a linear analysis is valid, the solution to the present random vibration problem can be constructed from the solution of a fundamental problem where the excitation is

(a) a unit plane wave, $e^{i(\omega t - kx)}$, for the one-dimensional case,

(b) a y-direction modulated unit plane wave, $e^{i(\omega t - kx)} \, e^{in\pi y/b}$, for the two-dimensional case.

It seems proper to call such a fundamental solution a frequency response function.

In the following sections, we will be mostly concerned with obtaining the frequency response functions for different structural configurations corresponding to a unit excitation of the type either (a) or (b) mentioned above. In each case, the frequency response function can then be used to compute the spectral density of the structural response. The spectral analysis of the radiated pressure induced by the structural motion also will be presented.

II. AN INFINITE BEAM RESTING ON A VISCOELASTIC FOUNDATION

The configuration of such a beam is shown in Fig. 1 (a and b). Fig. 1-a represents the case when the supports are considered to be infinitely rigid in the transverse direction, while Fig. 1-b represents the case when these supports are transversely elastic. As can be seen from Fig. 1, the structure is composed of an infinite number of bays, each of length ℓ. Also, it is to be noted that the representation of the viscoelastic foundation as shown in Fig. 1 is just one of several possible representations [27-30]. The inclusion of the spring k_1 is to accommodate some viscoelastic materials which deform instantaneously under loading. The values of the spring constants k_1, k_2 and the damping coefficient η_v depend on the specific chosen material.

The equation of motion of such a beam at any location not immediately over a support is given by

$$D \frac{\partial^4 W}{\partial x^4} + m_b \ddot{W} + F = P + P_1 \Big|_{z=0} \tag{2.1}$$

where

P = the turbulence pressure field neglecting the effect of the beam motion

P_1 = additional pressure generated by the beam motion

F = foundation reaction

W = transverse displacement of the beam

m_b = mass of the beam per unit length

D = flexural rigidity of the beam.

Since we are interested, at this stage, in obtaining the frequency response function only, a unit excitation $e^{i(\omega t - kx)}$ will be used instead of the

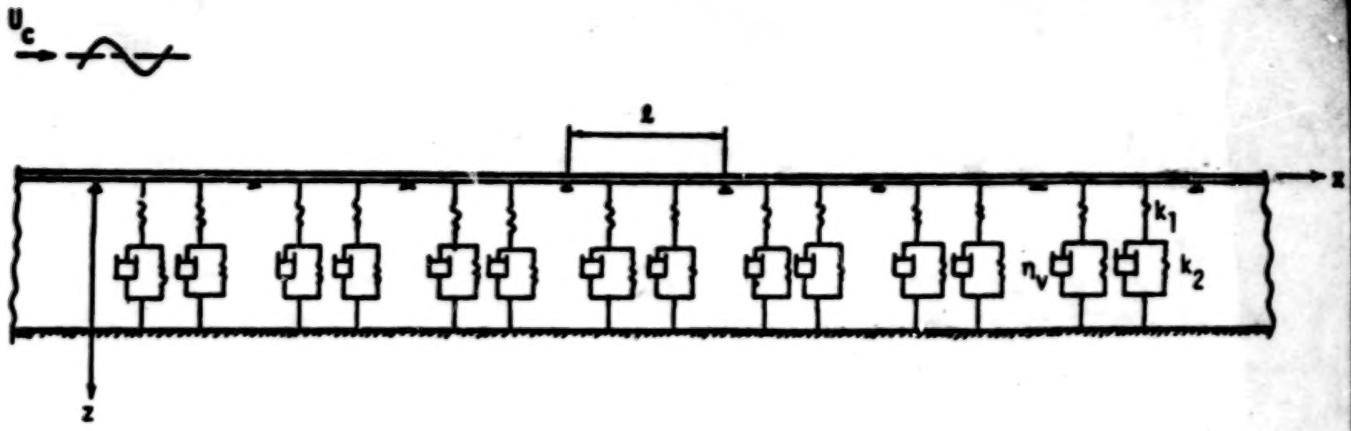

Fig. 1-a Infinite Periodic Beam on a Viscoelastic Foundation (Transversely Rigid Supports)

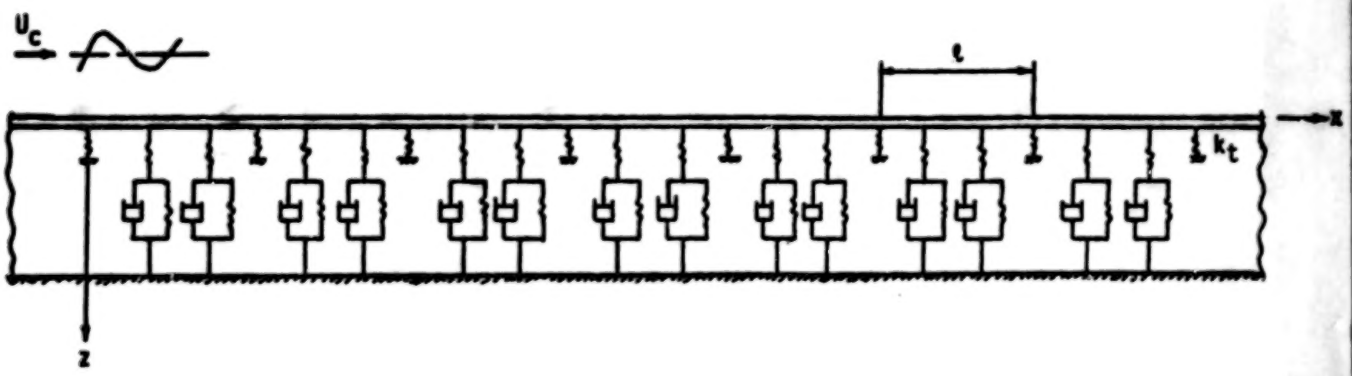

Fig. 1-b Infinite Periodic Beam on a Viscoelastic Foundation (Transversely Elastic Supports)

random pressure P. Also, if the periodic beam considered is actually a strip of periodically supported plate, the more appropriate value for D to be used in the computations would be the bending rigidity of the plate. By the same token, m_b and F would be mass and force per unit area, respectively.

The reaction of the foundation, F, is obtained as follows:

From Fig. 2, one finds that

$$W = W_1 + W_2$$

where

W_1 = relative displacement of point a w.r.t. point b

W_2 = relative displacement of point b w.r.t. point c

(which is the absolute value of the displacement of point b)

$$F = k_1 W_1 \tag{2.2}$$

$$F = k_2 W_2 + \eta_v \dot{W}_2 \tag{2.3}$$

To obtain an expression relating the reaction F and the total deflection W, differentiate both sides of Eq. (2.2)

$$\dot{F} = k_1 \dot{W} \ , \tag{2.4}$$

multiply Eq. (2.2) by k_2, Eq. (2.4) by η_v, Eq. (2.3) by k_1 and add,

$$(k_1 + k_2)F + \eta_v \dot{F} = k_1 k_2 (W_1 + W_2) + k_1 \eta_v (\dot{W}_1 + \dot{W}_2)$$

or $$(k_1 + k_2)F + \eta_v \dot{F} = k_1 k_2 W + k_1 \eta_v \dot{W} \tag{2.5}$$

Eq. (2.5) can be written in a more suitable form (for future discussions concerning the effect of the spring k_2) by dividing both sides by k_2

$$(1 + \frac{k_1}{k_2})F + \frac{\eta_v}{k_2} \dot{F} = k_1 W + \frac{k_1 \eta_v}{k_2} \dot{W} \tag{2.6}$$

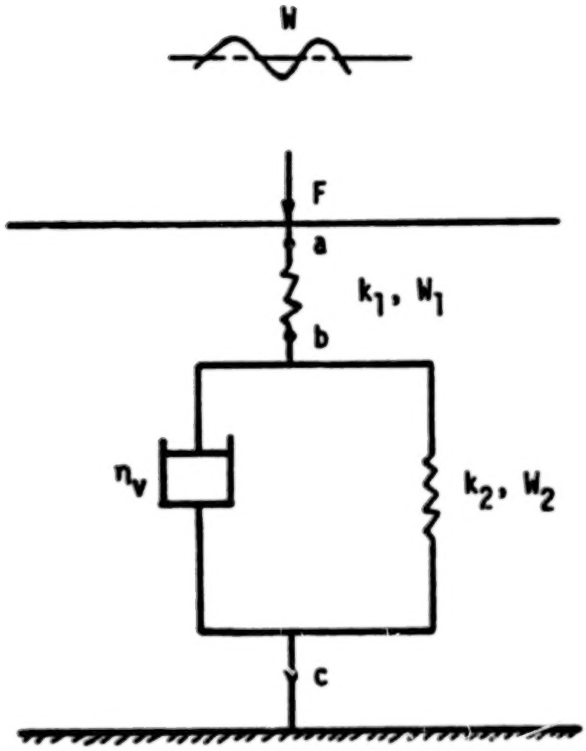

Fig. 2 Viscoelastic Foundation

Combining Eqs. (2.1) and (2.6), one obtains

$$\left\{ \left(1 + \frac{k_1}{k_2}\right) + \frac{\eta_v}{k_2} \frac{\partial}{\partial t} \right\} \left(D \frac{\partial^4 W}{\partial x^4} + m_b \ddot{W}\right) + k_1 W + \frac{k_1}{k_2} \eta_v \dot{W}$$

$$= \left\{ \left(1 + \frac{k_1}{k_2}\right) + \frac{\eta_v}{k_2} \frac{\partial}{\partial t} \right\} \left(P + P_1 \Big|_{z=0}\right) \tag{2.7}$$

For an infinitely long periodic beam, the wave propagation approach due to Brillouin and Mead can be applied most conveniently. Rewriting the exciting unit plane wave in the form,

$$e^{i(\omega t - kx)} = e^{i(\omega t - \mu_0 \cdot x/\ell)} \tag{2.8}$$

where $\mu_0 = k\ell$ is seen to be the phase difference of the exciting wave at two points separated by a distance ℓ along the beam. However, the structural response is not restricted to this phase difference although it must be spatially periodic with period ℓ. This periodicity condition is satisfied by expressing the structural response as follows:

$$W(x,t) = \sum_{n=-\infty}^{\infty} A_n \, e^{i(\omega t - \mu_n x/\ell)} \tag{2.9}$$

with $\mu_n = \mu_0 + 2n\pi$. This series must be made to satisfy the B.C.'s at the supports. Also, it is to be observed that corresponding to different μ_n, different wave components travel along the beam at difference speeds; namely

$$C_n = \frac{\omega \ell}{\mu_n} = \frac{\omega \ell}{\mu_0 + 2n\pi} \tag{2.10}$$

Each wave component can travel in either the positive or negative direction depending on the sign of μ_n. For small values of $|\mu_n|$, the absolute value

of C_n can be very large. The physical implication is that a subsonically convected excitation can generate supersonic waves in the structure. On the other hand, subsonic waves also can be generated by supersonically convected excitations since C_n become smaller for large values of n.

Another interesting relationship involves the wave lengths of the response components. If the usual definition of wave length is modified so that a negative-going wave has a negative wave length, then the wave length, λ_n, is related to C_n by

$$\lambda_n / C_n = \text{constant}$$

Thus, slower traveling waves have shorter wave lengths.

Now, to solve Eq. (2.7) for the displacement W, the reactive pressure P_1 has to be expressed in terms of W. The pressure P_1 which is induced by the structural motion on the upper side of the beam is governed by the convected wave equation

$$\left(\frac{\partial}{\partial t} + V \frac{\partial}{\partial x}\right)^2 P_1 = a_1^2 \nabla^2 P_1 \qquad (2.11)$$

where V = the flow velocity

a_1 = the speed of sound

∇^2 = Laplace operator

This induced pressure is subjected to the boundary condition

$$\rho_1 \left(\frac{\partial}{\partial t} + V \frac{\partial}{\partial x}\right)^2 W = - \left.\frac{\partial P_1}{\partial z}\right|_{z=0} \qquad (2.12)$$

and the radiation condition that it propagates in the domain $z < 0$.
The solution to Eq. (2.11), taking into account the above conditions, is given by Morse and Ingard [22]:

$$P_1\Big|_{z=0} = \sum_{n=-\infty}^{\infty} \frac{i\omega\rho_1 a_1 (C_n - V)^2}{C_n \sqrt{(C_n - V)^2 - a_1^2}} W_n \qquad (2.13)$$

where ρ_1 = fluid density surrounding the beam (air)

C_n = the propagation speed of the nth wave component of the response

W_n = nth component of the displacement

$= A_n e^{i(\omega t - \mu_n x/\ell)}$

Some general comments about the expression for P_1 as given in Eq. (2.13) are in order:

(i) When $C_n = V$, the contribution of such wave component to P_1 is zero.

(ii) When $|C_n - V| = a_1$, $P_1 \to \infty$ (shock wave effect)

(iii) The nth component of P_1 will give a damping effect whenever $|C_n - V| > a_1$. This would occur:

(a) If ω is very high which makes C_n very large (especially when C_n is negative)

(b) When $V > a_1$ and C_n is negative (or C_n is positive but $|C_n - V|$ is still greater than a_1)

(iv) The nth component of P_1 will act as an added mass if the quantity under the square root sign in Eq. (2.13) is negative; i.e., $|C_n - V| < a_1$

(v) When $V < a_1$ and ω is small ($C_n \simeq \frac{\omega\ell}{2\pi n}$), the nth component of P_1 will be approximately proportional to V^2.

Determination of the Coefficients A_n's:

Substituting Eq. (2.9) into Eq. (2.7), one obtains

$$D \frac{\partial^4 W}{\partial x^4} + C_e W = P + P_1\Big|_{z=0} \qquad (2.14)$$

where

$$C_e = \frac{-\omega^2 m_b \left(1 + \frac{k_1}{k_2} + i\omega\eta_v/k_2\right) + k_1 + i\omega k_1\eta_v/k_2}{1 + \frac{k_1}{k_2} + i\omega\eta_v/k_2} \tag{2.15}$$

$$W = \sum_{n=-\infty}^{\infty} W_n$$

Up to this point, nothing has been said about the boundary conditions at the supports. In the following sections, two cases will be considered:

A. The supports are assumed to be infinitely rigid in the transverse direction.

B. The supports are assumed to have some elasticity in that direction.

A. Transversely Rigid Supports

If the supports of a periodic beam are rigid, the displacements at these supports are zero. Hence, at the support x = 0,

$$W(0) = \sum_{n=-\infty}^{\infty} A_n = 0 \tag{2.16}$$

or

$$A_0 = - \sum_{\substack{n=-\infty \\ n\neq 0}}^{\infty} A_n \tag{2.17}$$

Thus, the displacement, W, and the pressure, P_1, can be expressed as (the common factor $e^{i\omega t}$ will be dropped from now on for convenience)

$$W = \sum_{\substack{n=-\infty \\ n\neq 0}}^{\infty} A_n (e^{-i\mu_n x/\ell} - e^{-i\mu_0 x/\ell}) \tag{2.18}$$

$$P_1 = \sum_{\substack{n=-\infty \\ n\neq 0}}^{\infty} i\omega\rho_1 a_1 \left(\frac{e^{-i\mu_n x/\ell}}{\overline{G}_n} - \frac{e^{-i\mu_0 x/\ell}}{\overline{G}_0}\right) A_n \tag{2.19}$$

where

$$\overline{G}_n = C_n\{(C_n - V)^2 - a_1^2\}^{\frac{1}{2}} / (C_n - V)^2 \qquad (2.20)$$

The coefficients A_n,s may be obtained by using the virtual work principle (i.e., when all the forces on and in the beam are in equilibrium, they should do no virtual work through any virtual displacement). Specifically, we assume a virtual displacement

$$\delta_m = \delta A_m \, (e^{-i\mu_m x/\ell} - e^{-i\mu_0 x/\ell}) \, . \qquad (2.21)$$

As usual in complex algebra, the conjugate of the virtual displacement, namely

$$\delta_m^* = \delta A_m \, (e^{i\mu_m x/\ell} - e^{i\mu_0 x/\ell}) \qquad (2.22)$$

is used in calculating the virtual work. Due to the spatial periodicity of the forcing function, the structural response and the virtual displacement, the result of an integration over an entire structure composed of B periodic elements is equal to B times that of integrating over one element. Since the total virtual work done is zero, the virtual work done within each periodic element is also zero and it is sufficient to apply the virtual work principle to just one periodic unit.

Now, the contribution of the 1st term in Eq. (2.14) to the virtual work is

$$\delta\overline{W}_{(1)} = \int_0^{\ell} \sum_{n=-\infty}^{\infty} A_n \, D\{(\tfrac{\mu_n}{\ell})^4 \, e^{-i\mu_n x/\ell} - (\tfrac{\mu_0}{\ell})^4 \, e^{-i\mu_0 x/\ell}\}$$

$$\delta A_m \, \{e^{i\mu_m x/\ell} - e^{i\mu_0 x/\ell}\} \, dx$$

$$= D\,[(\mu_n/\ell)^4 \, A_m + (\mu_0/\ell)^4 \sum_{\substack{n=-\infty \\ n\neq 0}}^{\infty} A_n] \cdot \ell \cdot \delta A_m \qquad (2.23)$$

Note that in obtaining Eq. (2.23), the following relationships have been used:

$$(1)\quad \int_0^{\ell} e^{-i\mu_m x/\ell} \cdot e^{i\mu_n x/\ell}\, dx = \begin{cases} 0 \ ; \ m \neq n \\ \ell \ ; \ m = n \end{cases} \tag{2.24}$$

$$(2)\quad \int_0^{\ell} e^{-i\mu_m x/\ell} \quad e^{i\mu_0 x/\ell}\, dx = \begin{cases} 0 \ ; \ m \neq 0 \\ \ell \ ; \ m = 0 \end{cases} \tag{2.25}$$

Similarly, for the other terms in Eq. (2.14)

$$\delta\bar{W}_{(2)} = C_e \int_0^{\ell} \sum_{n=-\infty}^{\infty} A_n (e^{-i\mu_n x/\ell} - e^{-i\mu_0 x/\ell}) \cdot \delta A_m \cdot (e^{i\mu_m x/\ell} - e^{i\mu_0 x/\ell})\, dx$$

$$= C_e \left\{ A_m + \sum_{\substack{n=-\infty \\ n\neq 0}}^{\infty} A_n \right\} \cdot \delta A_m \cdot \ell \tag{2.26}$$

$$\delta\bar{W}_p = -\int_0^{\ell} e^{-i\mu_0 x/\ell} (e^{i\mu_m x/\ell} - e^{i\mu_0 x/\ell})\, dx$$

$$= \begin{cases} 0 & ; \ m = 0 \\ \ell \cdot \delta A_m & ; \ m \neq 0 \end{cases} \tag{2.27}$$

$$\delta\bar{W}_{p_1} = -\int_0^{\ell} i\omega\rho_1 a_1 \sum_{n=-\infty}^{\infty} A_n \left\{ \frac{e^{-i\mu_n x/\ell}}{\bar{G}_n} - \frac{e^{-i\mu_0 x/\ell}}{\bar{G}_0} \right\} \delta A_m (e^{i\mu_m x/\ell} - e^{i\mu_0 x/\ell})\, dx$$

$$= -\left\{ \frac{i\omega\rho_1 a_1}{\bar{G}_m} A_m + \frac{i\omega\rho_1 a_1}{\bar{G}_0} \sum_{\substack{n=-\infty \\ n\neq 0}}^{\infty} A_n \right\} \delta A_m \cdot \ell \tag{2.28}$$

The virtual work done by the rotational spring, k_r, at the support $x = 0$ is

$$\delta\bar{W}_r = k_r\theta_r(0)(\delta A_m)'(0) = k_r W'(0)(\delta A_m)'(0)$$

where the prime, ', denotes differentiation w.r.t.x.

$$\delta\bar{W}_r = k_r \sum_{\substack{n=-\infty \\ n\neq 0}}^{\infty} i\, A_n \left\{-(\mu_n/\ell) + \frac{\mu_0}{\ell}\right\} \cdot i \cdot \delta A_m \cdot \left\{(\mu_m/\ell) - \frac{\mu_0}{\ell}\right\}$$

$$= k_r \sum_{\substack{n=-\infty \\ n\neq 0}}^{\infty} A_n \cdot \frac{2n\pi}{\ell} \cdot \frac{2m\pi}{\ell} \cdot \delta A_m \qquad (2.29)$$

The total virtual work, $\delta\bar{W}$, is

$$\delta\bar{W} = \delta\bar{W}_{(1)} + \delta\bar{W}_{(2)} + \delta\bar{W}_p + \delta\bar{W}_{p_1} + \delta\bar{W}_r = 0 \qquad (2.30)$$

Using Eq. (2.23) and Eqs. (2.26)-(2.30), we obtain a set of simultaneous linear equations for the coefficients A_n's as follows:

$$A_m\left(\mu_m^4 + C_e\frac{\ell^4}{D} - \frac{i\omega\rho_1 a_1}{\bar{G}_m}\frac{\ell^4}{D}\right) + \sum_{\substack{n=-\infty \\ n\neq 0}}^{\infty} A_n\left(\mu_0^4 + C_e\frac{\ell^4}{D} - \frac{i\omega\rho_1 a_1}{\bar{G}_0}\frac{\ell^4}{D}\right)$$

$$+ \sum_{\substack{n=-\infty \\ n\neq 0}}^{\infty} k_r\frac{\ell^3}{D}\cdot\frac{2n\pi}{\ell}\cdot\frac{2m\pi}{\ell}A_n = -\frac{\ell^4}{D} \qquad (2.31)$$

The structural damping of the beam and the supports can be accounted for by use of complex D and k_r

$$D = D'(1 + i\eta_b)$$

$$k_r = k_r'(1 + i\eta_r)$$

where η_b and η_r are the loss factors for the beam and the support materials respectively. Also, introducing the nondimensional quantities

$$\left.\begin{aligned} \Omega^2 &= m_b\omega^2 \frac{\ell^4}{D'} \\ \bar{\rho}_1 &= \rho_1 \omega a_1 \frac{\ell^4}{D'} \\ \gamma &= k_r' \ell/D' \\ \alpha &= k_1 \ell^4/D' \\ \beta &= k_2 \ell^4/D' \\ \bar{\eta} &= \omega\eta_v \ell^4/D' \\ \psi &= \omega\eta_v/k_2 \end{aligned}\right\} \qquad (2.32)$$

Eq. (2.31) can be simplified as

$$A_m \phi(m) + \phi(0) \sum_{\substack{n=-\infty \\ n\neq 0}}^{\infty} A_n + \sum_{\substack{n=-\infty \\ n\neq 0}}^{\infty} A_n \xi(n, m) = S \qquad (2.33)$$

where

$$\phi(m) = \mu_m^4 + \frac{-\Omega^2(1 + \frac{k_1}{k_2} + i\psi) + \alpha + i\bar{\eta}\frac{k_1}{k_2}}{(1 + \frac{k_1}{k_2} + i\psi)(1 + i\eta_b)} - \frac{\bar{\rho}_1}{\bar{G}_m(1 + i\eta_b)} \qquad (2.34)$$

$$\xi(n,m) = \gamma \cdot \frac{1 + i\eta_r}{1 + i\eta_b} \cdot (2n\pi) \cdot (2m\pi) \qquad (2.35)$$

$$S = -\frac{\ell^4/D'}{1 + i\eta_b} \qquad (2.36)$$

In practical applications the number of terms in each infinite sum in (2.33)

must be truncated. The truncated version of (2.33) may be written in a matrix form as

$$G\{A\} = \{S\} \tag{2.37}$$

where

$$g_{\ell j} = \phi(\ell)\delta_{\ell j} + \xi(\ell,j) + \phi(0) \tag{2.38}$$

$$\delta_{\ell j} = \text{Kronecher delta} = \begin{cases} 1 & \ell = j \\ 0 & \ell \neq j \end{cases}$$

$$\ell, j = -N, -(N-1), - - -, -2, -1, 1, 2, - - -, N-1, N$$

The choice of the number of simultaneous equations (=2N) depends on the desired accuracy in computing the values of A_n's.

In the remainder of this section, two special cases will be discussed. In the first case, the supports will be assumed to offer no rotational restraint to the beam, and in the second case the foundation will be assumed purely elastic.

(1) <u>No rotational restraint at the supports (i.e., $k_r = 0$):</u>

In this case Eq. (2.33) becomes

$$A_m \phi(m) + \phi(0) \sum_{\substack{n=-\infty \\ n\neq 0}}^{\infty} A_n = S \tag{2.39}$$

The solution of this equation is much simpler than that of Eq. (2.33) as to be explained below.

From Eq. (2.39), one observes that

$$A_m \phi(m) = \text{constant}$$

or

$$A_1 \phi(1) = A_2 \phi(2) = - - - - - - = A_N \phi(N) \tag{2.40}$$

Hence, combining Eqs. (2.39) and (2.40)

$$A_m \phi(m) = \frac{S}{1 + \phi(0) \sum_{\substack{n=-\infty \\ n\neq 0}}^{\infty} 1/\phi(n)} = \frac{S}{\phi(0) \sum_{n=-\infty}^{\infty} \{1/\phi(n)\}} \qquad (2.41)$$

which readily gives

$$A_m = \frac{S}{\phi(m)\phi(0) \sum_{n=-\infty}^{\infty} 1/\phi(n)} \qquad (2.42)$$

The number of terms required in Eq. (2.42) to obtain an accurate total deflection can be simply determined. First, we establish the dominant term in the series. Referring to this term as A_d, compute the ratio

$$r_n = |A_n/A_d| = \left|\frac{\phi(n_d)}{\phi(n)}\right| \qquad (2.43)$$

Defining the truncation as $-N \leq n \leq N$, a reasonable criterion for choosing N is

$$r_n \ll 1 \qquad \text{for } |n| > N \, .$$

(2) Elastic foundation:

As can be seen from Fig. 2, the foundation can be made elastic by choosing

(a) $k_2 = \infty$

or (b) $\eta_v = 0$

or both.

Case (a)

If $k_2 \to \infty$, then Eq. (2.15) becomes

$$C_e = -\omega^2 m_b + k_1 \qquad (2.44)$$

and Eq. (2.34) reduces to

$$\phi(m) = \mu_m^4 + \frac{-\Omega^2 + \alpha}{1 + i\eta_b} - \frac{i\bar{\rho}_1}{\bar{G}_m(1 + i\eta_b)} \tag{2.45}$$

while $\xi(n,m)$ and S remain unchanged.

Case (b)

When $\eta_v = 0$,

$$C_e = -\omega^2 m_b + \frac{k_1 k_2}{k_1 + k_2} \tag{2.46}$$

and

$$\phi(m) = \mu_m^4 - \frac{\Omega^2}{1 + i\eta_b} + \frac{\alpha\beta}{(\alpha + \beta)} \cdot \frac{1}{1 + i\eta_b} - i\,\frac{\bar{\rho}_1}{\bar{G}_m} \cdot \frac{1}{1 + i\eta_b} \tag{2.47}$$

Again $\xi(n,m)$ and S are unchanged.

Combination of cases (1) and (2) (i.e., no rational restraint at the supports and with an elastic foundation) will, of course, lead to further simplifications. The coefficients A_n's are obtained most simply from Eq. (2.42) with $\phi(m)$ given by either (2.45) or (2.47).

Once the coefficients A_n's are determined, the displacement W and other related quantities can be readily computed. For instance, the first derivative (w.r.t. x), W', is given by

$$W'(x) = \sum_{n=-\infty}^{\infty} A_n \left\{ -(i\,\frac{\mu_n}{\ell})\, e^{-i\mu_n x/\ell} + i\,\frac{\mu_0}{\ell}\, e^{-i\mu_0 x/\ell} \right\} \tag{2.48}$$

and

$$W'(0) = \sum_{n=-\infty}^{\infty} A_n(-i2n\pi/\ell) \tag{2.49}$$

Similarly, the second derivative is given by

$$W''(x) = \sum_{n=-\infty}^{\infty} A_n \left\{ (-i\,\frac{\mu_n}{\ell})^2\, e^{-i\mu_n x/\ell} - (-i\,\frac{\mu_0}{\ell})^2\, e^{i\mu_0 x/\ell} \right\} \tag{2.50}$$

$$W''(0) = \sum_{n=-\infty}^{\infty} A_n \left(-\frac{2n\pi}{\ell}\right)\left(\frac{\mu_0 + \mu_n}{\ell}\right) \tag{2.51}$$

Since we have substituted a unit plane wave for the excitation pressure P, the computed response as given in Eq. (2.18) (with the time variation factor $e^{i\omega t}$ omitted) is actually the frequency response function H(x,k). Therefore, we can write

$$H(x,k) = \sum_{n=-\infty}^{\infty} A_n \left\{ e^{-i\mu_n x/\ell} - e^{-i\mu_0 x/\ell} \right\} \tag{2.52}$$

where the A_n's are obtained by solving the matrix equation (2.37) or directly from Eq. (2.42).

B. Transversely Elastic Supports

Eventually if a periodic structure is used as a compliant surface, the supports are most likely ribs or stringers which have inertia and stiffness. In this section, we will assume that these supports can be replaced by springs characterized by a spring constant k_t in the transverse direction as shown in Fig. 1-b. The inertia of the supports will be neglected. An analysis similar to that of the previous section will apply here. Avoiding repetition of the previous section, the differences may be pointed out:

(1) The displacement at the internal supports are no longer equal to zero and the displacement is given by

$$W(x,t) = \sum_{n=-\infty}^{\infty} A_n \, e^{-i\mu_n x/\ell} \, e^{i\omega t} \tag{2.53}$$

(2) There will be an additional contribution to the virtual work. This comes from the elasticity of the supports. Following the

same procedure as in the previous section, the virtual work done by k_t at x = 0 is

$$\delta\bar{W}_t = k_t\, W(0)\, \delta A_m = \delta P_m \cdot k_t \sum_{n=-\infty}^{\infty} A_n \tag{2.54}$$

Then the relationship governing the coefficients A_n's becomes

$$A_m\, \phi(m) + \Gamma \sum_{n=-\infty}^{\infty} A_n + \gamma\mu_m \sum_{n=-\infty}^{\infty} A_n\mu_n = \begin{cases} -S\ ;\ m = 0 \\ 0\ ;\ m \neq 0 \end{cases} \tag{2.55}$$

where $\Gamma = k_t{}^3/D'$, γ and S are the same as before, and the expression for $\phi(m)$ is given by Eq. (2.34).

The first and second derivatives of the displacement are given by

$$W'(x,t) = \sum_{n=-\infty}^{\infty} A_n(-i\mu_n/\ell)\, e^{-i\mu_n x/\ell}\, e^{i\omega t} \tag{2.56}$$

$$W'(0,t) = \sum_{n=-\infty}^{\infty} A_n(-i\mu_n/\ell)\, e^{i\omega t} \tag{2.57}$$

$$W''(x,t) = \sum_{n=-\infty}^{\infty} A_n(-i\mu_n/\ell)^2\, e^{-i\mu_n x/\ell}\, e^{i\omega t} \tag{2.58}$$

$$W''(0,t) = \sum_{n=-\infty}^{\infty} -(\mu_n/\ell)^2\, A_n\, e^{i\omega t}\ , \tag{2.59}$$

and the frequency response function H(x,k) is given by

$$H(x,k) = \sum_{n=-\infty}^{\infty} A_n\, e^{-i\mu_n x/\ell} \tag{2.60}$$

Equations (2.48)-(2.52) and (2.56)-(2.60) will be used in the following sections.

It is worth noting that analyses of certain special cases discussed in the previous section, including the case of zero rotational constraints at the supports and the case of the elastic foundation, are also applicable here with the obvious modifications which correspond to the change in the B.C.'s at the supports.

III. FINITE PERIODIC BEAM ON A VISCOELASTIC FOUNDATION

The configuration of such a beam is shown in Fig. 3. Fig. 3-a shows a beam with transversely rigid supports, while Fig. 3-b shows the same beam with transversely elastic supports.

The response of a finite periodic beam to a unit excitation, $e^{i(\omega t-kx)}$, can be viewed as consisting of two parts:

(1) The response of an infinitely long periodic beam with the same periodic element. Such a response has already been discussed in the preceding sections.

(2) The response corresponding to the reflections from the end supports of the finite beam.

The waves reflected from the left-hand end support are positive-going waves, while the ones reflected from the right-hand end support are, naturally, negative-going waves. The reflected waves are free waves and can be viewed as the solution of the equation of motion without the excitation wave (i.e., by putting P = 0 in Eq. (2.14)). In other words, the motion is a free vibration of a semi-infinite periodic beam. It is important to note that the total response, which consists of parts (1) and (2) explained above, should satisfy the boundary conditions at the extreme ends of the finite beam.

The equation of motion for free vibration of the beam is given by

$$D \frac{\partial^4 W}{\partial x^4} + C_e W - P_1 \Big|_{z=0} = 0 \qquad (3.1)$$

The reactive pressure P_1 depends on the displacement W. For a semi-infinite periodic beam, there is no known closed-form solution for P_1.

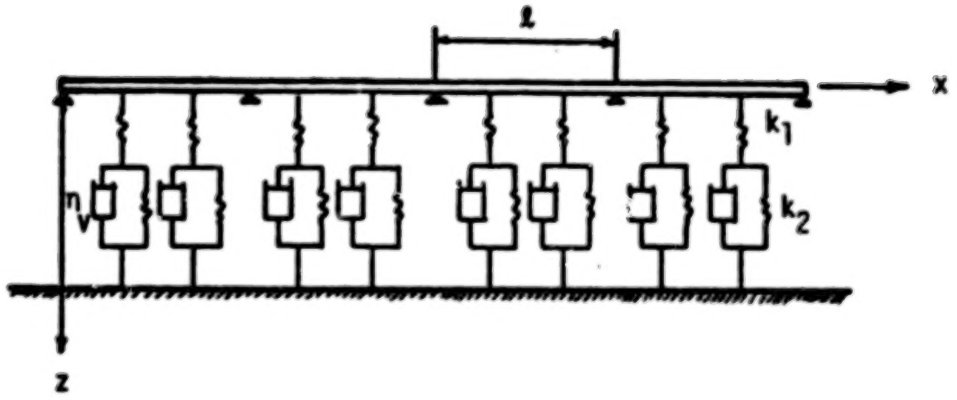

Fig. 3-a Finite Periodic Beam (Transversely Rigid Supports)

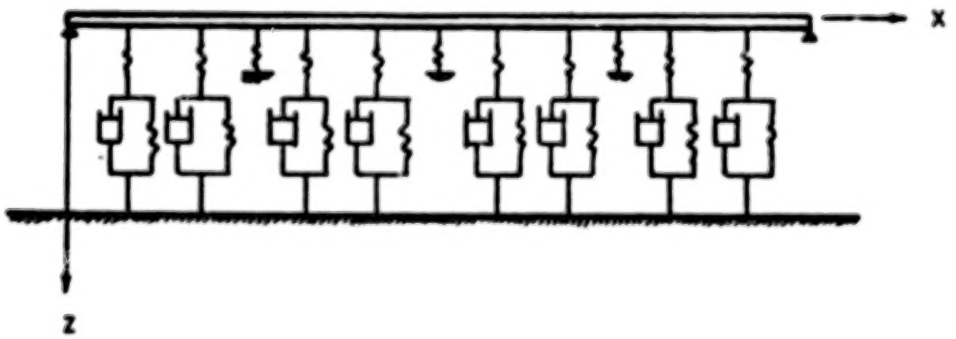

Fig. 3-b Finite Periodic Beam (Transversely Elastic Interior Supports)

Therefore, an iterative procedure will be used. Since the effect of P_1 is expected to be small, we will initially neglect such an effect (i.e., put $P_1\Big|_{z=0} = 0$ in Eq. (3.1)). Next, determine P_1 based on that solution of W, and a new displacement will be computed by solving Eq. (3.1) with previously determined P_1 treated as an external force. This will become clearer as we proceed.

Rewrite Eq. (3.1) (after putting $P_1 = 0$) as

$$\frac{\partial^4 W}{\partial x^4} - \bar{R} W = 0 \tag{3.2}$$

where $\bar{R} = -\frac{C_e}{D}$. The solution of Eq. (3.2) can be written as

$$W(x) = \sum_{n=1}^{4} A_n e^{\lambda_n x} \quad ; \quad 0 \leq x \leq \ell \tag{3.3}$$

in which the λ_n's are the four complex roots of $\bar{R}$ and they are

$$\left.\begin{aligned} \lambda_1 &= |\bar{R}|^{1/4} \; e^{i\frac{\theta}{4}} \\ \lambda_2 &= |\bar{R}|^{1/4} \; e^{i(\frac{\theta}{4} - \frac{\pi}{2})} \\ \lambda_3 &= |\bar{R}|^{1/4} \; e^{i(\frac{\theta}{4} + \frac{\pi}{2})} \\ \lambda_4 &= |\bar{R}|^{1/4} \; e^{i(\frac{\theta}{4} + \pi)} \\ \theta &= \tan^{-1}\left\{\frac{\mathrm{Im}(\bar{R})}{\mathrm{Re}(\bar{R})}\right\} \end{aligned}\right\} \tag{3.4}$$

where Re, Im denote the real and imaginary parts of a complex quantity, resp.

Now, consider a positive-going wave which has a propagation constant μ. The response produced by such a wave in a periodic structure has the essential property of which:

$$\text{vector at station } (r+1) = e^{\mu} \times \text{vector at station } (r) \tag{3.5}$$

where r and (r+1) are two stations on the periodic beam separated by a distance equal to the length of the periodic element, ℓ, as shown in Fig. 4. The components of such a vector can be taken as any four independent linear combinations of the displacement and its first three derivatives w.r.t.x.

The coefficients A_n's of Eq. (3.3) will be determined by using the wave property explained above, and the boundary conditions at the extreme ends of the beam. In what follows, two cases will be examined: transversely rigid supports, and transversely elastic supports.

A. Transversely Rigid Supports

For transversely rigid supports, the displacements at both ends of each periodic element ($x = 0, \ell$) are zero. Therefore, Eq. (3.3) gives

$$\sum_{j=1}^{4} A_j = 0 \tag{3.6}$$

and

$$\sum_{j=1}^{4} A_j e^{\lambda_j \ell} = 0 \tag{3.7}$$

Using the wave property expressed in Eq. (3.5) to relate the slopes at $x = 0$ and $x = \ell$,

$$W'(\ell) = e^{\mu} W'(0) \tag{3.8}$$

Substituting Eq. (3.3) into Eq. (3.8), we obtain

$$\sum_{j=1}^{4} A_j \lambda_j e^{\lambda_j \ell} = e^{\mu} \sum_{j=1}^{4} A_j \lambda_j \tag{3.9}$$

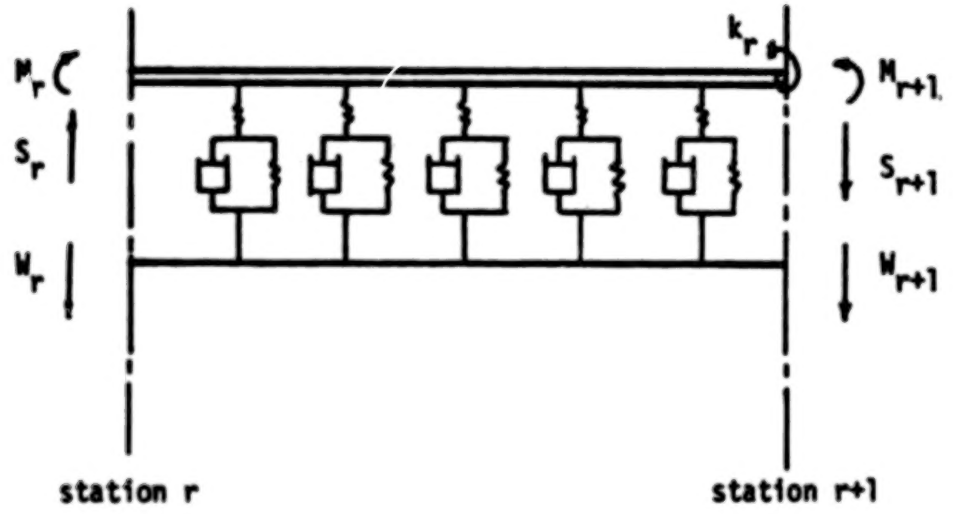

Fig. 4 A Single Periodic Element
(Transversely Rigid Supports)

Furthermore, one can observe (from Fig. 4) that

$$M_{r+1} - k_r W'(\ell) = D W''(\ell) \tag{3.10}$$

Since $M(x) = D W''(x)$, Eq. (3.10) becomes

$$W''(\ell) + \frac{k_r}{D} W'(\ell) = e^{\mu} W''(0)$$

or

$$\sum_{j=1}^{4} A_j \left(\lambda_j^2 + \frac{k_r}{D} \lambda_j\right) e^{\lambda_j \ell} = e^{\mu} \sum_{j=1}^{4} A_j \lambda_j^2 \tag{3.11}$$

Equations (3.6), (3.7), (3.9) and (3.11) form a set of simultaneous equations for the coefficients A_n's. However, these equations are not sufficient to determine the coefficients A_n's because the propagation constant μ is still unknown and the problem will reduce to an eigenvalue problem as to be demonstrated below.

Combining Eqs. (3.6) and (3.7), one obtains

$$A_2 = e_2^{-1} \{-A_3 e_3 - A_4 e_4\} \tag{3.12}$$

where

$$e_j = e^{\lambda_j \ell} - e^{\lambda_1 \ell} \quad ; \quad j = 2,3,4 \tag{3.13}$$

Substituting Eqs. (3.12), (3.13) into Eqs. (3.9) and (3.11) and simplifying,

$$G \{A\} = e^{\mu} Q \{A\} \tag{3.14}$$

where

$$\{A\} = \begin{Bmatrix} A_3 \\ A_4 \end{Bmatrix} \tag{3.15}$$

$$G = \begin{bmatrix} f_3 - f_2 e_2^{-1} e_3 & f_4 - f_2 e_2^{-1} e_4 \\ d_3 - S_1 & d_4 - S_2 \end{bmatrix} \tag{3.16}$$

$$Q = \begin{bmatrix} \xi_3 - \xi_2 e_2^{-1} e_3 & \xi_4 - \xi_2 e_2^{-1} e_4 \\ g_3 - g_2 e_2^{-1} e_4 & g_4 - g_2 e_2^{-1} e_4 \end{bmatrix} . \tag{3.17}$$

$$f_i = \lambda_i e^{\lambda_i \ell} - \lambda_1 e^{\lambda_1 \ell}$$

$$g_i = \lambda_i^2 - \lambda_1^2 \; ; \; \xi_i = \lambda_i - \lambda_1$$

$$d_i = (\lambda_i^2 + \frac{k_r}{D} \lambda_i) e^{\lambda_i \ell} \tag{3.18}$$

$$S_1 = d_1 + (d_2 - d_1) e_2^{-1} e_3$$

$$S_2 = d_1 + (d_2 - d_1) e_2^{-1} e_4 \qquad i = 1,2,3,4$$

Rewriting Eq. (3.14) in a more suitable form as

$$C \{A\} = e^{\mu} \{A\} \tag{3.19}$$

where

$$C = Q^{-1} G \tag{3.20}$$

Equation (3.19) is a standard eigenvalue problem in which e^{μ} is equal to the eigenvalues of the matrix C. These eigenvalues, denoted by Λ_1 and Λ_2, are pairwise reciprocal [15] and they are

$$\Lambda_{1,2} = \frac{1}{2} \left\{ C_{11} + C_{22} \pm \sqrt{(C_{11} - C_{22})^2 + 4 C_{12} C_{21}} \right\} \tag{3.21}$$

where C_{ij} is the (i,j)th element of the matrix C. The propagation constant μ is given by

$$\mu = \pm \log_e \Lambda_1 = \mp \log_e \Lambda_2$$

$$= \mu_R + i\mu_I \tag{3.22}$$

The real part of the propagation constant, μ_R, represents the decay of the amplitude of the propagating wave while μ_I represents its phase shift. We can see from Eq. (3.22) that two waves propagating in opposite directions will be generated in the structure. Also, the eigenvectors corresponding to μ and $-\mu$ can be determined. Of course, only the ratio between the two components A_3 and A_4 of each eigenvector is unique. This ratio can be used in conjunction with Eqs. (3.6) and (3.12) to determine the coefficients A_n's in terms of one of them (say 1, A_2/A_1, A_3/A_1 and A_4/A_1). If we denote

$$A_j/A_1 = \begin{cases} a_j^+ & ; \text{ for +ve going wave} \\ a_j^- & ; \text{ for -ve going wave} \end{cases}, \quad j=1 \div 4 \tag{3.23}$$

then Eq. (3.3) becomes

$$W(x) = \begin{cases} w_+ \sum_{j=1}^{4} a_j^+ e^{\lambda_j x} & ; \text{ +ve going wave} \\ w_- \sum_{j=1}^{4} a_j^- e^{\lambda_j x} & ; \text{ -ve going wave} \end{cases} \tag{3.24}$$

where w_+ and w_- are the amplitudes of the positive and negative going waves, respectively, and will be determined by using the B.C's at the extreme ends of the beam.

Now, to determine the induced pressure P_1, we have to solve Eq. (2.11) subjected to the B.C given by Eq. (2.12) and to the radiation condition that it propagates in the negative-z domain. For a positive going wave with μ as a propagation constant, let us assume that P_1 can be computed sufficiently accurately by the use of the following separable form:

$$P_1 = \sum_{n=-\infty}^{\infty} f_n(z) \; e^{-i(\mu_I + 2n\pi)\, x/\ell} \; e^{i\omega t} \tag{3.25}$$

Substituting Eq. (3.30) into Eq. (2.11) and simplifying, we obtain

$$f_n''(z) + k_n^2 f_n(z) = 0 \tag{3.26}$$

where

$$k_n^2 = [(a_1^2 - v^2)(i\bar{\mu}_n/\ell)^2 + \omega^2 + 2i\omega v(i\bar{\mu}_n/\ell)]/a_1^2 \tag{3.27}$$

and $\bar{\mu}_n = \mu_I + 2n\pi$. The solution to Eq. (3.25) can be written as

$$f_n(z) = B_1(n)\, e^{ik_n z} + B_2(n)\, e^{-ik_n z} \tag{3.28}$$

However, imposition of the radiation condition (i.e., P_1 can propagate in the domain $z < 0$ only) results in

$$B_2(n) = 0$$

and

$$f_n(z) = B_1(n)\, e^{ik_n z} \tag{3.29}$$

In order to determine $B_1(n)$, we use the B·C given by Eq. (2.12); namely

$$\left.\frac{\partial P_1}{\partial z}\right|_{z=0} = -\rho_1 \left[\frac{\partial}{\partial t} + V\frac{\partial}{\partial x}\right]^2 W$$

which gives

$$-\rho_1 \left[\sum_{j=1}^{4} \{-\omega^2 + 2i\omega V\lambda_j + V^2\lambda_j^2\}\, a_j^+\, w_+\, e^{\lambda_j x}\right]$$

$$= \sum_{n=-\infty}^{\infty} i\, k_n\, B_1(n) \exp\{-i\bar{\mu}_n\, x/\ell\}$$

Multiplying both sides of this equation by $e^{i\bar{\mu}_n x/\ell}$ and integrating w.r.t.x from 0 to ℓ, one obtains

$$B_1(n) = w_+\, \hat{B}_1(n)$$

where

$$\hat{B}_1(n) = \frac{\rho_1}{ik_n \ell} \sum_{j=1}^{4} a_j^+ \frac{(-\omega^2 + 2i\omega V\lambda_j + V^2\lambda_j^2)}{(i\bar{\mu}_n/\ell + \lambda_j)} \left\{1 - e^{\lambda_j \ell + i\bar{\mu}_n}\right\} \tag{3.30}$$

Combining Eqs. (3.30) and (3.35), the expression for the induced pressure P_1 becomes

$$P_1 = w_+ \sum_{n=-\infty}^{\infty} \hat{B}_1(n)\ e^{ik_n z}\ e^{-i\bar{\mu}_n x/\ell}\ e^{i\omega t} \tag{3.31}$$

and

$$P_1|_{z=0} = w_+ \sum_{n=-\infty}^{\infty} \hat{B}_1(n)\ e^{-i\mu_n x/\ell}\ e^{i\omega t} \tag{3.32}$$

Treating P_1 as an external force to Eq. (3.2), the particular solution of Eq. (3.2) (call it W_{p+}) is

$$W_{p+}(x) = w_+ Q_+(x) \tag{3.33}$$

where

$$Q_+(x) = \sum_{n=-\infty}^{\infty} [1/q_+(n)]\ e^{-i\mu_n x/\ell} \tag{3.34}$$

and

$$q_+(n) = [1/\hat{B}_1(n)]\ \{D(\bar{\mu}_n/\ell)^4 - C_e\ \omega^2\} \tag{3.35}$$

Combining Eqs. (3.3) and (3.33), we obtain

$$W(x) = \begin{cases} w_+ \left\{ \sum_{j=1}^{4} a_j^+ e^{\lambda_j x} + Q_+(x) \right\}; & \text{+ve going wave} \\ w_- \left\{ \sum_{j=1}^{4} a_j^- e^{\lambda_j x} + Q_-(x) \right\}; & \text{-ve going wave} \end{cases} \tag{3.36}$$

where $Q_-(x)$ has a similar form as that of $Q_+(x)$ with the obvious changes which correspond to a negative going wave (i.e., replace μ, a_j^+ and w_+ by $-\mu$, a_j^- and w_-, respectively).

Keeping in mind that the total solution should satisfy the boundary conditions at the extreme ends, the unknowns w_+ and w_- are then determined from such conditions. Assuming that both ends are identical to the internal supports (i.e., transversely rigid, and have the same rotational stiffness k_r), the total bending moment at both ends should be equal to zero; i.e.,

$$M_t(0) = M_t(\ell B) = 0 \tag{3.37}$$

where B is the number of the bays of the finite beam. The total moment at either end consists of the contributions of the forced response of the infinitely long beam and that of both the positive and negative going waves of the semi-infinite beams. In other words,

$$M_t(0) = 0 = M_+(0) + M_-(0) + M_{inf}(0) - k_r W_t'(0) \tag{3.38}$$

where $M_{inf}(x)$ = contribution of the forced response to the bending moment at x.

$W_t'(x)$ = total slope at x.

Note that the rotational spring k_r at $x = 0$ is not a part of the periodic element between $x = 0$ and $x = \ell$ which explains the presence of the last term of Eq. (3.38). Similarly,

$$M_t(\ell B) = 0 = M_+(\ell B) + M_-(\ell B) + M_{inf}(\ell B) \tag{3.39}$$

Substituting for the values of M_+, M_- and W_t' in Eqs. (3.38) and (3.39), we obtain two simultaneous equations for w_+ and w_- as to be explained below. Note that

$$W_t'(0) = w_+ \{ \sum_{j=1}^{4} a_j^+ \lambda_j + Q_+(0) \} + w_- \{ \sum_{j=1}^{4} a_j^- \lambda_j + Q_-(0) \} + W_{inf}'(0) \quad (3.40)$$

and $M(\ell B) = e^{\mu B} M(0)$. Thus, Eq. (3.38) becomes

$$w_+ \{ \sum_{j=1}^{4} a_j^+ \lambda_j^2 + Q_+''(0) - \frac{k_r}{D} (\sum_{j=1}^{4} a_j^+ \lambda_j + Q_+'(0)) \}$$

$$+ w_- \{ \sum_{j=1}^{4} a_j^- \lambda_j^2 + Q_-''(0) - \frac{k_r}{D} (\sum_{j=1}^{4} a_j^- \lambda_j + Q_-'(0)) \} = \frac{k_r}{D} W_{inf}'(0) - W_{inf}''(0) \quad (3.41)$$

and Eq. (3.39) reduces to

$$w_+ \{ e^{\mu B} \sum_{j=1}^{4} a_j^+ \lambda_j^2 + Q_+''(0)\, e^{i\mu_I B} \} + w_- \{ e^{-\mu B} \sum_{j=1}^{4} a_j^- \lambda_j^2 + Q_-''(0)\, e^{-i\mu_I B} \}$$

$$= -W_{inf}''(\ell B) \quad (3.42)$$

Hence, from Eqs. (3.41) and 3.42), we find

$$w_+ = \frac{\beta_2 \{ \frac{k_r}{D} W_{inf}'(0) - W_{inf}''(0) \} + \alpha_2 W''(\ell B)}{\beta_2 \alpha_1 - \beta_1 \alpha_2} \quad (3.43)$$

$$w_- = \frac{\beta_1 \{ \frac{k_r}{D} W_{inf}'(0) - W_{inf}''(0) \} + \alpha_1 W''(\ell B)}{\beta_1 \alpha_2 - \beta_2 \alpha_1} \quad (3.44)$$

where

$$\left.\begin{aligned} \alpha_1 &= \sum_{j=1}^{4} a_j^+ \lambda_j^2 + Q_+''(0) - \frac{k_r}{D} \{ \sum_{j=1}^{4} a_j^+ \lambda_j + Q_+'(0) \} \\ \alpha_2 &= \sum_{j=1}^{4} a_j^- \lambda_j^2 + Q_-''(0) - \frac{k_r}{D} \{ \sum_{j=1}^{4} a_j^- \lambda_j + Q_-'(0) \} \\ \beta_1 &= e^{\mu B} \sum_{j=1}^{4} a_j^+ \lambda_j^2 + e^{i\mu_I B} Q_+''(0) \\ \beta_2 &= e^{-\mu B} \sum_{j=1}^{4} a_j^- \lambda_j^2 + e^{-i\mu_I B} Q_-''(0) \end{aligned}\right\} \quad (3.45)$$

Once w_+ and w_- are determined, the total displacement (which is the sum of the displacements given in Eqs. (3.36) and (2.18) with the term $e^{i\omega t}$ omitted) and other related quantities are readily determined. Since we have substituted a unit plane wave for the excitation pressure P, the computed response is actually the frequency response function H. Therefore, we can write

$$H(x,\frac{\omega}{U_c}) = w_+ \{\sum_{j=1}^{4} a_j^+ e^{\lambda_j x} + Q_+(x)\} + w_- \{\sum_{j=1}^{4} a_j^- e^{\lambda_j x} + Q_-(x)\}$$

$$+ \sum_{n=-\infty}^{\infty} A_n \{e^{-i(\mu_0+2n\pi)x/\ell} - e^{-i\mu_0 x/\ell}\} \; ; \; 0 \leq x \leq \ell \qquad (3.46)$$

Again, μ_0 is the forcing wave propagation constant and the coefficients A_n's are obtained from Eq. (2.33).

It is to be noted that the frequency response function or any related quantities outside ($0 \leq x \leq \ell$) can be obtained most simply from Eq. (3.46) by using the wave property given in Eq. (3.5) (note that for a negative-going wave the term $e^{-\mu}$ replaces e^{μ} in Eq. (3.5).

B. Transversely Elastic Supports

The analysis in this section is basically the same as that of the previous one (i.e., finite beam on rigid supports). However, there are some differences in the B.C.'s at the internal supports and in the number of free waves which may propagate in the structure. This will become clear as we proceed to calculate the coefficients A_n's of Eq. (3.3).

Using the wave property as expressed in Eq. (3.3), we obtain for

(1) the displacement

$$W(\ell) = e^{\mu} W(0)$$

or
$$\sum_{j=1}^{4} A_j e^{\lambda_j \ell} = e^{\mu} \sum_{j=1}^{4} A_j . \tag{3.47}$$

(ii) the slope

The same relationship as in Eq. (3.9).

(iii) the moment

The same relationship as in Eq. (3.11).

(iv) the shearing force (referring to Fig. 5)

$$S_{r+1} - k_t W(\ell) = D W'''(\ell)$$

or
$$W'''(\ell) + \frac{K_t}{D} W(\ell) = e^{\mu} W'''(0) \tag{3.48}$$

Substituting Eq. (3.48) into Eq. (3.3),

$$\sum_{j=1}^{4} (\lambda_j^3 + \frac{k_t}{D}) A_j e^{\lambda j \ell} = e^{\mu} \sum_{j=1}^{4} A_j \lambda_j^3 \tag{3.49}$$

Combining Eqs. (3.9), (3.11), (3.47) and (3.49), we obtain a set of simultaneous equations relating the coefficients A_j's and the propagation constant μ. This set of simultaneous equations can be written in a matrix form as

$$\overline{G} \{A\} = e^{\mu} \overline{Q} \{A\} \tag{3.50}$$

where $\{A\}^T = [A_1, A_2, A_3, A_4]$ (3.51)

$$\overline{G} = \begin{bmatrix} e^{\lambda_1 \ell} & e^{\lambda_2 \ell} & e^{\lambda_3 \ell} & e^{\lambda_4 \ell} \\ \lambda_1 e^{\lambda_1 \ell} & \lambda_2 e^{\lambda_2 \ell} & \lambda_3 e^{\lambda_3 \ell} & \lambda_4 e^{\lambda_4 \ell} \\ (\lambda_1^2 + \frac{k_r}{D}) e^{\lambda_1 \ell} & (\lambda_2^2 + \frac{k_r}{D}) e^{\lambda_2 \ell} & (\lambda_3^2 + \frac{k_r}{D}) e^{\lambda_3 \ell} & (\lambda_4^2 + \frac{k_r}{D}) e^{\lambda_4 \ell} \\ (\lambda_1^3 + \frac{k_t}{D}) e^{\lambda_1 \ell} & (\lambda_2^3 + \frac{k_t}{D}) e^{\lambda_2 \ell} & (\lambda_3^3 + \frac{k_t}{D}) e^{\lambda_3 \ell} & (\lambda_4^3 + \frac{k_t}{D}) e^{\lambda_4 \ell} \end{bmatrix} \tag{3.52}$$

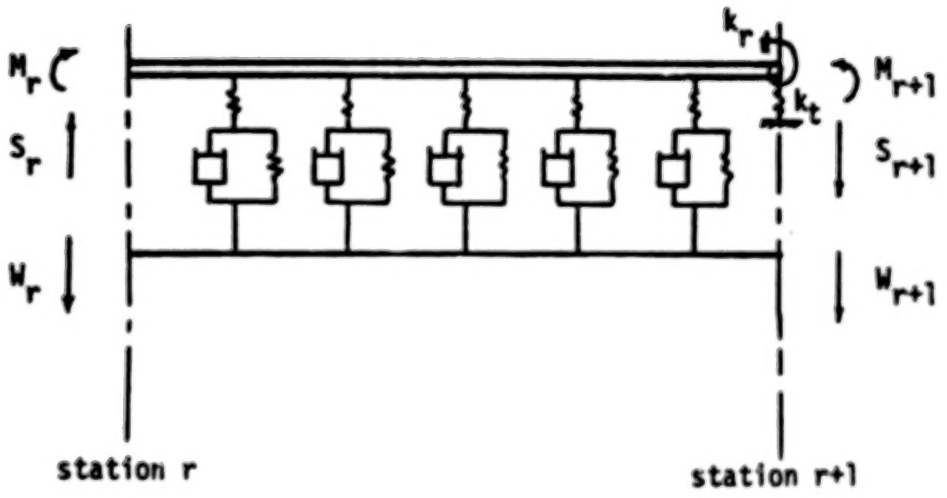

Fig. 5. A Single Periodic Element
(Transversely Elastic Supports)

$$\overline{Q} = \begin{bmatrix} 1 & 1 & 1 & 1 \\ \lambda_1 & \lambda_2 & \lambda_3 & \lambda_4 \\ \lambda_1^2 & \lambda_2^2 & \lambda_3^2 & \lambda_4^2 \\ \lambda_1^3 & \lambda_2^3 & \lambda_3^3 & \lambda_4^3 \end{bmatrix} \tag{3.53}$$

k_t = the spring constant of the elastic support,

and T denotes the transpose of a matrix. A matrix of the form given in Eq. (3.53) is called a vandermonde matrix. Since the roots λ_j's can be assumed distinct, it can be shown that this matrix is nonsingular and therefore $\overline{Q}^{-1}$ exists [23].

The remainder of the analysis can be carried out parallel to that of the previous section. Rewrite Eq. (3.50) in the form of

$$\overline{C}\{A\} = e^{\mu}\{A\} \tag{3.54}$$

where

$$\overline{C} = \overline{Q}^{-1}\,\overline{G} \tag{3.55}$$

The matrix $\overline{C}$ is cross symmetric and possesses two pairs of reciprocal eigenvalues [16]. If these eigenvalues are denoted by $\Lambda_j (j = 1 \to 4)$, and let

$$\Lambda_1 = \frac{1}{\Lambda_3} \quad , \quad \Lambda_2 = \frac{1}{\Lambda_4} \tag{3.56}$$

then the corresponding two pairs of propagation constants are

$$\begin{aligned} \mu_1 &= \log_e \Lambda_1 = -\mu_3 \\ \mu_2 &= \log_e \Lambda_2 = -\mu_4 \end{aligned} \tag{3.57}$$

In other words, there will be two free waves propagating in the positive direction with the propagation constants μ_1 and μ_2, and two free waves propagating in the opposite direction with $-\mu_1$ and $-\mu_2$. Also, the eigenvectors corresponding to the different propagation constants can be determined. Of course, only the normalized eigenvectors (the components of an eigenvector divided by one of them) are unique. If we denote A_j/A_1 (corresponding to μ_k) as $\hat{a}_{j,k}$, then the displacement W_k due to the free wave with propagation constant μ_k can be written as

$$W_k(x) = w_k \sum_{j=1}^{4} \hat{a}_{j,k}\, e^{\lambda_j x} \tag{3.58}$$

where w_k is the amplitude of the wave and will be determined from the B.C.'s at the extreme ends of the finite beam.

The effect of the induced pressure P_1 can be accounted for in a manner similar to that explained in the previous section. To do that, let $P_{1,k}$ be the pressure induced by the wave with propagation constant μ_k, and let it be expressed as follows:

$$P_{1,k}\Big|_{z=0} = w_k \sum_{n=-\infty}^{\infty} \hat{B}_{1,k}(n)\, \exp\{-(\mu_{I,k} + 2n\pi)\, x/\ell\}\, e^{i\omega t} \tag{3.59}$$

where $\hat{B}_{1,k}(n)$ is given by Eq. (3.30) and $\mu_{I,k}$ is the imaginary part of μ_k. Similarly, let the particular solution of Eq. (3.1), with $P_1\big|_{z=0}$ replaced by $P_{1,k}\big|_{z=0}$, be W_k^P. It is simple to show that

$$W_k^P = w_k\, \overline{W}_k \tag{3.60}$$

where
$$\overline{W}_k = \sum_{n=-\infty}^{\infty} \hat{B}_{1,k}(n)\, \frac{e^{-i(\mu_{I,k} + 2n\pi)\, x/\ell}}{D\left(\frac{\mu_{I,k} + 2n\pi}{\ell}\right)^4 - C_e\, \omega^2} \tag{3.61}$$

We shall now proceed to determine the unknowns w_k's, using the B.C.'s at the two extreme ends of the entire beam. Let the supports at the extreme ends be infinitely rigid in the transverse direction, and let their rotational stiffness be k_r. Expressed mathematically, these conditions are

$$W_t(0) = \sum_{k=1}^{4} \{W_k^P(0) + W_k(0)\} + W_{inf}(0) = 0 \tag{3.62}$$

$$W_t(\ell B) = \sum_{k=1}^{4} \{W_k^P(\ell B) + W_k(\ell B)\} + W_{inf}(\ell B) = 0 \tag{3.63}$$

$$M_t(0) = \sum_{k=1}^{4} \overline{M}_k(0) + M_{inf}(0) - k_r W_t'(0) = 0 \tag{3.64}$$

$$M_t(\ell B) = \sum_{k=1}^{4} \overline{M}_k(\ell B) + M_{inf}(\ell B) = 0 \tag{3.65}$$

where $\overline{M}_k(x)$ is the moment corresponding to $\{W_k^P(x) + W_k(x)\}$, and the subscript t denotes the total value (i.e., total displacement, moment, etc.). Application of Eqs. (3.62)-(3.65) results in a set of simultaneous equations for the unknowns w_k's. These equations are combined into a matrix equation as follows:

$$V(w_k) = \{R\} \tag{3.66}$$

where

$$\{R\}^T = [-W_{inf}(0),\ -W_{inf}(\ell B),\ \frac{k_r}{D} W_{inf}'(0) - W_{inf}''(0),\ -W_{inf}''(\ell B)], \tag{3.67}$$

and the elements of the matrix V are given by

$$v_{1,k} = \sum_{j=1}^{4} \hat{a}_{j,k} + \overline{W}_k(0)$$

$$v_{2,k} = e^{\mu_k B} \sum_{j=1}^{4} \hat{a}_{j,k} + e^{i\mu_{I,k} B}\, \overline{W}_k(0)$$

$$v_{3,k} = \sum_{j=1}^{4} \hat{a}_{j,k} \lambda_j^2 + \bar{W}_k''(0) - \frac{k_r}{D} \{ \sum_{j=1}^{4} \hat{a}_{j,k} \lambda_j + \bar{W}_k(0) \}$$

$$v_{4,k} = e^{\mu_k B} \sum_{j=1}^{4} \hat{a}_{j,k} \lambda_j^2 + \bar{W}_k''(0)\, e^{i\mu_{I,k} B}$$

$$k = 1 \rightarrow 4$$

Once the unknowns w_k's are determined, the total displacement is readily determined by summing up the displacements corresponding to the free waves W_k's and that of the infinite beam. Since we have substituted a unit plane wave for the excitation pressure P, the total displacement is actually the frequency response function H. Therefore,

$$H(x, \frac{\omega}{U_c}) = \sum_{k=1}^{4} \{ W_k(x, \frac{\omega}{U_c}) + W_k^P(x, \frac{\omega}{U_c}) \} + H_{inf}(x, \frac{\omega}{U_c}) \qquad (3.68)$$

where $H_{inf}(x, \frac{\omega}{U_c})$ is given by Eq. (2.60).

Again, the frequency response function or other related quantities outside ($0 \leq x \leq \ell$) can be easily obtained from Eq. (3.68) by using the wave property given in Eq. (3.5) (note that for a negative-going wave, $e^{-\mu}$ replaces e^{μ} in Eq. (3.5)).

IV. TWO-DIMENSIONAL CASE: AN INFINITELY LONG PANEL BACKED BY AN AIR CAVITY

In the preceding sections, some possible designs of passive compliant surfaces have been analyzed using simplified one-dimensional models of periodic beams. Such simplified analyses reveal basic characteristics of real structures, but more accurate representation requires the use of two-dimensional models.

In this section, an infinitely long panel backed by an air cavity of depth d is considered. The side walls of the cavity are assumed to be either acoustically hard or acoustically soft and both cases will be dealt with in this investigation. The panel is supported by pre-tensioned circular solid wires at distant ℓ apart. The tension in each wire is T. The configuration of such a panel is shown in Fig. 6.

The equation of motion of such a panel, not directly over a wire, is given by

$$D\nabla^4 W + m_p \ddot{W} = P + (P_1 - P_2)\Big|_{z=-d} \tag{4.1}$$

where

$$\nabla^4 = \frac{\partial^4}{\partial x^4} + 2\frac{\partial^4}{\partial x^2 \partial y^2} + \frac{\partial^4}{\partial y^4}$$

P = the turbulence pressure field (if the panel were motionless)

P_1 = induced additional pressure generated above the panel

P_2 = pressure variation transmitted into the cavity

m_p = mass per unit area of the panel

D = flexural rigidity of the panel.

Again, we shall determine first the frequency response function. For this purpose, P is replaced by the sth plane wave $e^{i(\omega t - kx)}\, e^{is\pi y/b}$.

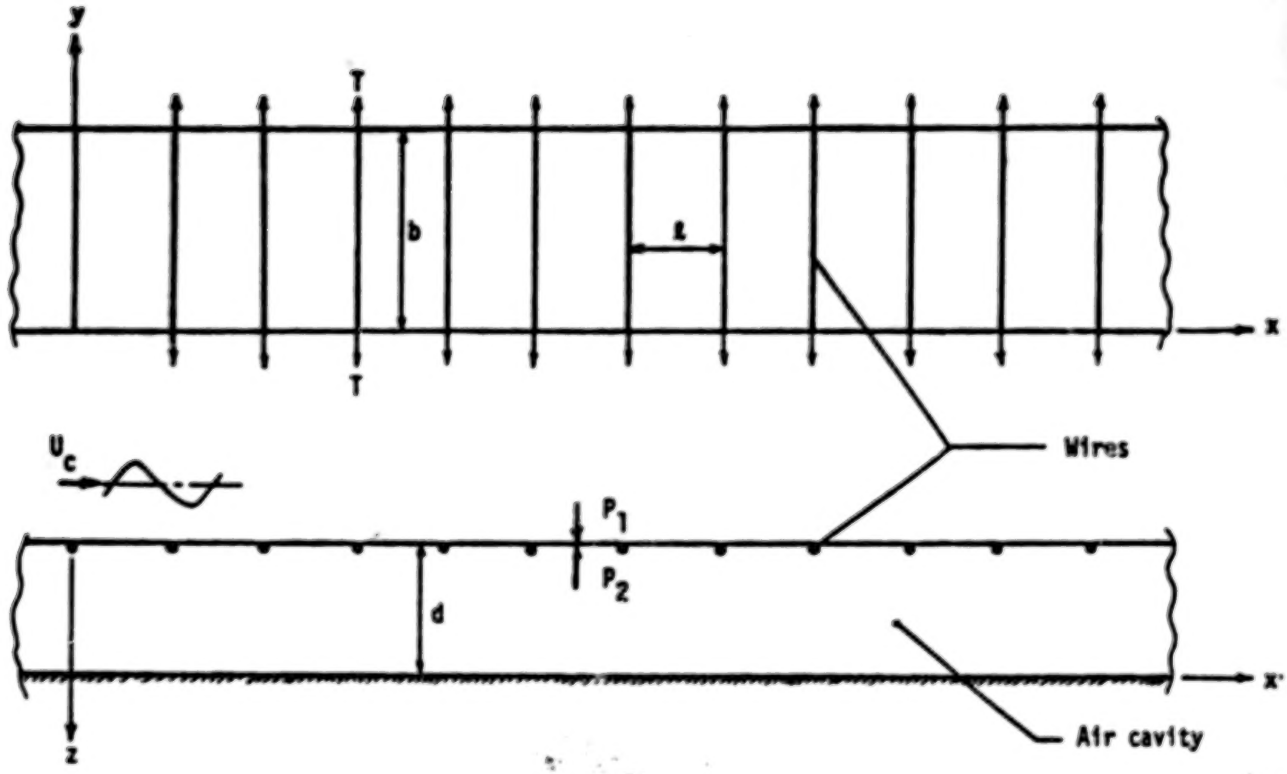

Fig. 6 An Infinite Panel Backed by an Air Cavity

The panel is assumed to be simply supported at both sides y = 0,b. Accordingly, the boundary conditions for W are

$$W(x,0,t) = W(x,b,t) = 0 \tag{4.2}$$

The pressure P_1 which is induced by the panel motion is governed by the convective wave motion

$$(\frac{\partial}{\partial t} + V \frac{\partial}{\partial x})^2 P_1 = a_1^2 \nabla^2 P_1 \ . \tag{4.3}$$

This induced pressure, P_1, is subjected to the B.C.

$$\rho_1 (\frac{\partial}{\partial t} + V \frac{\partial}{\partial x})^2 W = - \left. \frac{\partial P_1}{\partial z} \right|_{z=-d} \tag{4.4}$$

and the radiation condition that it propagates in the domain $z < 0$.

The pressure wave P_2 which is also generated by the panel motion and transmitted into the cavity is governed by the equation

$$\frac{\partial^2 P_2}{\partial t^2} = a_2^2 \nabla^2 P_2 \tag{4.5}$$

where a_2 is the speed of sound in the cavity. If the side walls of the cavity are acoustically hard, then the boundary conditions for P_2 are

$$\frac{\partial P_2}{\partial z} = 0 \quad \text{at} \quad z = 0 \tag{4.6}$$

$$\frac{\partial P_2}{\partial y} = 0 \ \text{along} \ y = 0,b \tag{4.7}$$

$$\left. \frac{\partial P_2}{\partial z} \right|_{z=-d} = -\rho_2 \ddot{W} \tag{4.8}$$

where ρ_2 is the air density inside the cavity.

Since the displacement must be spatially periodic (in the x-direction) and must satisfy the B.C. (4.2), it is convenient to write the displacement W due to the excitation $e^{i(\omega t - kx)}\, e^{is\pi y/b}$ as follows:

$$W_s(x,y,t) = \sum_{m=1}^{\infty} \sum_{n=-\infty}^{\infty} A_{mn}\, e^{-i\mu_n x/\ell} \sin\left(\frac{m\pi}{b} y\right) e^{i\omega t} \tag{4.9}$$

where $\mu_n = \mu_0 + 2n\pi$ and μ_0 is the forcing wave propagation constant ($= k\ell$). Again, our immediate objective is to determine the coefficients A_{mn}'s.

In view of the B.C. given in Eq. (4.4), the induced pressure P_1 may be expressed in a form similar to that of the displacement; namely

$$P_1(x,y,z,t) = \sum_{m=1}^{\infty} \sum_{n=-\infty}^{\infty} e^{-i\mu_n x/\ell} \sin\left(\frac{m\pi}{b} y\right) f_{mn}(z)\, e^{i\omega t} \tag{4.10}$$

Substituting Eq. (4.10) into Eq. (4.3) and simplifying, one obtains

$$f''_{mn}(z) + k_{mn}^2 f_{mn}(z) = 0 \tag{4.11}$$

where $$k_{mn}^2 = \frac{\omega^2}{a_1^2} - \frac{2\omega V}{a_1^2}\frac{\mu_n}{\ell} + \frac{V^2}{a_1^2}\left(\frac{\mu_n}{\ell}\right)^2 - \left(\frac{\mu_n}{\ell}\right)^2 - \left(\frac{m\pi}{b}\right)^2 \tag{4.12}$$

The solution to Eq. (4.11) can be written as

$$f_{mn}(z) = B_1(m,n)\, e^{ik_{mn}z} + B_2(m,n)\, e^{-ik_{mn}z} \tag{4.13}$$

Since P_1 can propagate in the negative z-domain only, $B_2(m,n)$ must be equal to zero and Eq. (4.13) reduces to

$$f_{mn}(z) = B_1(m,n)\, e^{ik_{mn}z} \tag{4.14}$$

Using the B.C. given by Eq. (4.4),

$$B_1(m,n) = \frac{-i\rho_1\omega a_1(C_n - V)^2 e^{ik_{mn}d}}{C_n\{(C_n - V)^2 - a_1^2 - (\frac{m\pi}{b} \cdot \frac{\ell}{\mu_n} a_1)^2\}^{\frac{1}{2}}} A_{mn} \qquad (4.15)$$

where $C_n = \frac{\omega\ell}{\mu_n}$. If we substitute Eqs. (4.14) and (4.15) into Eq. (4.10), we obtain

$$P_1(x,y,z,t) = \sum_{m=1}^{\infty} \sum_{n=-\infty}^{\infty} \hat{B}_1(m,n)\, e^{ik_{mn}(z+d)}\, e^{-i\mu_n x/\ell} \sin(\tfrac{m\pi}{b}y)\, e^{i\omega t} \qquad (4.16)$$

and

$$P_1(x,y,z,t)\Big|_{z=-d} = \sum_{m=1}^{\infty} \sum_{n=-\infty}^{\infty} \hat{B}_1(m,n)\, e^{-i\mu_n x/\ell} \sin(\tfrac{m\pi}{b}y)\, e^{i\omega t} \qquad (4.17)$$

where $\hat{B}_1(m,n) = B_1(m,n)\, e^{-ik_{mn}d}$. It is to be noted that the comments which have been made concerning the effect of P_1 on the response are the same for both the one-dimensional and two-dimensional cases (see page 16).

Similarly, because of the B.C. (4.8), a convenient form for P_2 is

$$P_2(x,y,z,t) = \sum_{m=0}^{\infty} \sum_{n=-\infty}^{\infty} A_{mn}\, F_{mn}(z)\, e^{-i\mu_n x/\ell} \cos(\tfrac{m\pi}{b}y)\, e^{i\omega t} \qquad (4.18)$$

The B.C.'s given by Eq. (4.7) are automatically satisfied. Substituting Eq. (4.18) into Eq. (4.5) and simplifying, one obtains

$$F''_{mn}(z) + K_{mn}^2 F(z) = 0 \qquad (4.19)$$

where $$K_{mn}^2 = \frac{\omega^2}{a_2^2} - (\frac{\mu_n}{\ell})^2 - (\frac{m\pi}{b})^2 \quad . \qquad (4.20)$$

The solution to Eq. (4.19) may be written as

$$F_{mn}(z) = D_1(m,n)\, e^{iK_{mn}z} + D_2(m,n)\, e^{-iK_{mn}z} \qquad (4.21)$$

Imposition of Eq. (4.6) results in

$$D_1(m,n) = D_2(m,n) \equiv D(m,n)$$

and
$$F_{mn}(z) = 2D(m,n) \cos (K_{mn} z) \tag{4.22}$$

The B.C. given by Eq. (4.9) leads to

$$\sum_{m=0}^{\infty} \sum_{n=-\infty}^{\infty} A_{mn}\, e^{-i\mu_n x/\ell} \cos \left(\frac{m\pi}{b} y\right) D(m,n)\, K_{mn} \sin (K_{mn} d)$$

$$= \rho_2\, \omega^2 \sum_{m=1}^{\infty} \sum_{n=-\infty}^{\infty} A_{mn}\, e^{-i\mu_n x/\ell} \sin \left(\frac{m\pi}{b} y\right) \tag{4.23}$$

Multiplying both sides of Eq. (4.23) by $e^{i\mu_{n'} x/\ell} \cos \left(\frac{m'\pi}{b} y\right)$ and integrating over $(0 < x < \ell;\ 0 < y < b)$,

$$A_{m'n'}\, \ell \frac{b}{2} \hat{f}(m')\, D(m',n')\, K_{m'n'} \sin (K_{m'n'} d)$$

$$= \rho_2\, \omega^2\, \ell \sum_{m=1}^{\infty} A_{mn'} \int_0^b \sin \left(\frac{m\pi}{b} y\right) \cos \left(\frac{m'\pi}{b} y\right) dy$$

which becomes, after simplification,

$$A_{m'n'}\, D(m',n') = \frac{2\, \rho_2\, \omega^2}{\hat{f}(m')\, K_{m'n'} \sin (K_{m'n'} d)} \sum_{m=1}^{\infty} A_{mn'} \frac{2m}{\pi(m^2 - m'^2)} \tag{4.24}$$

where
$$\hat{f}(m') = \begin{cases} 1 & ;\ m' \neq 0 \\ 2 & ;\ m' = 0\ . \end{cases} \tag{4.25}$$

Substituting Eq. (4.24) into Eq. (4.18) gives

$$P_2(x,y,z,t) = \rho_2\, \omega^2 \sum_{m=0}^{\infty} \sum_{n=-\infty}^{\infty} \frac{4 \cos (K_{mn} z)}{\hat{f}(m) \cdot K_{mn} \sin (K_{mn} d)}\ e^{-i\mu_n x/\ell}$$

$$\cos\left(\frac{m\pi}{b}y\right) \sum_{\substack{r=1 \\ m+r=\text{odd}}}^{\infty} A_{rn} \frac{r}{\pi(r^2 - m^2)} \cdot e^{i\omega t} \qquad (4.26)$$

Exchanging the symbols r and m, and reversing the summation order in Eq. (4.26) to make it compatible with the form of the displacement W, the expression for P_2 becomes

$$P_2(x,y,z,t)\Big|_{z=-d} = \rho_2 \omega^2 \sum_{m=1}^{\infty} \sum_{n=-\infty}^{\infty} A_{mn} e^{-i\mu_n x/\ell} \left\{ \sum_{\substack{r=0 \\ r+m=\text{odd}}}^{\infty} \frac{4m}{f(r)\pi(m^2-r^2)} \right.$$

$$\left. \cot(K_{rn}d) \cos\left(\frac{r\pi}{b}y\right)/K_{rn} \right\} e^{i\omega t} \qquad (4.27)$$

It is to be noted that when K_{rn} is imaginary, the quantity $\dfrac{\cot(K_{rn}d)}{K_{rn}}$ becomes $-\dfrac{\text{Coth}(|K_{rn}|d)}{|K_{rn}|}$. This means that the nth component of P_2 would act as an added mass.

Determination of the coefficients A_{mn}'s:

The virtual work principle will be used to determine A_{mn}'s. The total virtual work done by all the forces on and in the panel (including those due to the wires) should be equal to zero. To calculate the virtual work, we will consider one periodic element only for the same reasoning given for the one-dimensional case. Let the virtual displacement be

$$\delta W = \delta A_{m'n'} e^{-i\mu_{n'}x/\ell} \sin\left(\frac{m'\pi}{b}y\right) e^{+i\omega t} \qquad (4.28)$$

As usual in complex algebra, the complex conjugate of δW will be used in calculating the virtual work.

Let the virtual work done by $\left\{ D\,\nabla^4 \bar{W} + m_p \ddot{\bar{W}} - P_1 \Big|_{z=-d} \right\}$ be $\delta\bar{W}_1$.

$$\delta\bar{W}_1 = \int_0^b \int_0^\ell \sum_{m=1}^{\infty} \sum_{n=-\infty}^{\infty} \delta A_{m'n'}\, e^{-i(\mu_n - \mu_{n'})x/\ell}\, A_{mn}$$

$$\sin\left(\frac{m\pi}{b} y\right) \sin\left(\frac{m'\pi}{b} y\right) \phi(m,n)\, dx\, dy \qquad (4.29)$$

where

$$\phi(m,n) = \left\{ \left(\frac{\mu_n}{\ell}\right)^4 + 2\left(\frac{m\pi}{b} \cdot \frac{\mu_n}{\ell}\right)^2 + \left(\frac{m\pi}{b}\right)^4 \right\} D - m_p \omega^2$$

$$+ \frac{i\, \rho_1\, \omega a_1 (C_n - V)^2}{C_n \sqrt{(C_n - V)^2 - a_1^2 - \left(a_1 \frac{m\pi}{b} \frac{\ell}{\mu_n}\right)^2}} \qquad (4.30)$$

Carrying out the integration in Eq. (4.29) and simplifying, we obtain

$$\delta\bar{W}_1 = \ell \frac{b}{2} A_{m'n'}\, \delta A_{m'n'}\, \phi(m',n') \qquad (4.31)$$

Similarly, the virtual work done by P_2 is

$$\delta\bar{W}_{P_2} = \int_0^b \int_0^\ell P_2 \Big|_{z=-d}\, e^{i\mu_{n'} x/\ell} \sin\left(\frac{m'\pi}{b} y\right) dx\, dy$$

$$= \delta A_{m'n'}\, \ell \sum_{m=1}^{\infty} A_{mn'} \left[\frac{\rho_2\, \omega^2\, m}{\pi(m^2 - r^2)} \cdot \frac{4 \cot(K_{rn} d)}{\hat{f}(r)\, K_{rn}} \right.$$

$$\left. \int_0^b \sin\left(\frac{m'\pi}{b} y\right) \cos\left(\frac{r\pi}{b} y\right) dy \right]$$

$$= \frac{b}{2}\, \ell \sum_{m=1}^{\infty} A_{mn'}\, \psi(m,m',n')\, \delta A_{m'n'} \qquad (4.32)$$

where

$$\psi(m,m',n) = \sum_{\substack{r=0 \\ m+r=odd \\ m'+r=odd}}^{\infty} \frac{4\,\rho_2\,\omega^2\,mm'}{(m^2-r^2)\hat{f}(r)\pi^2} \cdot \frac{4\cot(K_{rn}d)}{K_{rn}} \tag{4.33}$$

The virtual work done by the excitation $e^{is\pi y/b}\, e^{i(\omega t - kx)}$ is

$$\delta\bar{W}_p = -\int_0^b\int_0^{\ell} e^{-i\mu_0 x/\ell}\, e^{i\mu_{n'} x/\ell}\, A_{m'n'} \sin\left(\frac{m'\pi}{b} y\right)$$

$$e^{is\pi y/b}\, dy = \bar{\alpha}(s,m',n') \tag{4.34}$$

where

$$\bar{\alpha}(s,m',n') = \begin{cases} -\ell\,\delta A_{m'n'}\, \dfrac{(m'\pi/b)\,\{1-(-1)^{s+m'}\}}{\left(\frac{m'\pi}{b}\right)^2 - \left(\frac{s\pi}{b}\right)^2}\,\delta_{n'0} & ;\ s \neq m' \\ -i\,\ell\,\delta A_{m'n'}\,\dfrac{b}{2}\,\delta_{n'0} & ;\ s = m' \end{cases} \tag{4.35}$$

The wire, because of its elastic and inertial properties, will produce shearing forces and moments in the panel along the line of attachment. The virtual work done by the shearing forces is (say at x = 0)

$$\delta\bar{W}_s = \int_0^b \left(E_w I_w \frac{\partial^4 W}{\partial y^4} + \rho_w A_w \frac{\partial^2 W}{\partial t^2} - T\frac{\partial^2 W}{\partial y^2}\right) \delta W(0,y)\, dy$$

$$= \int_0^b \sum_{m=1}^{\infty} \sum_{n=-\infty}^{\infty} \left\{E_w I_w \left(\frac{m\pi}{b}\right)^4 - \rho_w A_w \omega^2 + T\left(\frac{m\pi}{b}\right)^2\right\}$$

$$A_{mn}\,\delta A_{m'n'} \sin\left(\frac{m\pi}{b} y\right) \sin\left(\frac{m'\pi}{b} y\right) dy$$

$$= \frac{b}{2} \sum_{n=-\infty}^{\infty} A_{m'n}\,\delta A_{m'n'}\,\xi(m',n) \tag{4.36}$$

where

E_w = Young's modulus of the wire materials

I_w = moment of inertia of the wire about the x-axis

ρ_w = density of the wire material

A_w = cross sectional area of the wire

T = tension applied to the wire

and

$$\xi(m',n) = E_w I_w \left(\frac{m'\pi}{b}\right)^4 - \rho_w A_w \omega^2 + T\left(\frac{m'\pi}{b}\right)^2 \tag{4.37}$$

Also, the virtual work done by the torsional moments in the wire is

$$\delta\bar{W}_m = \int_0^b \left\{-GC \frac{\partial^3 W}{\partial x \partial y^2} + \rho_w J_w \frac{\partial}{\partial x} \ddot{W}\right\} \delta W'(0,y)\, dy \tag{4.38}$$

where G is the shear modulus, C is the Saint-Venant constant of uniform torsion, and J_w is the polar moment of inertia of the wire. Carrying out the integration in Eq. (4.38) and simplifying:

$$\delta\bar{W}_m = \frac{b}{2} \sum_{n=-\infty}^{\infty} A_{m'n}\, \delta A_{m'n'}\, \Gamma(m',n,n') \tag{4.39}$$

where

$$\Gamma(m',n,n') = \left\{-GC\left(\frac{m'\pi}{b}\right)^2 + \rho_w J_w \omega^2\right\} \frac{\mu_n \mu_{n'}}{\ell^2} \tag{4.40}$$

Since the total virtual work must be zero,

$$\delta\bar{W}_1 + \delta\bar{W}_{p_2} + \delta\bar{W}_s + \delta\bar{W}_m + \delta\bar{W}_p = 0 \tag{4.41}$$

Substituting into this equation the values of $\delta\bar{W}_1$, $\delta\bar{W}_{p_2}$, $\delta\bar{W}_p$, $\delta\bar{W}_s$ and $\delta\bar{W}_m$ from Equations (4.29), (4.32), (4.34), (4.36) and (4.39), respectively, we obtain a set of simultaneous equations for the coefficients A_{mn}'s.

$$A_{m'n'}\,\phi(m',n') + \sum_{m=1}^{\infty} A_{mn'}\,\psi(m',m,n') + \frac{1}{\ell}\sum_{n=-\infty}^{\infty} A(m',n,n')\,A_{m'n}$$

$$= \overline{B}(s,m',n') \tag{4.42}$$

where

$$\overline{B}(s,m',n') = \begin{cases} \dfrac{2}{b}\,\dfrac{(m'\pi/b)}{(\frac{m'\pi}{b})^2 - (\frac{s\pi}{b})^2}\left\{1 - (-1)^{s+m'}\right\}\delta_{n'0} & ;\ s \neq m' \\ i\,\delta_{n'0} & ;\ s = m' \end{cases} \tag{4.43}$$

and $A(m',n,n') = E(m',n') + \Gamma(m',n,n')$. (4.44)

Moreover, we can write a truncated version of Eq. (4.42) in a matrix form

$$[K_{mn\alpha\beta}]\,\{A_{\alpha\beta}\} = \{\overline{B}(s,m,n)\} \tag{4.45}$$

where

$$K_{mn\alpha\beta} = \phi(m,n)\,\delta_{m\alpha}\,\delta_{n\beta} + \psi(m,n,\alpha)\,\delta_{n\beta} + \frac{A(m,\beta,n)}{\ell}\,\delta_{m\alpha} \tag{4.46}$$

$m = 1,2,3, \ldots, N_1$

$\alpha = 1,2,3, \ldots, N_1$

$n = -N_2, \ldots, -1,0,1, \ldots, N_2$

$\beta = -N_2, \ldots, -1,0,1, \ldots, N_2$

The choice of N_1 and N_2 depends on the accuracy desired in computing the coefficients A_{mn}'s.

In the preceding analysis we considered the side walls of the cavity to be acoustically hard and we obtained a set of simultaneous equations governing the coefficients A_{mn}'s. Now, we turn to the case where the side walls are assumed to be acoustically soft. In this case, we will have a different expression for P_2 and, accordingly, the virtual work done by P_2 will differ from that of the acoustically-hard-walls case.

The governing equation for the pressure P_2 is still Eq. (4.5), but the B.C.'s are now

$$\frac{\partial P_2}{\partial z} = 0 \quad \text{at} \quad z = 0 \tag{4.47}$$

$$P_2 = 0 \quad \text{along} \quad y = 0,b \tag{4.48}$$

$$\left.\frac{\partial P_2}{\partial z}\right|_{z=-d} = -\rho_2 \ddot{W} \tag{4.49}$$

which replace Eqs. (4.6)-(4.8). In view of the B.C.'s (4.48) and (4.49), let the pressure P_2 be expressed as

$$P_2(x,y,z,t) = \sum_{m=1}^{\infty} \sum_{n=-\infty}^{\infty} \bar{f}_{mn}(z)\, e^{-i\mu_n x/\ell} \sin\left(\frac{m\pi}{b} y\right) e^{i\omega t} \tag{4.50}$$

Following a procedure similar to that used in the case of acoustically hard walls, one can show easily that $\bar{f}_{mn}(z)$ can be expressed as

$$\bar{f}_{mn}(z) = C_1(m,n)\, e^{iK_{mn}z} + C_2(m,n)\, e^{-iK_{mn}z} \tag{4.51}$$

where K_{mn}^2 is given by Eq. (4.20). Using the B.C. given by Eq. (4.47), one finds that $C_1(m,n)$ is equal to $C_2(m,n)$. Furthermore, the B.C. (4.49) gives

$$C_1(m,n) = [\rho_2\omega^2/\{2K_{mn} \sin(K_{mn}d)\}]\, A_{mn} \tag{4.52}$$

Combining Eqs. (4.50) through (4.52), we obtain

$$P_2(x,y,z,t) = \sum_{m=1}^{\infty} \sum_{n=-\infty}^{\infty} A_{mn}\, e^{-i\mu_n x/\ell} \sin\left(\frac{m\pi}{b} y\right) \cdot \frac{\rho_2\omega^2 \cos(K_{mn}z)}{K_{mn} \sin(K_{mn}d)}\, e^{i\omega t} \tag{4.53}$$

and

$$P_2(x,y,z,t)\Big|_{z=-d} = \sum_{m=1}^{\infty} \sum_{n=-\infty}^{\infty} \frac{\rho_2 \omega^2}{K_{mn}} \cot (K_{mn} d)\, e^{-i\mu_n x/\ell}$$

$$A_{mn} \sin \left(\frac{m\pi}{b} y\right) e^{i\omega t} \qquad (4.54)$$

Now, the virtual work done by the pressure P_2 is

$$\delta \bar{W}_{P_2} = \int_0^b \int_0^{\ell} \sum_{m=1}^{\infty} \sum_{n=-\infty}^{\infty} \frac{\rho_2 \omega 2}{K_{mn}} \cot (K_{mn} d)\, e^{-i\mu_n x/\ell}$$

$$A_{mn} \sin \left(\frac{m\pi}{b} y\right) \delta A_{m'n'}\, e^{i\mu_{n'} x/\ell} \sin \left(\frac{m'\pi}{b} y\right) dx\, dy$$

$$= \ell \frac{b}{2} \delta A_{m'n'} \cdot \frac{\rho_2 \omega 2}{K_{m'n'}} \cot (K_{m'n'} d)\, A_{m'n'} \qquad (4.55)$$

Therefore, using Eq. (4.55) instead of Eq. (4.32), we obtain a new set of simultaneous linear equations for the coefficients A_{mn}'s

$$A_{m'n'} \bar{\phi}(m',n') + \frac{1}{\ell} \sum_{n=-\infty}^{\infty} \Lambda(m',n,n')\, A_{m'n} = \bar{\beta}(s,m',n') \qquad (4.56)$$

where $$\bar{\phi}(m',n') = \phi(m',n') + \rho_2 \omega^2 \frac{\cot (K_{m'n'} d)}{K_{m'n'}} \quad , \qquad (4.57)$$

and $\bar{\beta}(s,m',n')$ is given by Eq. (4.43). Moreover, we can write a truncated Eq. (4.56) in a matrix form

$$[\bar{K}_{mn\alpha\beta}]\, \{A_{\alpha\beta}\} = \{\bar{\beta}(s,m,n)\} \qquad (4.58)$$

where $$\bar{K}_{mn\alpha\beta} = \bar{\phi}(m,n)\, \delta_{m\alpha} \delta_{n\beta} + \frac{1}{\ell} \Lambda(m,\beta,n)\, \delta_{m\alpha} \quad , \qquad (4.59)$$

$$m = 1,2, \ldots, N_3$$

$$\alpha = 1,2, \ldots, N_3$$

$$n = -N_4, \ldots, -1, 0, 1, \ldots, N_4$$

$$\beta = -N_4, \ldots, -1, 0, 1, \ldots, N_4 ,$$

and $(2N_3 + 1)$ and $(2N_4 + 1)$ are the number of significant modes in the y and x directions, respectively.

Once the coefficients A_{mn}'s are determined from Eq. (4.42) or Eq. (4.57), the frequency response function of the structure due to the sth component of the pressure wave, $e^{is\pi y/b}\, e^{i(\omega t - kx)}$, is readily determined; namely

$$H_s(x,y,k) = \sum_{m=1}^{\infty} \sum_{n=-\infty}^{\infty} A_{mn}\, e^{-i\mu_n x/\ell} \sin\left(\frac{m\pi}{b} y\right) \qquad (4.60)$$

V. STRUCTURAL RESPONSE

In the preceding sections, we were mainly concerned with the frequency response function, H. The next question is whether or not desired structural motion can be generated by boundary layer turbulence excitations. Under such excitations, the structural response is a random process and should be characterized in terms of statistical quantities such as spectral density, mean square value, ..., etc.

If we accept the frozen pattern hypothesis for the turbulence field, then after reaching stochastic stationarity the displacement W may be expressed as

$$W(x,y,t) = \int_{-\infty}^{\infty} \sum_{s=-\infty}^{\infty} H_s(x,y,k)\, \tilde{f}_s\, e^{i\omega t}\, dF(k) \tag{5.1}$$

where $E\{dF(k_1)\, dF^*(k_2)\} = \delta(k_1 - k_2)\, S_p(k_1)\, dk_1\, dk_2$

$$|\tilde{f}_s|^2 = f_s ,$$

and f_s is given by Eq. (1.4). The frequency response function H_s is given in Eq. (4.60). The autocorrelation function of the displacement W is

$$\Gamma_w(x,y,t_1,t_2) = E\{W(x,y,t_1)\, W^*(x,y,t_2)\} \tag{5.2}$$

Combining Eqs. (5.1), (5.2) and noting that the Fourier components $\tilde{f}_s$ are uncorrelated, we get

$$R_w(x,y,\tau) = \Gamma_w(x,y,t_1-t_2) = \int_{-\infty} \sum_{s=-\infty}^{\infty} |H_s(x,y,k|^2\, f_s$$

$$S_p(k)\, e^{ikU_c\tau}\, dk \tag{5.3}$$

The spectral density of the displacement, Φ_w, is the Fourier transform of the autocorrelation function; i.e.,

$$\Phi_w(x,y,\Omega) = \frac{1}{2\pi}\int_{-\infty}^{\infty} e^{-i\Omega\tau}\, R_w(x,y,\tau)\, d\tau$$

$$= \frac{1}{2\pi}\int_{-\infty}^{\infty}\int_{-\infty}^{\infty}\sum_{s=-\infty}^{\infty} |H_s(x,y,k)|^2\, f_s\, S_p(k)$$

$$e^{i(kU_c - \Omega)\tau} dk\, d\tau$$

$$= \frac{1}{U_c}\int_{-\infty}^{\infty}\sum_{s=-\infty}^{\infty} |H_s(x,y,\tfrac{\omega}{U_c})|^2\, f_s\, S_p(\tfrac{\omega}{U_c})\, \delta(\Omega - \omega)\, d\omega$$

$$= \frac{S_p(\frac{\Omega}{U_c})}{U_c}\sum_{s=-\infty}^{\infty} |H_s(x,y,\tfrac{\Omega}{U_c})|^2\, f_s$$

or

$$\Phi_w(x,y,\omega) = S_p(\omega)\sum_{s=-\infty}^{\infty} |H_s(x,y,\tfrac{\omega}{U_c})|^2\, f_s \tag{5.4}$$

For the one-dimensional case, Φ_w becomes

$$\Phi_w(x,\omega) = S_p(\omega)\, |H(x,\tfrac{\omega}{U_c})|^2 \tag{5.5}$$

If the drag reduction mechanism hypothesized in Reference [3] is true, then a good design is one that can respond to the boundary layer excitations in a desirable manner within a particular frequency range. The root mean square value of the structural response attributed to a frequency range (ω_ℓ, ω_u) is

$$W_{r.m.s}(x,y) = \left[\int_{\omega_\ell}^{\omega_u} \Phi_w(x,y,\omega)\, d\omega\right]^{\frac{1}{2}} \tag{5.6}$$

where ω_ℓ and ω_u are the lower and upper limits of the frequency range, respectively.

To carry out the integration in Eq. (5.6), we need an expression for the turbulence spectrum. Considerable amount of information is available on experimentally determined boundary-layer turbulence spectra at various free stream velocities. See, for example, [21,24]. In particular, Bull [24] has done extensive spectral density measurements for subsonic boundary layer pressure fluctuations. Therefore, numerical calculations in this thesis are based on Bull's spectrum but with the decay factor in the convection direction omitted, and the results will be presented in the section dealing with the numerical results.

VI. SPECTRAL DENSITIES OF P_1 AND $(P_1 + P)$

A. Spectral Density of P_1

Let the frequency response function of P_1 due to the excitation $e^{is\pi y/b}\, e^{i(\omega t - kx)}$ be $H_{1,s}(x,y,k)$. After reaching stochastic stationarity, the pressure P_1 can be expressed as

$$P_1(x,y,t) = \int_{-\infty}^{\infty} \sum_{s=-\infty}^{\infty} \tilde{f}_s\, H_{1,s}(x,y,k)\, e^{i\omega t}\, dF(k) \tag{6.1}$$

Carrying out an analysis similar to that of the displacement, the spectral density of P_1 (for the two-dimensional case) can be expressed as

$$\Phi_{p_1 p_1}(x,y,\omega) = \sum_{s=-\infty}^{\infty} f_s \left| H_{1,s}(x,y,\tfrac{\omega}{U_c}) \right|^2 S_p(\omega) \tag{6.2}$$

where $H_{1,s}(x, \frac{\omega}{U_c})$ is obtained from Eq. (4.17), namely

$$H_{1,s}(x,y, \tfrac{\omega}{U_c}) = \sum_{m=1}^{\infty} \sum_{n=-\infty}^{\infty} \hat{B}_1(m,n)\, e^{-i\mu_n x/\ell} \sin\left(\tfrac{m\pi}{b} y\right) \tag{6.3}$$

For the one-dimensional case,

$$\Phi_{p_1 p_1}(x,\omega) = \left| H_1(x, \tfrac{\omega}{U_c}) \right|^2 S_p(\omega) \tag{6.4}$$

In this case H_1 depends on the configuration of the beam. For example, in the case of an infinitely long beam on rigid supports, H_1 is given by Eq. (2.19).

B. Spectral Density of $(P + P_1)$

Let

$$\hat{P} = P + P_1 \tag{6.5}$$

The autocorrelation function, $\Gamma_{\hat{p}\hat{p}}(x,y,t_1,t_2)$, of $\hat{P}$ is given by

$$\Gamma_{\hat{p}\hat{p}}(x,y,t_1,t_2) = E\{\hat{P}(x,y,t_1)\,\hat{P}(x,y,t_2)\} \tag{6.6}$$

$$= E\{P(x,y,t_1)\,P(x,y,t_2)\} + E\{P_1(x,y,t_1)\,P_1(x,y,t_2)\}$$

$$+ E\{P(x,y,t_1)\,P_1(x,y,t_2)\} + E\{P(x,y,t_2)\,P_1(x,y,t_1)\} \tag{6.7}$$

When the stochastic stationarity of P and P_1 is reached, Eq. (6.7) becomes

$$R_{\hat{p}\hat{p}}(x,y,\tau) = R_{pp}(x,y,\tau) + R_{p_1p_1}(x,y,\tau) + R_{pp_1}(x,y,\tau)$$

$$+ R_{p_1p}(x,y,\tau) \tag{6.8}$$

The spectral density of $\hat{p}$ is merely the Fourier transform of $R_{\hat{p}\hat{p}}(x,y,\tau)$; i.e.,

$$\Phi_{\hat{p}\hat{p}}(x,y,\omega) = \Phi_{pp}(x,y,\omega) + \Phi_{pp_1}(x,y,\omega) + 2\mathrm{Re}\{\Phi_{pp_1}(x,y,\omega)\} \tag{6.9}$$

Expressing p and p_1 as in Eqs. (1.5) and (6.1), respectively,

$$R_{p_1p}(x,y,\tau) = E\left\{\int_{-\infty}^{\infty}\int \sum_{s=-\infty}^{\infty} \tilde{f}_s\, H_{1,s}(x,y,k_1) \sum_{r=-\infty}^{\infty} \tilde{f}_r\, e^{ik_2x}\, e^{-ir\pi y/b}\right.$$

$$\left. e^{i(k_1t_1 - k_2t_2)U_c}\, dF(k_1)\, dF^*(k_2)\, dk_1\, dk_2\right\} \tag{6.10}$$

$$= \int_{-\infty}^{\infty} \sum_{s=-\infty}^{\infty} f_s\, H_{1,s}(x,y,k)\, e^{ikx}\, e^{-is\pi y/b}\, e^{ikU_c\tau}\, S_p(k)\, dk \tag{6.11}$$

Taking the Fourier transform of Eq. (6.11) and simplifying,

$$\Phi_{pp_1}(x,y,\omega) = e^{i\frac{\omega}{U_c}x}\left\{\sum_{s=-\infty}^{\infty} f_s\, H_{1,s}(x,y,\tfrac{\omega}{U_c})\, e^{-is\pi y/b}\right\} S_p(\omega) \tag{6.12}$$

Similarly,

$$\Phi_{pp}(x,y,\omega) = \sum_{s=-\infty}^{\infty} f_s \; S_p(\omega) \tag{6.13}$$

Combining Eqs. (6.2), (6.12) and (6.13), we find that

$$\Phi_{\hat{p}\hat{p}}(x,y,\omega) = S_p(\omega) \left[\sum_{s=-\infty}^{\infty} f_s \left\{ 1 + |H_{1,s}(x,y,\frac{\omega}{U_c})|^2 + 2\mathrm{Re}\left(e^{i\frac{\omega}{U_c}x} \; e^{-is\pi y/b} \; H_{1,s}(x,y,\frac{\omega}{U_c}) \right) \right\} \right] \tag{6.14}$$

For the one-dimensional case, one obtains

$$\Phi_{\hat{p}\hat{p}}(x,\omega) = S_p(\omega) \left[1 + |H_1(x,\frac{\omega}{U_c})|^2 + 2\mathrm{Re}\{ e^{i\frac{\omega}{U_c}x} \; H_1(x,\frac{\omega}{U_c}) \} \right] \tag{6.15}$$

VII. NUMERICAL RESULTS

In the preceding sections, we have derived expressions for the frequency response functions and the root mean square values of the displacements for a number of structural configurations. In this section, a parametric study will be presented on the effect of the changes in span length, plate thickness,..., etc., on the structural response as represented by the change in frequency response function and the root mean square value. In order to carry out the computations, the pressure spectrum $S_p(\omega)$ has to be specified for which we chose Bull's spectrum as shown in Fig. 7. The coordinates of the figure are $S_p(\omega)\ V/q_0^2\ \delta^*$ and $\omega\delta^*/V$ where

V = free stream velocity

q_0 = dynamic pressure = $\frac{1}{2}\rho V^2$

δ^* = displacement thickness of the boundary layer

The displacement thickness is related to the boundary layer thickness δ by

$$\delta^* = \delta/8 \tag{7.1}$$

and according to Schlichting [25]

$$\delta(x) = 0.37 \times R^{-1/5} \tag{7.2}$$

where x = distance from the leading edge to the location where δ is to be evaluated

$R = Vx/\nu_a$ = Reynold's number

ν_a = kinematic viscosity of the fluid medium (air).

Traditionally the boundary-layer thickness is measured to where the velocity is equal to 0.99 V.

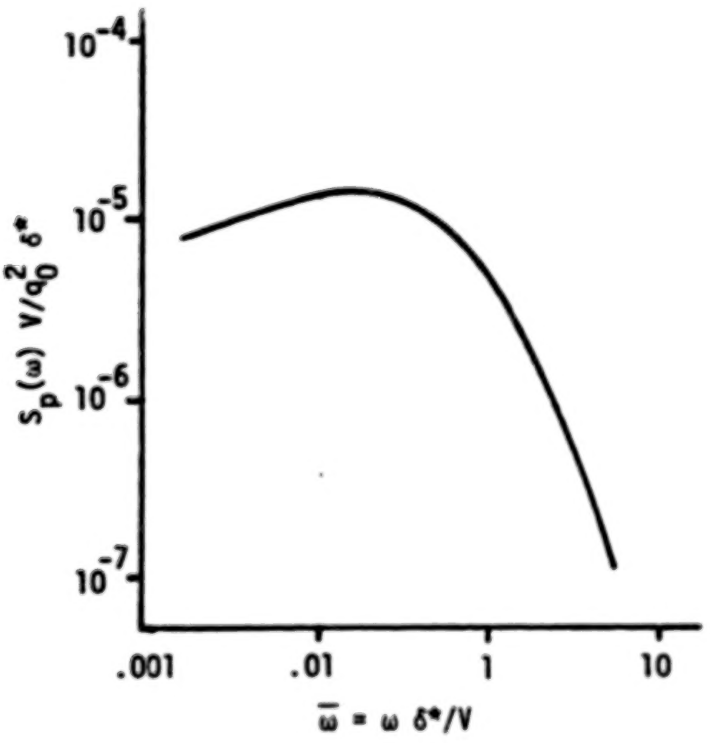

Fig. 7 Bull's Experimental Spectrum

Bull has fitted his experimental data by the expression

$$S_p(\omega) = \frac{q_0^2 \delta^*}{V} \{ 3.7\, e^{-2\bar{\omega}} + 0.8\, e^{-.47\bar{\omega}} - 3.4\, e^{-8\bar{\omega}} \} \times 10^{-5} \qquad (7.3)$$

where $\bar{\omega} = \omega\delta^*/V$ (7.4)

Thus, for a certain flow velocity V, δ^* can be determined and in turn $S_p(\omega)$ can be computed.

Since the vibration is random, a measure of its magnitude is the root mean square value which takes the place of the amplitude of a deterministic vibration. Also, there is lack of a universally agreed upon notion replacing the usual concept of wave length. However, we shall propose the term dominant wave length as a measure of the spatial variation of the total vibration which is computed from the dominant peak frequency of the response spectrum.

The numerical results presented hereafter have been obtained by using a double-precision procedure on the IBM 360/75 digital computer. Some brief comments about the computer programs involved are discussed in Appendix I. These numerical results cover: (i) the one-dimensional and (ii) the two-dimensional cases.

(i) The One-Dimensional Case

The structure which is idealized as a periodic beam is assumed to be made of mylar with the following properties:

ρ (density) = 1.3915×10^3 k_g/m^3

$D = Eh^3/12(1-\nu^2)$

$\nu = .3$ (Poisson's ratio)

h = beam thickness (to be determined).

$E = 2.757 \times 10^9$ N/m^2

$m_b = \rho h$ (mass per unit area)

The physical constants of the air above the beam are

$$\rho_1 = 0.1227 \ k_g/m^3$$

$$a_1 = 340.036 \ m/sec$$

$$\nu_a = 2.88 \times 10^{-5} \ m^2/sec$$

A parametric study using the above values has been carried out to obtain an optimal design, in terms of the following physical quantities, which meets the requirements set forth in reference [5]:

(a) the periodic length ℓ

(b) the beam thickness h

(c) the rotational stiffness k_r

(d) the foundation material properties (k_1, k_2, η_v)

(e) the elasticity of the supports k_t (in the case of elastic support).

As explained in the text, the one-dimensional case includes both infinite and finite beams having supports which can be assumed transversely rigid or elastic. In all of these cases, the computations are made for the mid-span point ($x = \ell/2$). Also, the convection velocity U_c is taken as .8 of the flow velocity V which is chosen as 30.48 m/sec. The different numerical results, corresponding to different cases, are presented in the following subsections.

A. An Infinite Beam on Rigid Supports

Our parametric study has been restricted within the following ranges of values:

$$\ell = (2.54 \sim 6.35) \times 10^{-3} \ m$$

$$h = (5.08 \sim 25.4) \times 10^{-6} \ m$$

$$k_1 = (2.714 \sim 13.57) \times 10^5 \ N/m^3$$

$$k_2 = (2.714 \times 10^5 \sim 2.714) \times 10^{15} \ N/m^3$$

$$\eta_v = 0 \sim 2.714 \times 10^{4} \text{ N-sec/m}^2$$

$$k_r = 4.448 \times 10^{-3} \sim 4.448 \times 10^{-1} \text{ N-m/m/rad.}$$

The results of our study are described below:

(1) A typical response of the beam, represented by the square of the absolute value of the frequency response function, is shown in Fig. 8. It can be seen from this figure that there is a dominant peak occurring at a certain frequency, say f_{max}. The peak region is the dominant part of the structural response and, therefore, our attention will be focused on it.

For the relatively low flow velocity (V = 30.48 m/sec) considered herein, the peak response frequency appears to be near the fundamental natural frequency of the system. An estimate of this natural frequency can be obtained by considering a simply supported beam of length ℓ resting on an elastic foundation of stiffness k_1 (i.e., $k_2 = \infty$). The natural frequency of the nth mode is given by

$$f_n = \frac{1}{2\pi}\sqrt{\frac{D(n\pi/\ell)^2 + k_1}{m_b}} \tag{7.5}$$

If we use the values:

$$\ell = 3.81 \times 10^{-3} \text{ m}$$

$$h = 5.08 \times 10^{-6} \text{ m}$$

$$k_1 = 2.714 \times 10^{5} \text{ N/m}^3$$

then the fundamental natural frequency f_1 is approximately equal to 990 Hz. The peak frequency f_{max} computed by using the above ℓ, h and k_1 values as seen in Figs. 8 and 10 is 900 Hz. The slight discrepancy between 990 and 900 is due to the fact that other factors which affect f_{max} have not been included in Eq. (7.5). Such factors are the convection velocity, the rotational stiffness, and the interaction between neighboring spans.

(2) Within the range of parameters investigated, the dominant wave component is found to be associated with an n value between -2 and 2. Some samples of the coefficients A_n's indicative of relative importance of different wave components are shown in Tables 1-3. It is important to mention that these A_n's were computed from Eq. (2.33) or its simplified versions and by truncating the number of simultaneous equations to 16 (i.e., N = 8), It was found from the computations that a minimum of N = 8 was necessary to obtain a reasonable accuracy especially at or near the peak frequency.

(3) The change in the periodic length, ℓ, greatly affects the structural response including its amplitude, peak frequency, and the dominant wave length. As expected, an increase in ℓ generally leads to a reduction in the peak frequency and an increase in the amplitude. The wave length of the nth wave component is related to the periodic length ℓ as follows:

$$\frac{\lambda_n}{\ell} = \frac{1}{n + \frac{f_{max}\,\ell}{U_c}} \tag{7.6}$$

where we assumed that this component contributed to the response at the peak frequency f_{max}. Since the dominant terms are those corresponding to n between -2 and 2, the design criterion concerning the wave length should be checked against the wave length of each of these components. For instance, when $n = \mp 2$, the absolute value of the R.H.S. of Eq. (7.6) is approximately equal to 1/2 (since the value of $f_{max}\,\ell/U_c$ is small within the range of values being considered). Therefore, the corresponding wave lengths $\lambda_{-2,2}$ are approximately equal to $\ell/2$. Consequently, these two wave lengths can easily satisfy the wave length requirement ($\leq 2.54 \times 10^{-3}$ m

for values of ℓ ranging from (2.54 to 3.81) x 10^{-3}m. The term which poses a great difficulty in meeting the wave length requirement is A_{-1}. The wave length associated with this term is obtained from Eq. (7.6) (by putting n equal to -1):

$$\frac{\lambda_{-1}}{\ell} = \frac{1}{-1 + \frac{f_{max}\,\ell}{U_c}} \tag{7.7}$$

The absolute value of the R.H.S. of Eq. (7.7) is always greater than one. Therefore, to obtain the desired wave length, ℓ has to be less than 2.54 x 10^{-3}m. However, such a small ℓ would increase f_{max} beyond the desired frequency range. As a compromise we have chosen ℓ as 3.81 x 10^{-3}m for this parametric study (which might not satisfy the wave length requirement but it keeps f_{max} within the desired frequency range).

(4) The thickness h has a great effect on the amplitude and on the peak frequency of the response. An increase in h shifts f_{max} to a higher value and generally leads to a decrease in the amplitude.

(5) The increase in the stiffness k_1 reduces the amplitude and increases the peak frequency f_{max}. (See Fig. 9)

(6) The change in the stiffness k_2 does not affect the peak frequency appreciably. However, an increase in k_2 increases the amplitude. The limiting case of an infinite k_2 is simply that of an elastic foundation of stiffness k_1. The effect of the change of k_2 on the response is shown in Fig. 10.

(7) The increase in the damping coefficient η_v, for the range of values used, leads to an increase in the amplitude without any significant change in the peak frequency. (See Fig. 11) The structural response corresponding to the special case of $\eta_v = 0$ is shown in Fig. 12.

(8) An increase in the rotational stiffness k_r increases the peak frequency and slightly increases the amplitude. (See Fig. 13)

Some representative root mean square values of the response, and the wave lengths of the dominant components are shown in Table 4. As can be seen from this table, the root mean square value, $W_{r.m.s.}$, is smaller than the desired values for most of the cases shown. Also, the wave length λ_{-1} is always higher than the desired value for the reasons we explained before.

It should be noted that, unless stated otherwise on the figure itself, the following values have been used in computing the response shown in Figures 8 through 13:

$$\ell = 3.81 \times 10^{-3} \text{ m}$$

$$h = 5.08 \times 10^{-6} \text{ m}$$

$$k_1 = 2.714 \times 10^{5} \text{ N/m}^3$$

$$k_2 = 2.714 \times 10^{5} \text{ N/m}^3$$

$$k_r = 4.448 \times 10^{-3} \text{ N-m/m/rad.}$$

$$\eta_v = 2.714 \times 10^{3} \text{ N-sec/m}^3$$

$$\eta_r = .01$$

$$\eta_b = 0$$

B. An Infinite Beam on Transversely Elastic Supports

The only difference between the structural configuration of the beam considered here and that of an infinite beam on transversely rigid supports is in the introduction of transversely elastic springs, each characterized by a spring constant k_t, at the supports. Therefore, in this section, we are mainly concerned with the effect of these transversely elastic supports on the structural response. Such effect is shown in Figs. 14-17. Figure 14 shows a typical response of the beam over a wide range of frequencies, while Figs. 15-17 focus on the peak region only. Based on these figures,

we conclude that:

(1) The elastic spring constant, k_t, has a considerable effect on the location of the peak frequency. As k_t increases, the peak frequency is shifted to a higher value until it approaches that of the transversely rigid-support case (i.e., $k_t = \infty$). Thus, by choosing a small k_t, it is possible to reduce the periodic length to as small as 2.54×10^{-3}m so that the requirement for wave length can be satisfied without raising f_{max} to outside the desired frequency range.

(2) The amplitude of the response increases as the value of k_t decreases. Therefore, a suitable choice of k_t can help in bringing the amplitude to the desired value.

Typical values of the root mean square displacements and the wave length of the dominant terms are shown in Table 5. It can be clearly seen that, except for the first one, the amplitude and the frequency of all cases presented fit the desired ranges. Moreover, the wave length λ_{-1} of the component $n = -1$ is very close to the desired value of 2.5×10^{-3}m (the difference is approximately 1%).

It is to be noted that the following values have been used in computing the response shown in Figs. 14-17:

$$\ell = 2.54 \times 10^{-3}\text{m}$$

$$h = 5.08 \times 10^{-6}\text{m}$$

$$k_r = 4.448 \times 10^{-3} \text{ N-m/m/rad.}$$

$$\eta_v = 2.714 \times 10^{3} \text{ N-sec/m}^3$$

$$\eta_r = .01$$

$$\eta_b = 0.0$$

Table 1. Sample of the Coefficients A_n is (in meters)

n	-8	-7	-6	-5	-4	-3	-2	-1	0 *
$Re(A_n)$	4.26×10^{-5}	6.35×10^{-5}	1.03×10^{-4}	1.85×10^{-4}	3.88×10^{-4}	1.19×10^{-3}	-1.06×10^{2}	-1.75×10^{-3}	1.29×10^{-2}
$Im(A_n)$	-2.26×10^{-3}	-3.43×10^{-3}	-5.58×10^{-3}	-1.03×10^{-2}	-2.26×10^{-3}	-7.5×10^{-2}	5.5×10^{-1}	1.5×10^{-1}	-8.09×10^{-1}
n	1	2	3	4	5	6	7	8	-
$Re(A_n)$	6.6×10^{-3}	-7.44×10^{-3}	-9.65×10^{-4}	-3.63×10^{-4}	-1.78×10^{-4}	-1.01×10^{-4}	-6.09×10^{-5}	-4.19×10^{-5}	-
$Im(A_n)$	-1.75×10^{-1}	3.11×10^{-1}	4.04×10^{-2}	1.54×10^{-2}	7.77×10^{-3}	4.47×10^{-3}	2.84×10^{-3}	1.9×10^{-3}	-

$\ell = 3.81 \times 10^{-3}$ m; $h = 5.08 \times 10^{-6}$ m; $\eta_v = 2.714 \times 10^{3}$ N sec/m^3

$k_1 = 2.714 \times 10^{5}$ N/m^3; $k_2 = 2.714 \times 10^{5}$ N/m^3; $k_r = 4.448 \times 10^{-3}$ N-m/m/rad; $\eta_r = .01$

f = 898 HZ (peak frequency) ; * dominant term

Table 2. Sample of the Coefficients A_n's (in meters)

n	-8	-7	-6	-5	-4	-3	-2	-1*	0
$Re\{A_n\}$	-2.08×10^{-5}	-3.04×10^{-5}	-5.18×10^{-5}	-9.14×10^{-5}	-1.93×10^{-4}	-5.25×10^{-4}	-2.79×10^{-3}	8.63×10^{-3}	-8.05×10^{-4}
$Im\{A_n\}$	5.334×10^{-8}	8.128×10^{-8}	1.33×10^{-7}	2.33×10^{-7}	4.57×10^{-7}	1.24×10^{-6}	6.09×10^{-6}	1.3×10^{-5}	-2.6×10^{-5}
n	1	2	3	4	5	6	7	8	-
$Re\{A_n\}$	5.5×10^{-3}	8.89×10^{-4}	3.81×10^{-4}	1.18×10^{-4}	6.29×10^{-5}	3.73×10^{-5}	2.4×10^{-5}	1.62×10^{-5}	-
$Im\{A_n\}$	3.68×10^{-5}	-3.73×10^{-6}	-9.6×10^{-7}	-4.01×10^{-7}	-2.05×10^{-7}	-1.10×10^{-7}	-7.5×10^{-8}	-5.08×10^{-8}	-

$\ell = 2.54 \times 10^{-3}$ m; $h = 5.08 \times 10^{-6}$ m; $\eta_v = 2.714 \times 10^4$ N. sec/m^3

$k_1 = 2.714 \times 10^5$ N/m^3; $K_2 = 2.714 \times 10^5$ N/m^3; $k_r = 4.448 \times 10^{-3}$ N-m/m/rad; $\eta_r = .01$

f = 898 HZ (not near a peak) ; * dominant term

Table 3. Sample of the Coefficients A_n's (in meters)

n	-8	-7	-6	-5	-4	-3	-2	-1	0
$Re\{A_n\}$	-2.49×10^{-3}	-3.81×10^{-3}	-6.09×10^{-3}	-1.1×10^{-2}	-2.36×10^{-2}	-6.59×10^{-2}	-4.26×10^{-1}	6.19×10^{-1}	1.0287
$Im\{A_n\}$	6.85×10^{-4}	1.067×10^{-3}	1.72×10^{-3}	3.04×10^{-3}	6.6×10^{-3}	1.82×10^{-2}	1.193×10^{-1}	-1.73×10^{-1}	3.20×10^{-1}
n	1*	2	3	4	5	6	7	8	-
$Re\{A_n\}$	-1.27	1.09×10^{-1}	3.23×10^{-2}	1.42×10^{-2}	7.54×10^{-3}	4.47×10^{-3}	2.87×10^{-3}	1.95×10^{-3}	-
$Im\{A_n\}$	3.55×10^{-1}	-3.06×10^{-2}	-9.04×10^{-3}	-3.96×10^{-3}	-2.108×10^{-3}	-1.24×10^{-3}	-8.05×10^{-4}	-5.46×10^{-3}	-

$\ell = 2.54 \times 10^{-3}$ m $h = 5.08 \times 10^{-6}$ m $\eta_v = 0.0$ N sec/m^3

$k_1 = 2.714 \times 10^5$ N/m^3 $k_2 = \infty$ N/m^3 $K_r = 4.448 \times 10^{-3}$ N-m/m/rad; $\eta_r = .01$

f = 1585 HZ(peak frequency); * dominant term

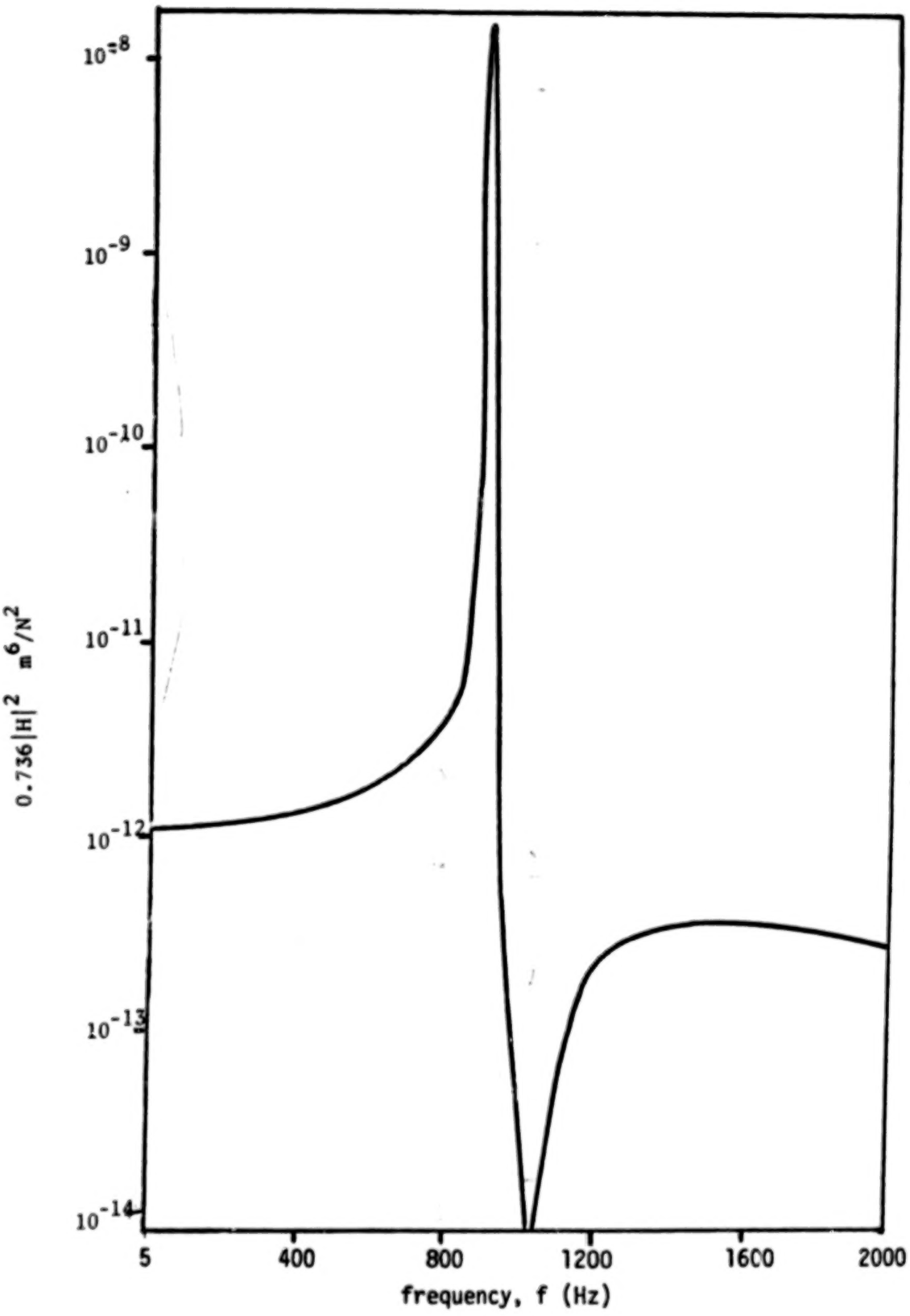

Fig. 8 Response of an Infinite Beam (Transversely Rigid Supports)

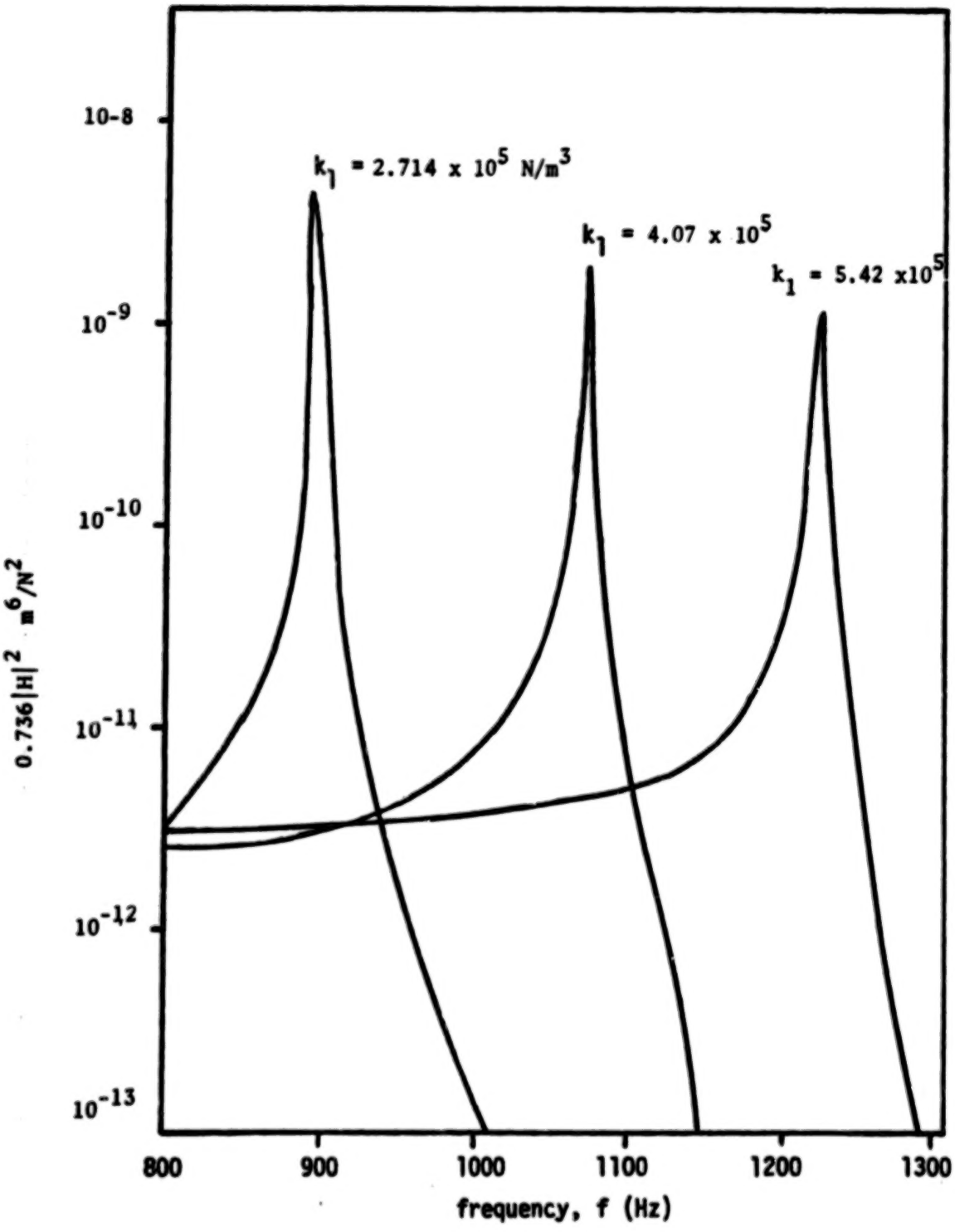

Fig. 9 Effect of k_1 on the Response

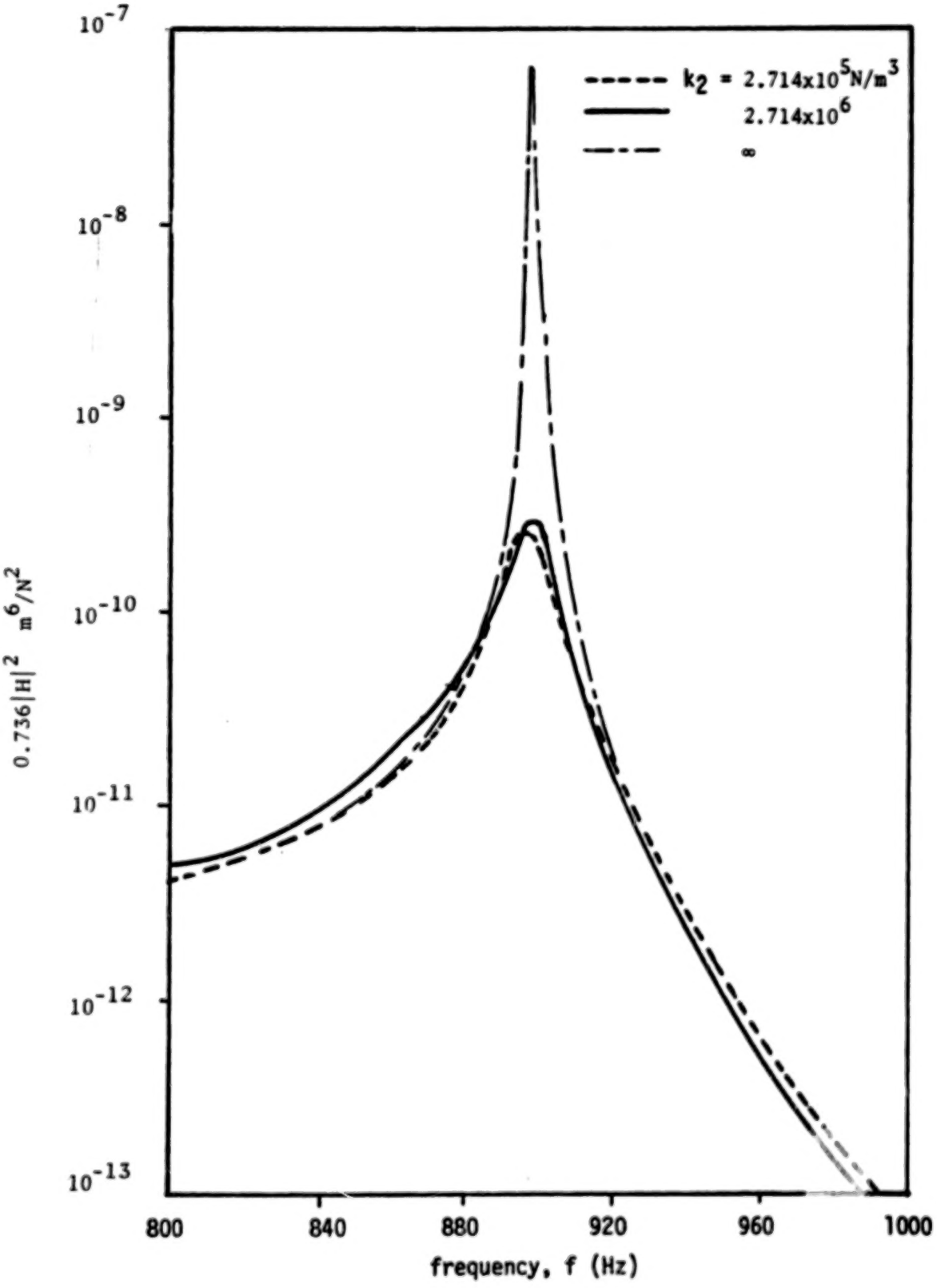

Fig. 10 Effect of k_2 on the Response

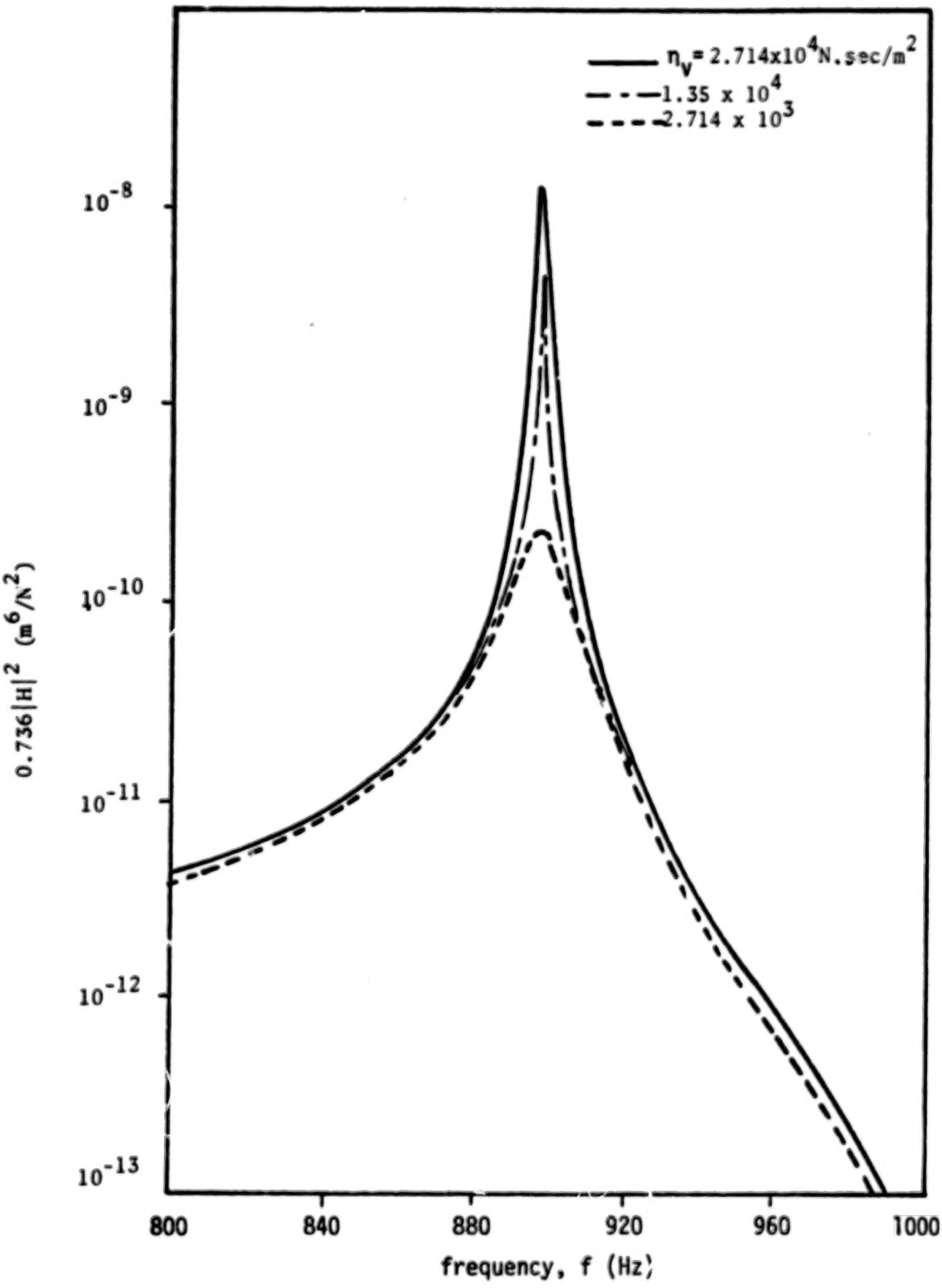

Fig. 11 Effect of η_v on the Response

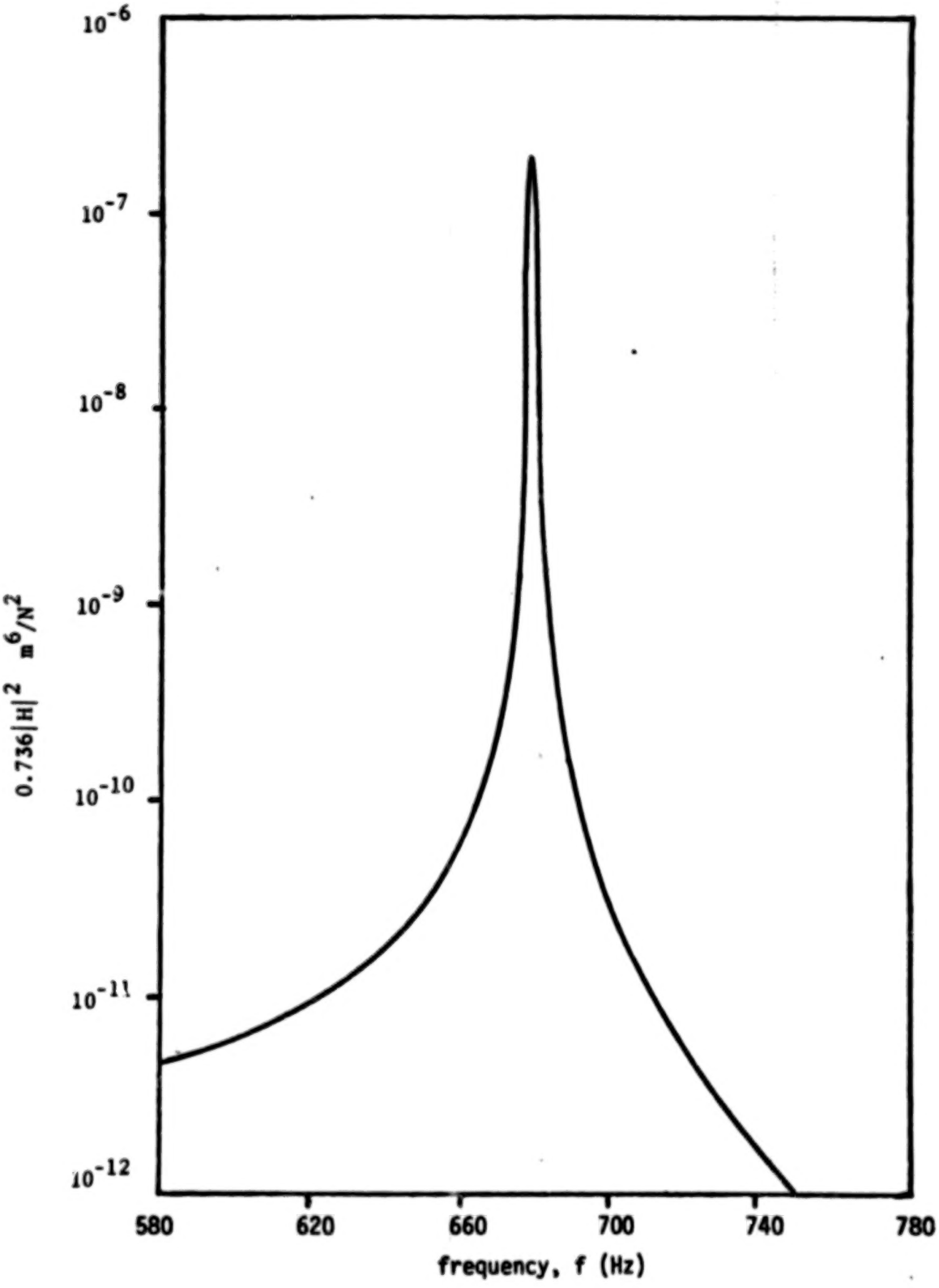

Fig. 12 Response of the Beam When the Foundation is Elastic ($n_v = 0$)

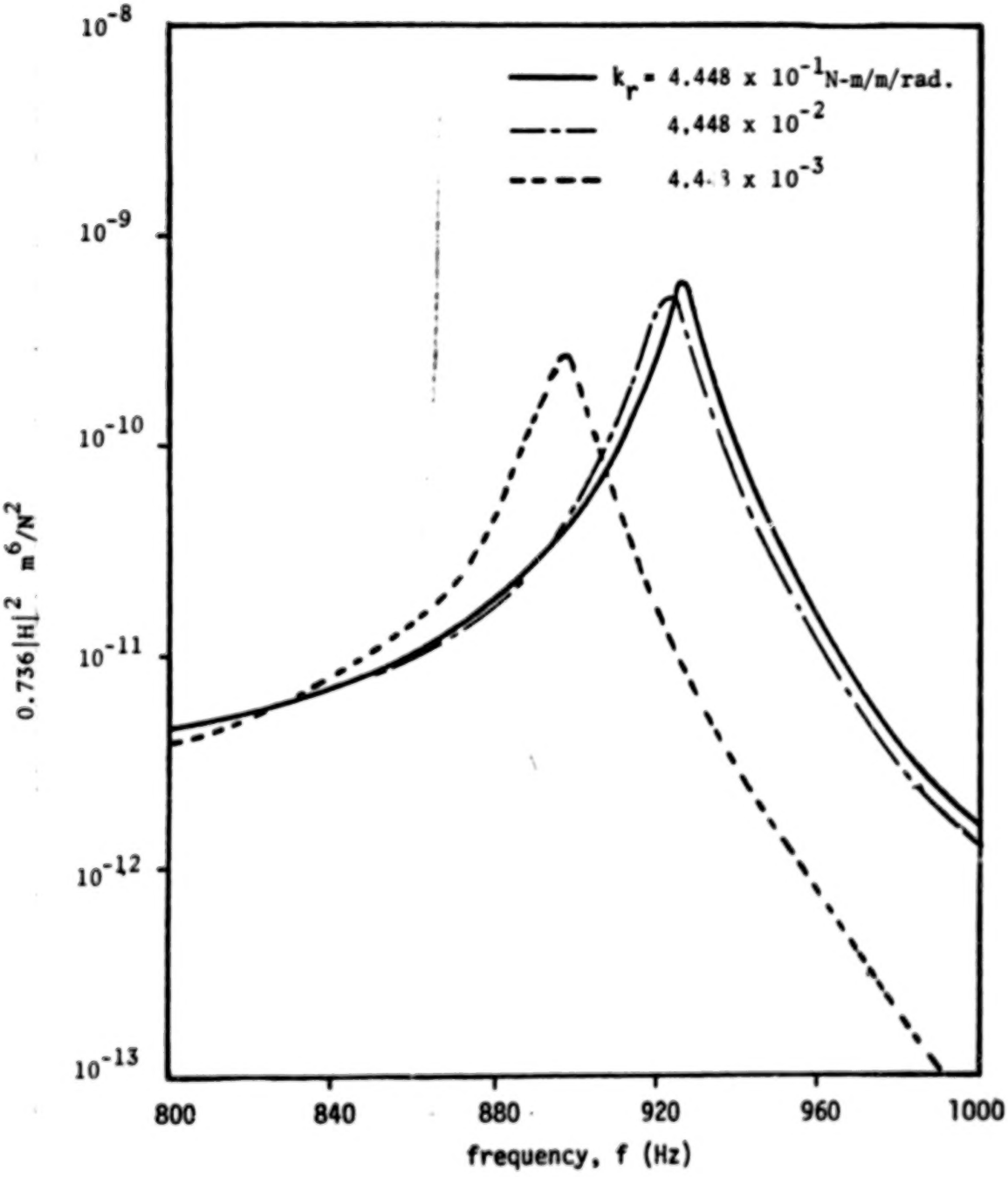

Fig. 13 Effect of k_r on the Response

Table 4. Sample of Displacements and Wave Length of an Infinite Beam on Transversely Rigid Supports

K_1 N/m^3	K_2 N/m^3	η_r N-sec/m^3	K_T N-m/m/rad	f_{max} HZ	Peak range HZ	$W_{r.m.s.}$ m	$\lvert\lambda_{-1}\rvert$ m	$\lvert\lambda_{-2}\rvert$ m
5.42×10^5	2.74×10^5	1.35×10^4	4.448×10^{-3}	1223	1200-1252	5.53×10^{-6}	4.7×10^{-3}	2.1×10^{-3}
4.071×10^5	"	"	"	1073	1050-1102	6.73×10^{-6}	4.57×10^{-3}	2.07×10^{-3}
2.714×10^5	"	"	"	898	850-950	9.78×10^{-6}	4.42×10^{-3}	2.03×10^{-3}
"	"	2.714×10^3	"	898	875-927	2.08×10^{-5}	"	"
"	2.714×10^6	"	"	897	875-927	4.11×10^{-6}	"	"
"	2.714×10^5	0	"	679	650-702	3.56×10^{-5}	4.24×10^{-3}	2.0×10^{-3}
"	"	2.714×10^3	4.448×10^{-2}	924	850-950	5.76×10^{-6}	4.45×10^{-3}	2.052×10^{-3}
"	"	2.714×10^3	4.448×10^{-1}	927	900-952	5.58×10^{-6}	4.45×10^{-3}	2.052×10^{-3}

$\ell = 3.81 \times 10^{-3}$ m ; $h = 5.08 \times 10^{-6}$ m ; $\eta_r = .01$

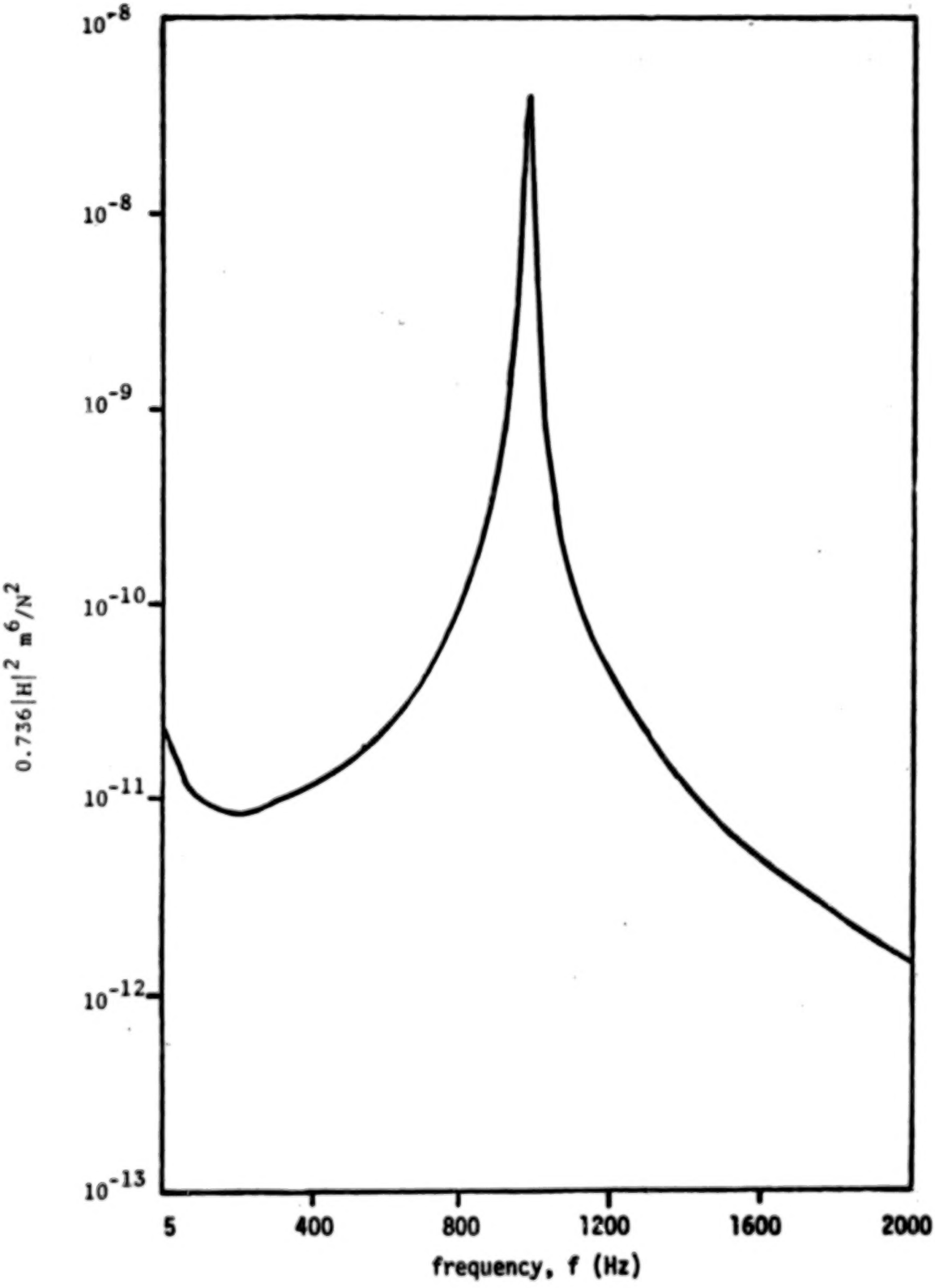

Fig. 14 Response of an Infinite Periodic Beam (Transversely Elastic Supports)

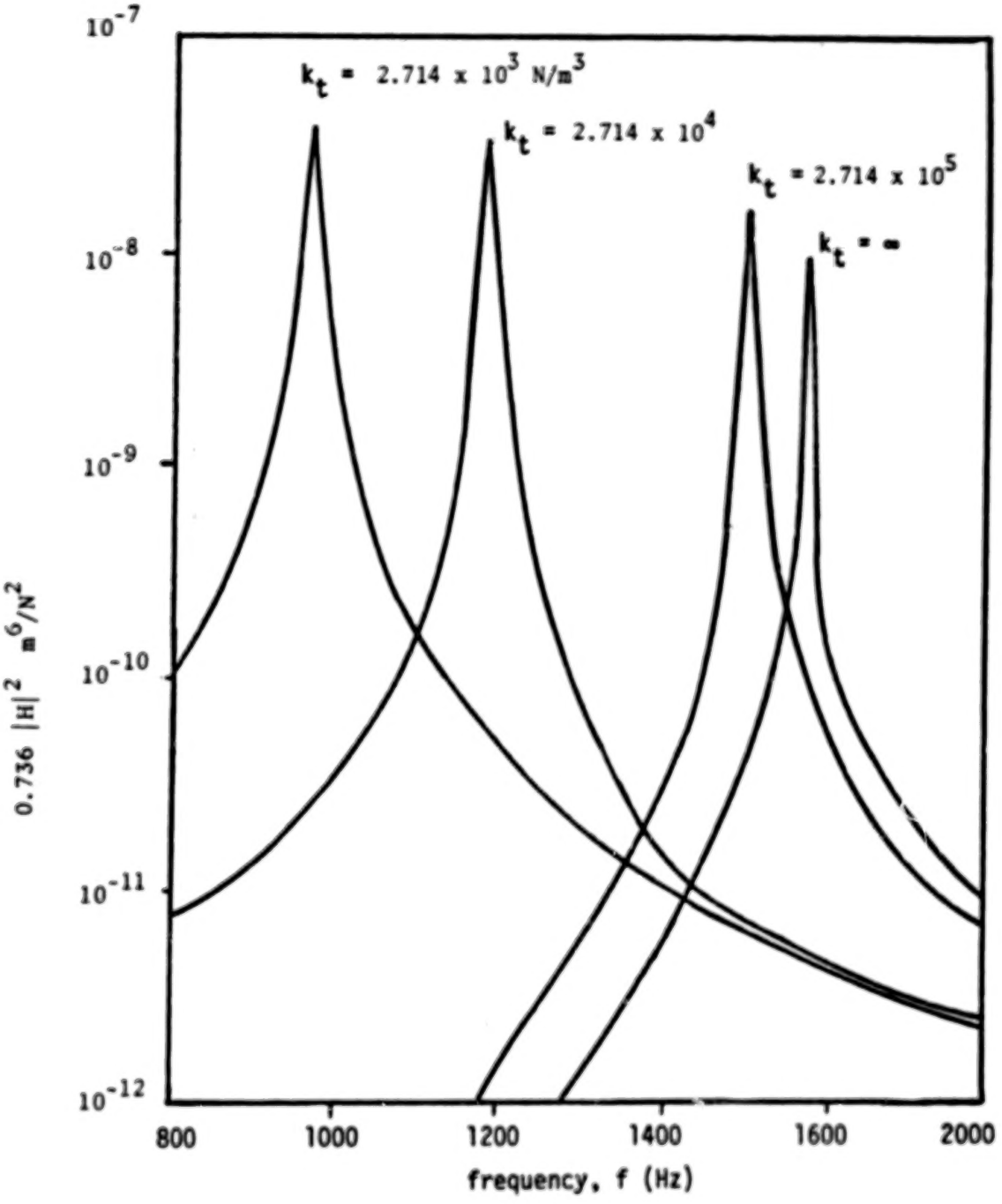

Fig. 15 Effect of k_t on the Response

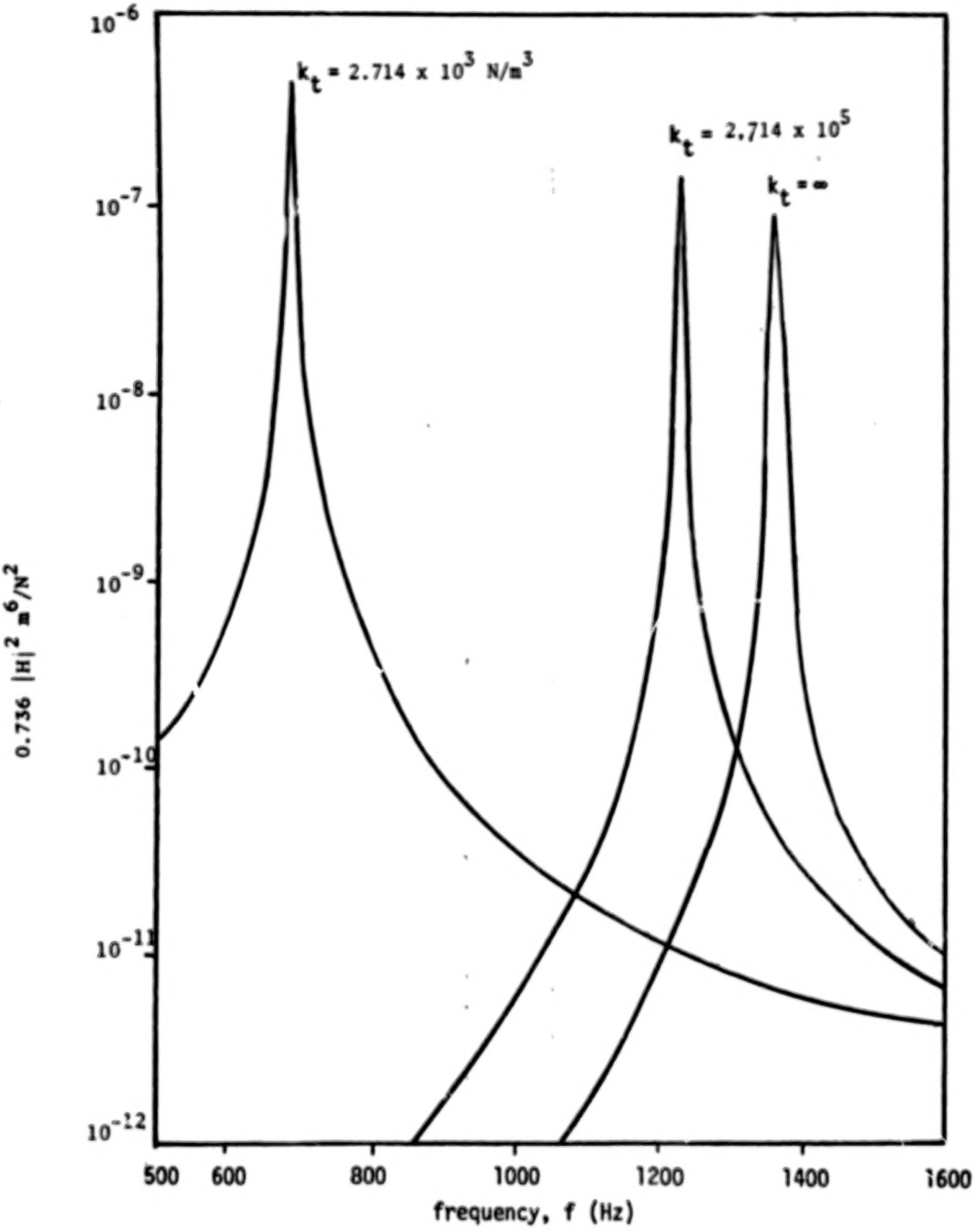

Fig. 16 Response of an Infinite Beam on an Elastic Foundation ($n_v = 0$)

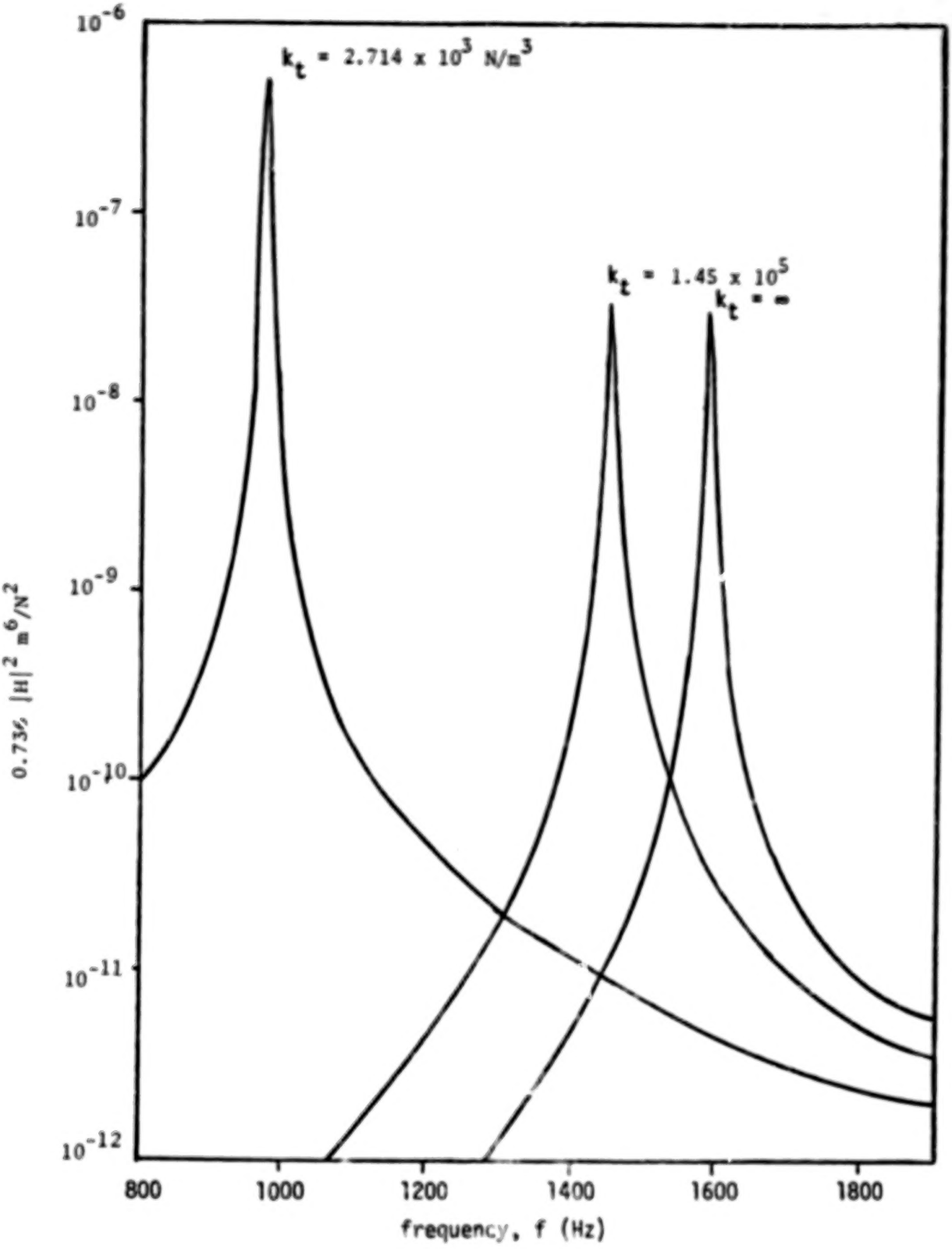

Fig. 17 Response of an Infinite Beam on an Elastic Foundation (k_2 = ∞)

Table 5. Sample of Displacements and Wave Lengths of an Infinite Beam on Transversely Elastic Supports

k_2 N/m^3	η_v N-sec/m^3	k_r N-m/m/rad	k_t N/m^3	f_{max} Hz	Peak range Hz	$W_{r.m.s.}$ m	$\lvert\lambda_{-1}\rvert$ m	$\lvert\lambda_{-2}\rvert$ m
2.714×10^5	2.714×10^3	4.448×10^{-3}	2.714×10^5	1513	1475-1539	2.52×10^{-5}	2.997×10^{-3}	1.38×10^{-3}
"	"	"	2.714×10^4	1189	1160-1210	4.318×10^{-5}	2.895×10^{-3}	1.35×10^{-3}
"	"	"	2.714×10^3	972	900-950	4.6×10^{-5}	2.82×10^{-3}	1.34×10^{-3}
"	2.714×10^4	"	2.714×10^2	942	925-975	5.1×10^{-5}	2.79×10^{-3}	1.33×10^{-3}
"	0	"	2.714×10^3	695	675-725	1.678×10^{-4}	2.71×10^{-3}	1.32×10^{-3}
"	0	"	2.714×10^3	975	950-1000	1.65×10^{-4}	2.82×10^{-3}	1.34×10^{-3}

$\ell = 2.54\times10^{-3}$ m; $h = 5.08\times10^{-6}$ m; $k_1 = 2.714\times10^5$ N/m^3, $\eta_v = .01$

C. Finite Periodic Beam

In this section, numerical results of the structural response of a 5-span periodic beam will be presented. These results correspond to two cases: (a) the interior supports are transversely rigid, (b) the interior supports are transversely elastic. In both cases, each of the end supports is assumed to be rigid in the transverse direction, and to possess a rotational stiffness k_r. The physical data used in the computations for these cases are the same as those used previously for the corresponding infinitely-long beams. Also, the response referred to is for the midpoint of the first span.

(a) Transversely Rigid Interior Supports

Comparisons between the structural response of a finite beam and that of an infinitely long beam, other physical data being identical, are presented in Figs. 18-20. Each of these figures shows the square of the absolute value of the frequency response function vs. the frequency. Figure 18 shows the comparison when a viscoelastic foundation is used for both finite and infinite beams, while in the case of Figs. 18 and 20 the foundation is purely elastic.

As expected, the response curve for each finite beam contains multiple peaks clustered in frequency zones. Within the frequency range shown in the figures, the response peaks are clustered roughly in the first free-wave propagation zone [15]. The number of peaks in each zone is expected to be equal to the number of spans of the finite periodic beam. However, it is possible that some of those peaks might not appear because of the amount of damping present in the system or because of the choice of a coarse frequency interval in the computations.

TABLE OF CONTENTS

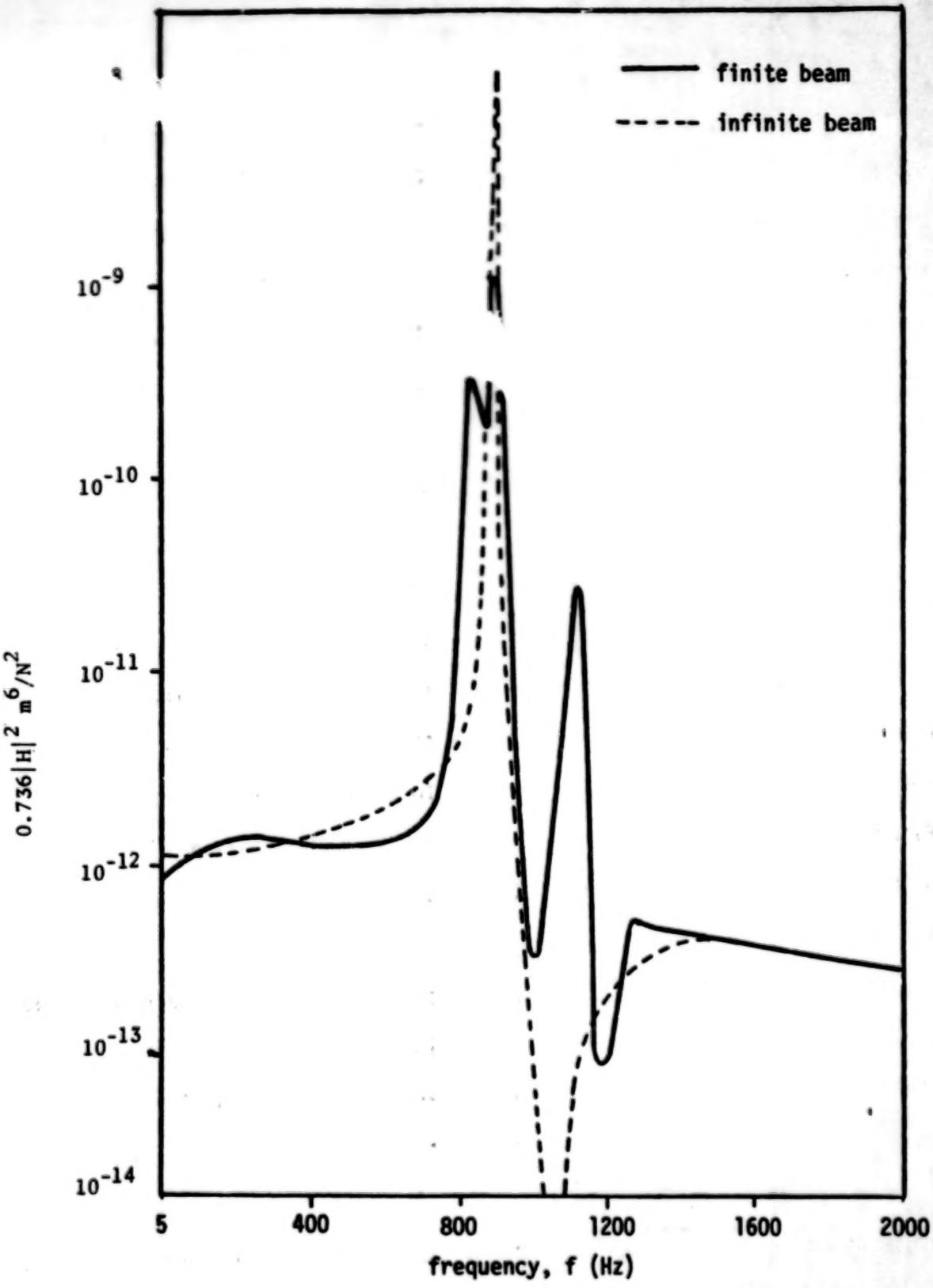

Fig. 18 Response of a Periodic Beam on a Viscoelastic Foundation (Transversely Rigid Supports)

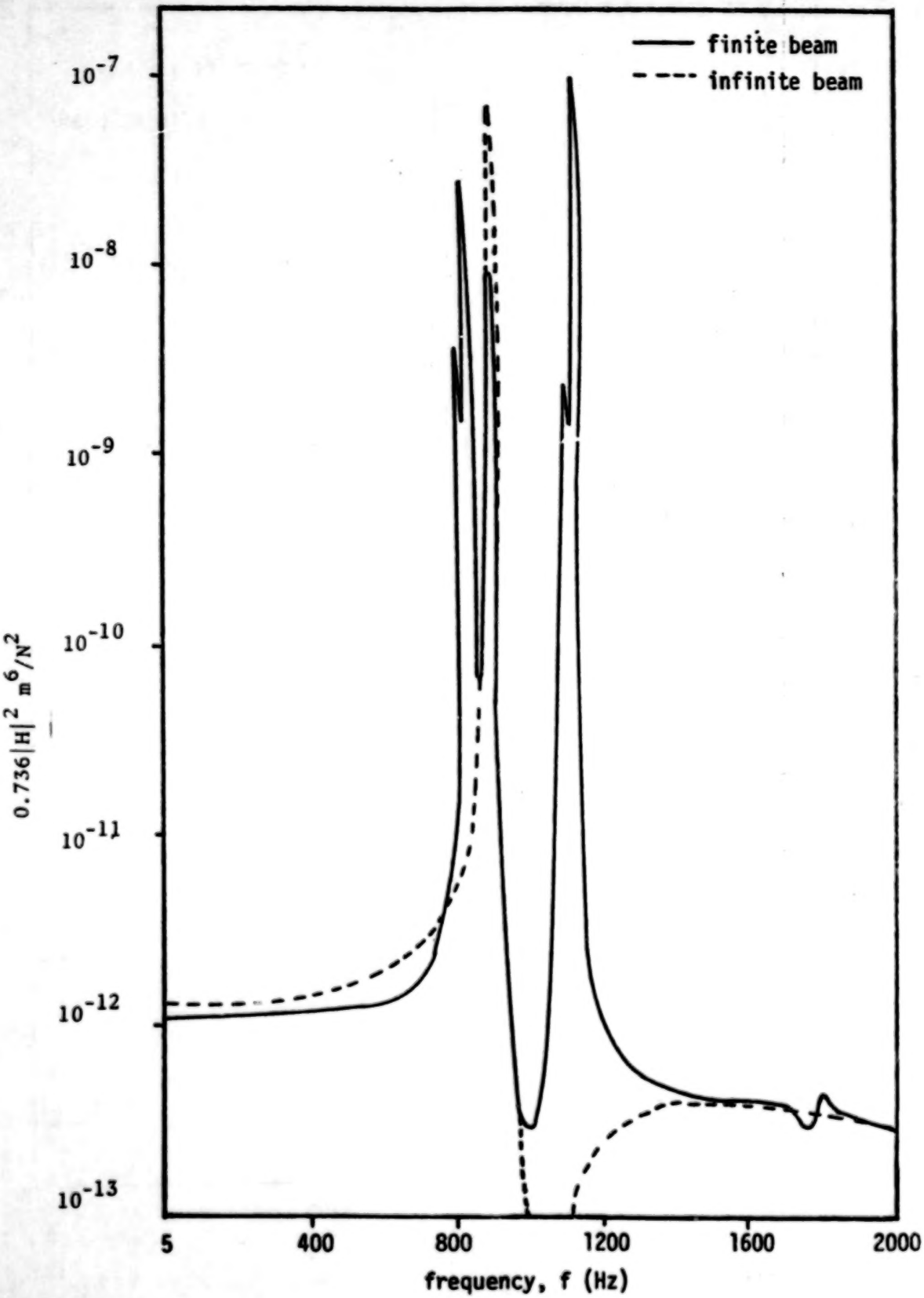

Fig. 19 Response of a Periodic Beam (Transversely Rigid Supports, $k_2 = \infty$)

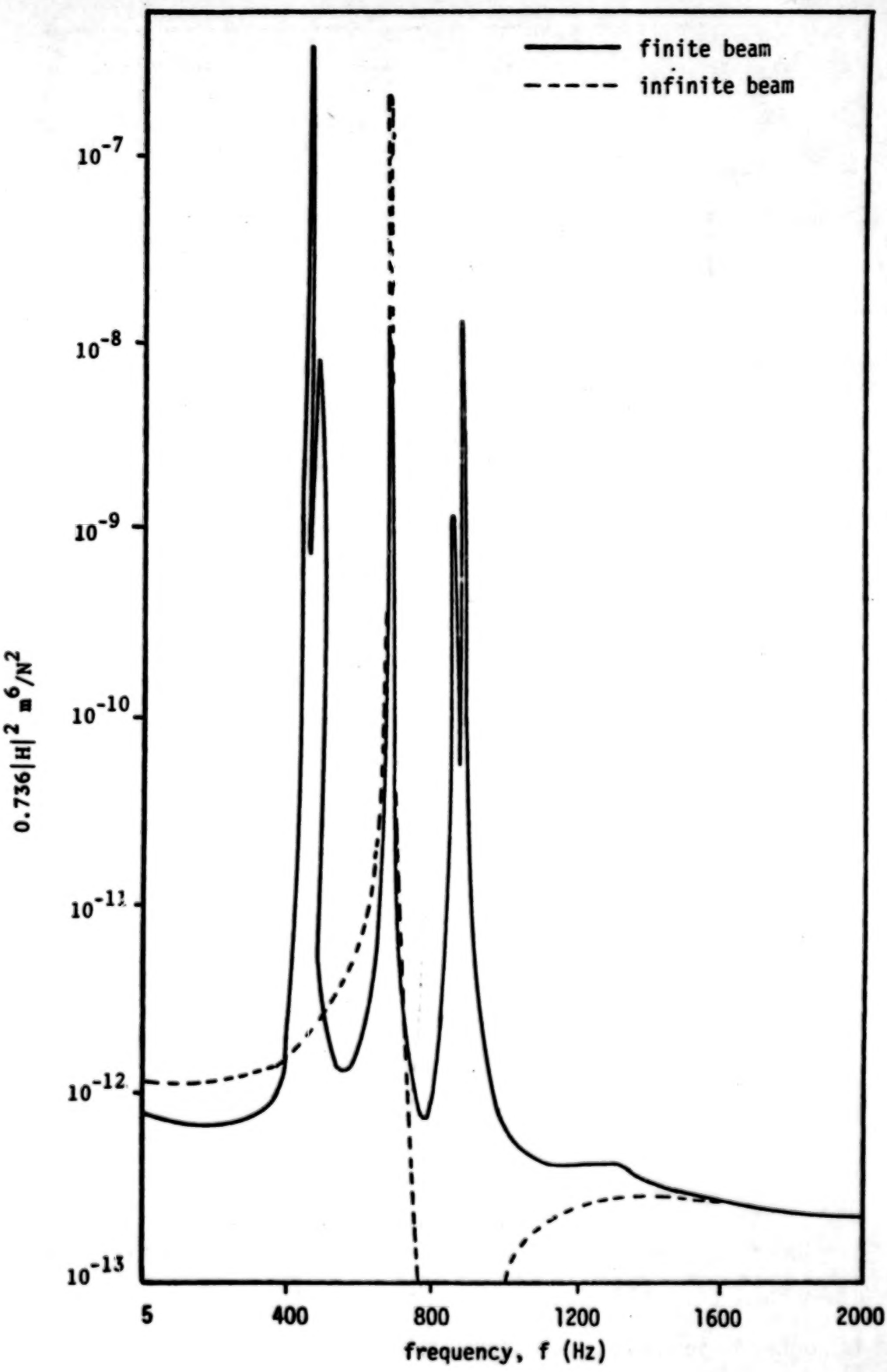

Fig. 20 Response of a Periodic Beam (Transversely Rigid Supports, $\eta_v = 0$)

(b) Transversely Elastic Interior Supports

In this case, there are four free waves which might propagate in the finite beam, compared to only two free waves in the case of transversely rigid-support case. This increase in the number of waves, and the ill-conditioned matrices involved make the computations more complicated. More specifically, the vandermonde matrix given in Eq. (3.53) and the system of simultaneous equations relating the unknowns w_k's (i.e., Eq. (3.66)) are very ill-conditioned (meaning a small error in the elements of these matrices would magnify leading to much larger errors). Although there are special techniques to deal with such matrices (see Appendix I), the computational accuracy can suffer greatly from any numerical errors which might arise in the course of computations.

A comparison between the structural response of a finite beam and that of an infinite one, other physical data being identical, is shown in Fig. 21. Only the response near and within the first free-wave propagation zone is shown in the figure. Again, the response contains multiple peaks clustered roughly within this free-wave propagation zone. However, the number of peaks as shown in Fig. 21 exceeds the expected number, that is the number of spans of the finite beam. It is believed that some of those peaks have resulted from the numerical errors which might have occurred due to the ill-conditioned matrices already mentioned.

(ii) The Two-Dimensional Case

In this case, the panel is assumed to be made of mylar of which the physical properties have been previously mentioned in connection with the one-dimensional case. The wires are assumed to be made of steel which has the following properties:

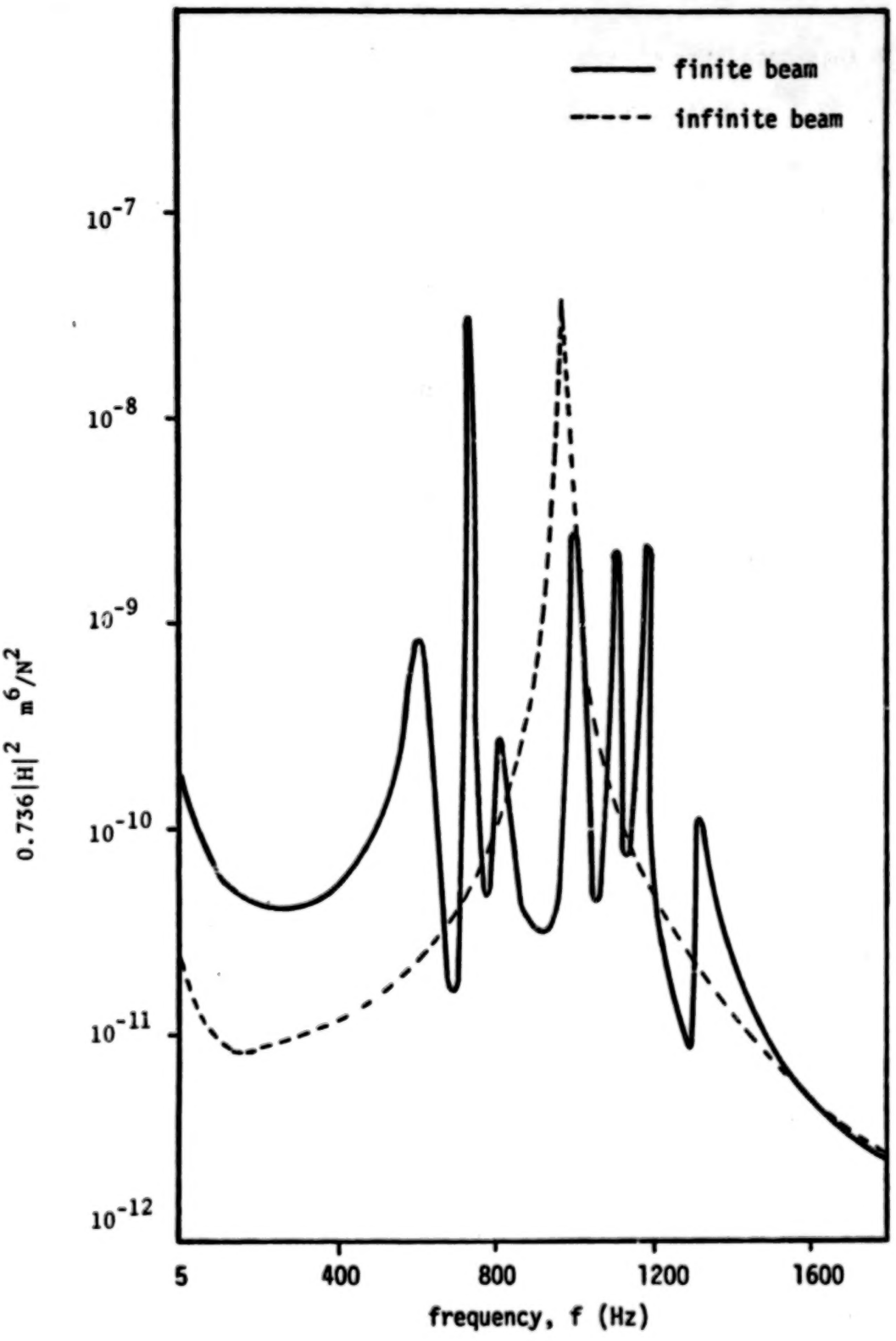

Fig. 21 Response of a Periodic Beam (Transversely Elastic Supports)

$$G = 7.92 \times 10^{10} \text{ N/m}^2$$

$$\rho_w = 7.68 \times 10^{3} \text{ kg/m}^3$$

$$\sigma_a = 9.65 \times 10^{7} \text{ N/m}^2$$

$$E_w = 2.068 \times 10^{11} \text{ N/m}^2$$

Again, a parametric study using the above values has been carried out to obtain an optimal design, in terms of the following physical quantities, which meets the requirements set forth in reference [5]:

(1) the periodic length ℓ

(2) the panel thickness h

(3) the panel width b

(4) the wire diameter D

(5) the cavity depth d

(6) the tension applied to each wire, T.

Before presenting the results of our parametric study, some introductory remarks might be helpful:

(a) In light of the results of the parametric study carried out for the one-dimensional case, we have chosen ℓ as 2.54×10^{-3}m. This value of ℓ is expected to be near the "best" choice for meeting the wave length requirement and, at the same time, keeping the peak region within the desired frequency range.

(b) The wire diameter has been chosen as proportional to the panel thickness h, namely

$$D = \gamma h \tag{7.8}$$

The proportionality constant γ can be chosen arbitrarily but one should keep in mind that a large γ would make the wires act as rigid supports (a reasonable choice might be 2-6).

(c) To make sure that the allowable stress of the wire material, σ_a, would not be exceeded, the tension T has been chosen as

$$T \leq \sigma_a A_W . \tag{7.9}$$

(d) It is to be noted that all computations for structural response have been carried out at the midpoint ($x = \ell/2$, $y = b/2$) of the first panel. Also, the number of modes has been chosen as 5 in the x-direction and 14 in the y-direction.

(e) For simpler representation of the numerical results, let us rewrite Eq. (5.4) as

$$\Phi_w(x, y, \omega) = \left|\hat{H}(x, y, \frac{\omega}{U_c})\right|^2 S_p(\omega) \tag{7.10}$$

where $\hat{H}$ is the "total" frequency response function of the panel and is given by

$$\left|\hat{H}(x, y, \omega)\right|^2 = \sum_{s=-\infty}^{\infty} \left|H_s(x, y, \frac{\omega}{U_c})\right|^2 f_s . \tag{7.11}$$

The results of our parametric study are summarized as follows:

(1) A typical relationship between $|\hat{H}|^2$ and the frequency f is shown in Fig. 22 (peaks are not drawn to scale). As can be seen, there are two peak regions: the first one occurs at a very low frequency range while the second one occurs at a much higher range. When the values (in meters), $h = 8.98 \times 10^{-6}$, $\ell = 2.54 \times 10^{-3}$, $b = 1.778 \times 10^{-1}$ and $d = 2.54 \times 10^{-2}$ were used in the computations, the first peak region was found around 10 Hz and the second one near 990 Hz.

To explain the occurrence of these two peak regions, consider a simpler case of a panel of length ℓ and width b which is simply supported along all sides and vibrating in vacuum. Assuming a sine series solution in both directions, the natural frequency for the nth mode in the x-direction and the mth mode in the y-direction for such a panel is given by

$$f_{n,m} = \frac{\pi}{2}\sqrt{\frac{D}{\rho_p h}}\left\{\left(\frac{n}{\ell}\right)^2 + \left(\frac{m}{b}\right)^2\right\} \qquad (7.12)$$

where ρ_p is the panel mass per unit area ($= m_p/h$). Using the values for h, ℓ, b and d mentioned above in Eq. (7.12) gives

$$f_{n,m} = 9.12\ \{100n^2 + (m^2/49)\}$$

The first few natural frequencies (i.e., n = 1) are all very close to 912 Hz. Therefore, the second peak region in Fig. 22 is mainly due to the panel resonance. The presence of the external flow and the cavity appears to result in only minor shift in resonance frequency.

Secondly, if we consider a simply supported wire of length b, area A_w and subjected to a tensile force T, then the natural frequency of the mth mode can be computed from

$$f_m = \frac{m}{2b}\sqrt{\frac{T}{\rho_w A_w} + \frac{E_w I_w}{\rho_w A_w}\left(\frac{m\pi}{b}\right)^2} \qquad (7.13)$$

For a wire diameter of .001 inches, the second term under the square root sign of Eq. (7.13) is much smaller than the first one. Therefore,

$$f_m \simeq \frac{m}{2b}\sqrt{\frac{T}{\rho_w A_w}} \leq \frac{m}{2b}\sqrt{\frac{\sigma_a}{\rho_w}} = 3.15\ m$$

For $1 \leq m \leq 14$, the natural frequencies have a range 3-45 Hz. This means that the first peak region in Fig. 22 is mainly due to the wire resonance.

The first and second peak regions of the panel response are plotted in much larger scales in Figs. 23 and 24, respectively.

Since drag reduction is expected to depend primarily on the second peak region response, our attention will be focused henceforth on this region and any reference to the response will have the restricted meaning of the second peak region.

(2) The panel thickness has a great effect on both the amplitude and the location of the peak region. An increase in the thickness h shifts the peak region to a higher frequency range and generally reduces the amplitude.

(3) The effect of the bending rigidity of the wire on the panel response represented by the term $E_w I_w \frac{\partial^4 w}{\partial y^4}$ in Eq. (4.36) is negligible.

(4) Neglecting the contribution of the torsional moments acting on the wire, represented by the term $\Gamma(m', n, n')$ in Eq. (4.40), to the virtual work slightly reduces the computed response amplitude.

(5) The change in the tension T has very little effect on the structural response of this region (2nd peak), as long as the tensile stress in the wire remains unchanged (Thus, the cross-sectional area of the wire must be changed correspondingly).

(6) The change in the panel width $(1.778 \sim 3.048) \times 10^{-1}$m significantly alters the locations and the amplitudes of the individual peaks of this peak region (see Figs. 24 and 25).

(7) No significant change in the structural response was noticed when the cavity depth was changed $(2.54 \sim 1.27) \times 10^{-3}$m (see Figs. 24 and 26).

Again, it is to be noted that the following values have been used in computing the response shown in Figs. 22-26:

$$\ell = 2{,}54 \times 10^{-3}\ \text{m}$$

$$h = 8.98 \times 10^{-6}\ \text{m}$$

$$T = 4.448 \times 10^{-2}\ \text{N}$$

$$D = 2.54 \times 10^{-5}\ \text{m}$$

The root mean square value of the displacement, $W_{r.m.s.}$, is computed from Eq. (5.6). A typical $W_{r.m.s.}$ of 1.74×10^{-4} m has been obtained when using the above data and choosing a cavity depth $d = 2.54 \times 10^{-2}$ m and a panel width $b = 1.778 \times 10^{1}$ m. This value of $W_{r.m.s.}$ is based on the second peak frequency range 970-1045 Hz, and it can be reduced by including structural damping in the computations. Therefore, damping materials or devices can perhaps be used to adjust the response level to within the desired range.

Finally, the spectral density $\Phi_{p_1 p_1}$ of the induced pressure P_1 is plotted in Fig. 27 over a frequency range of 5-2000 Hz, and again in Fig. 28 in a larger scale within the second peak region.

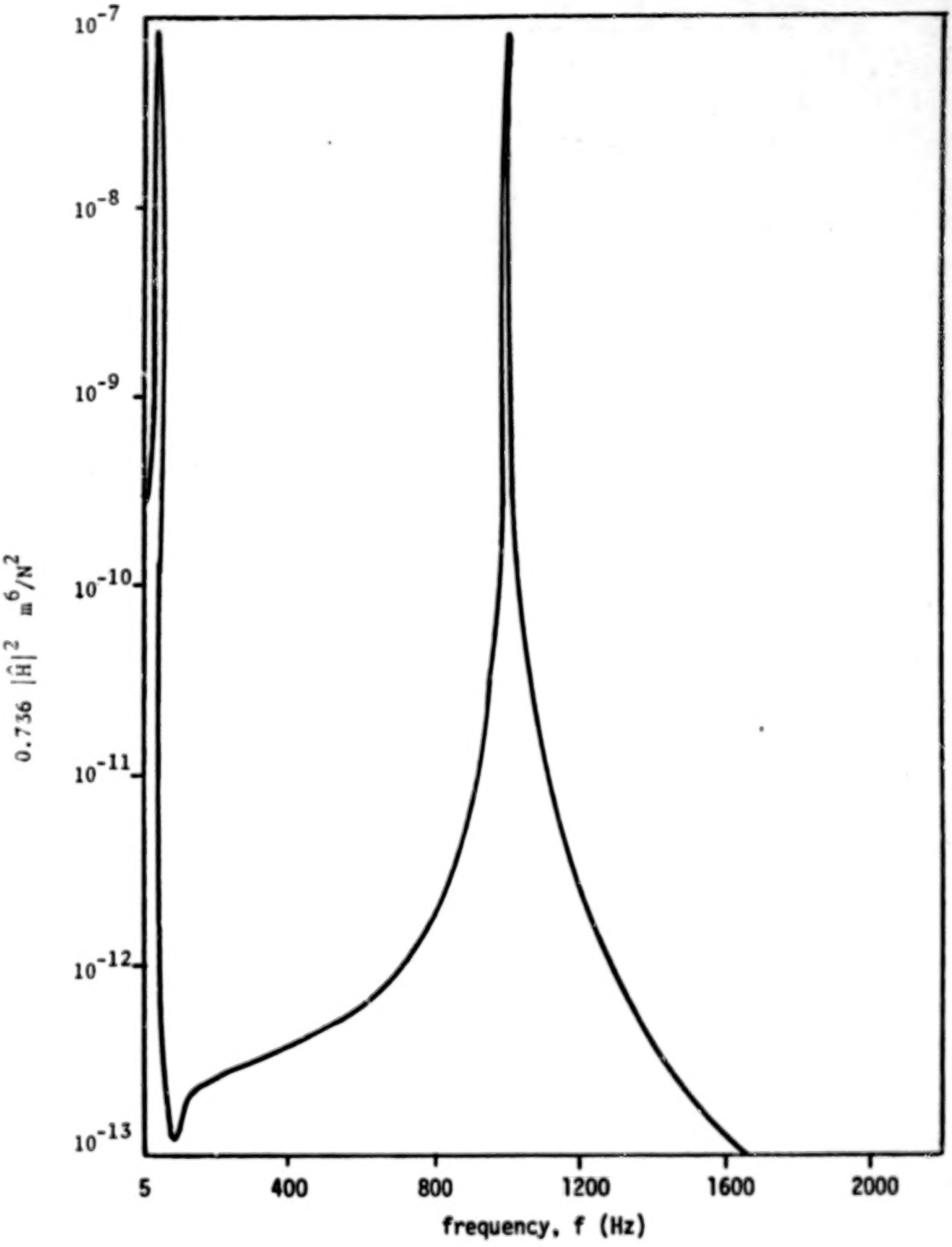

Fig. 22 Panel Response

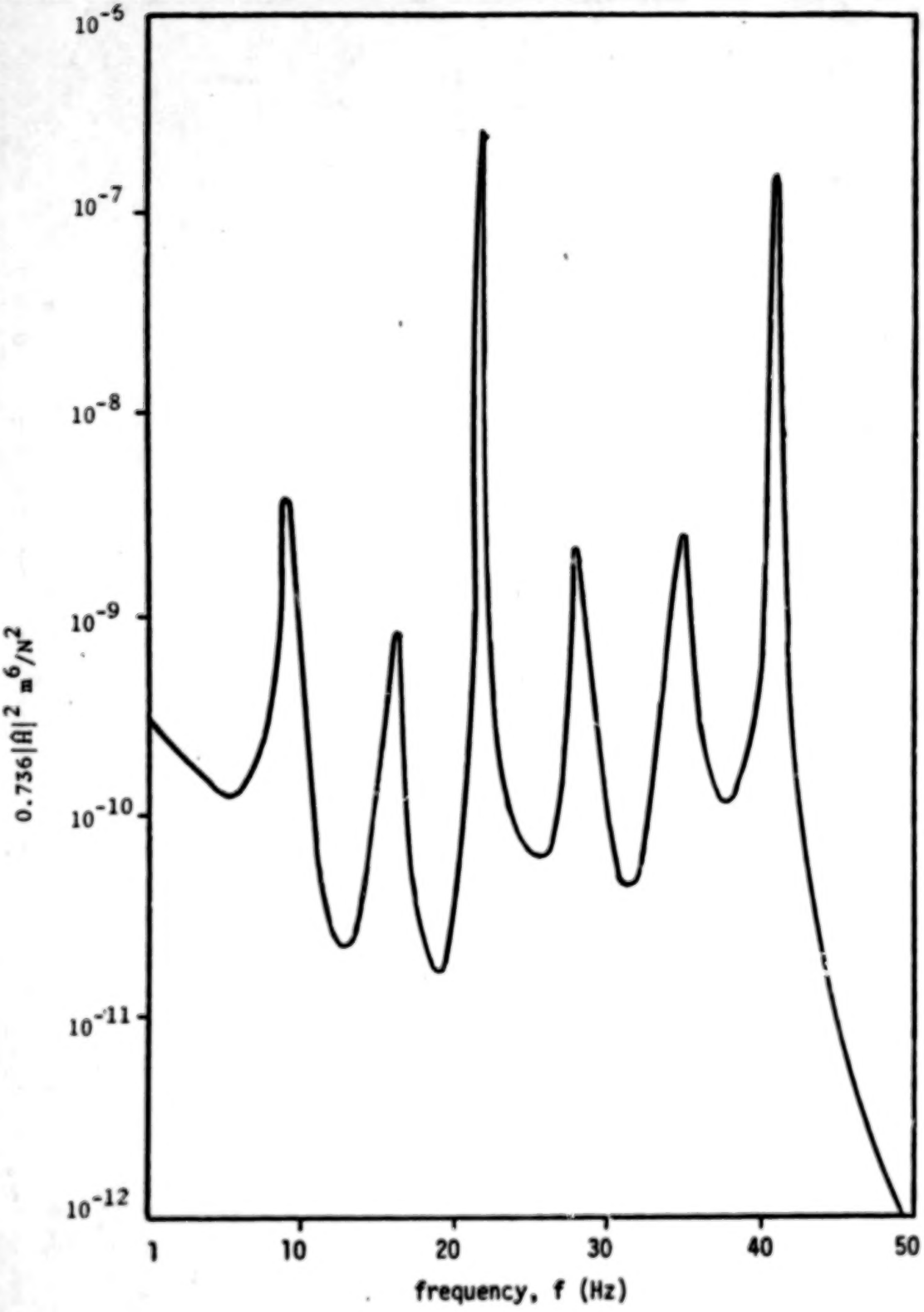

Fig. 23 Panel Response (1st Peak Region)

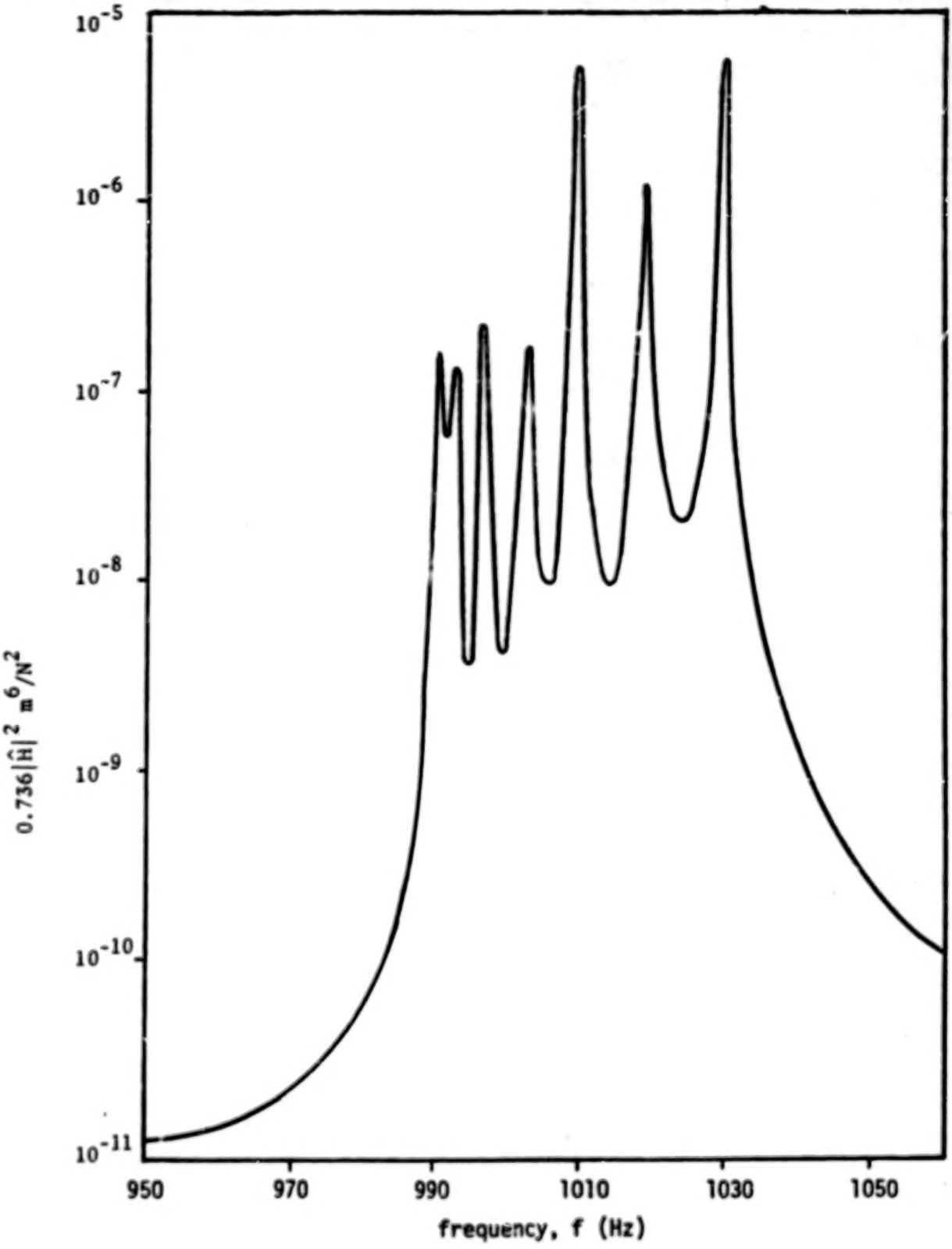

Fig. 24 Panel Response (2nd Peak Region, b = 0.1778 m, d = 0.0254 m)

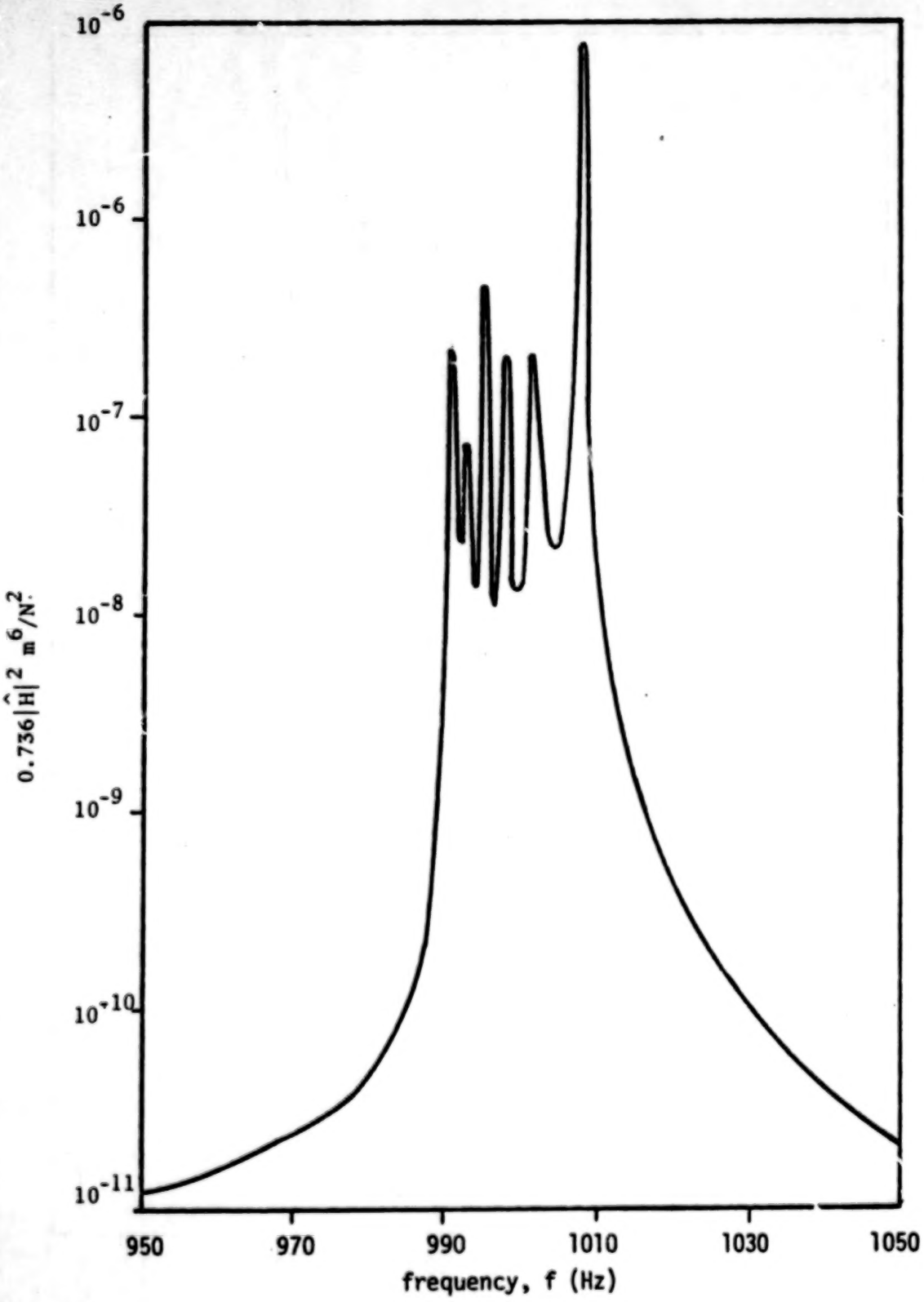

Fig. 25 Panel Response (b = 0.3048 m, d = 0.0254 m)

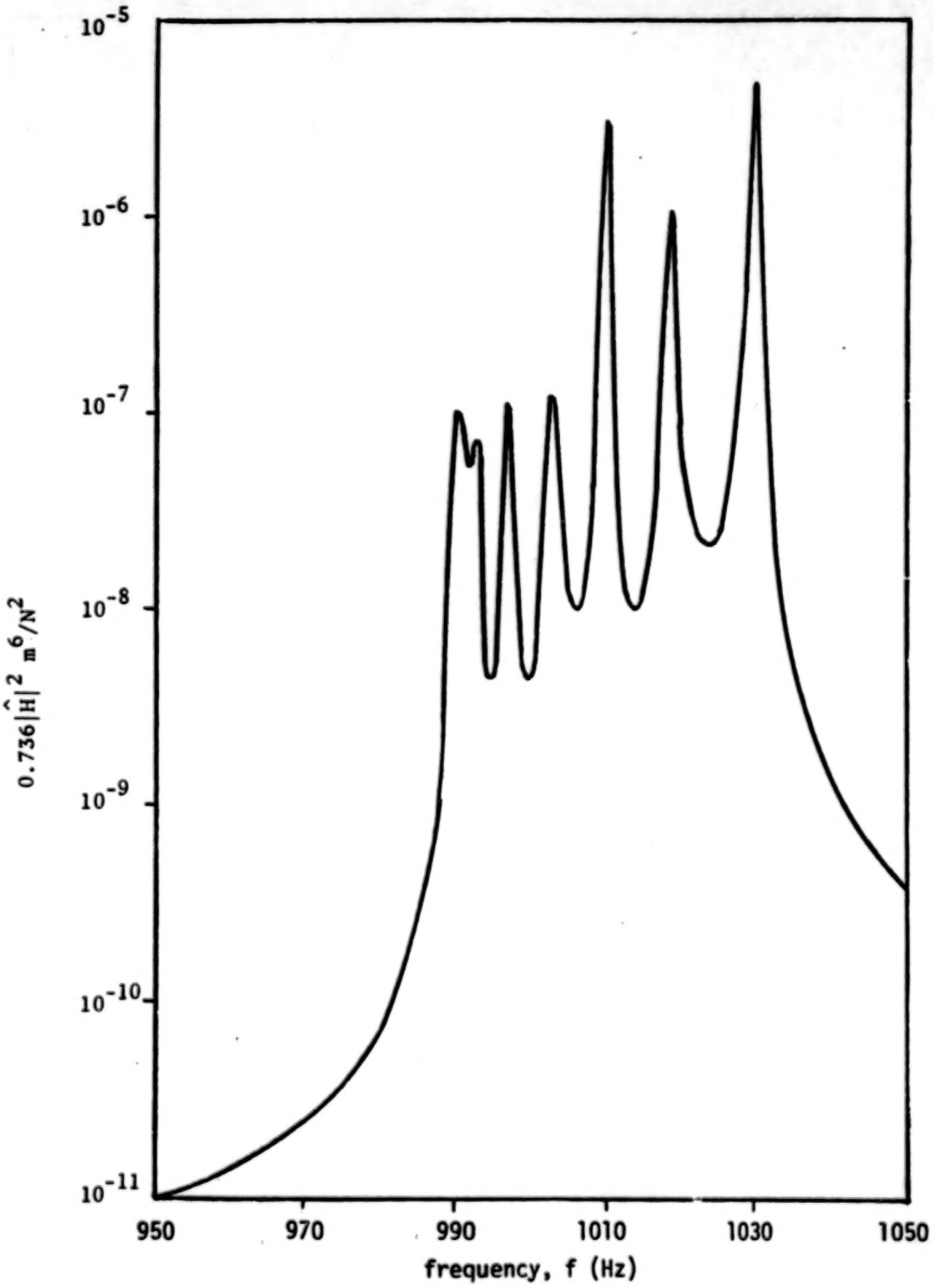

Fig. 26 Panel Response (2nd Peak Region, b = 0.1778 m, d = 0.0127 m)

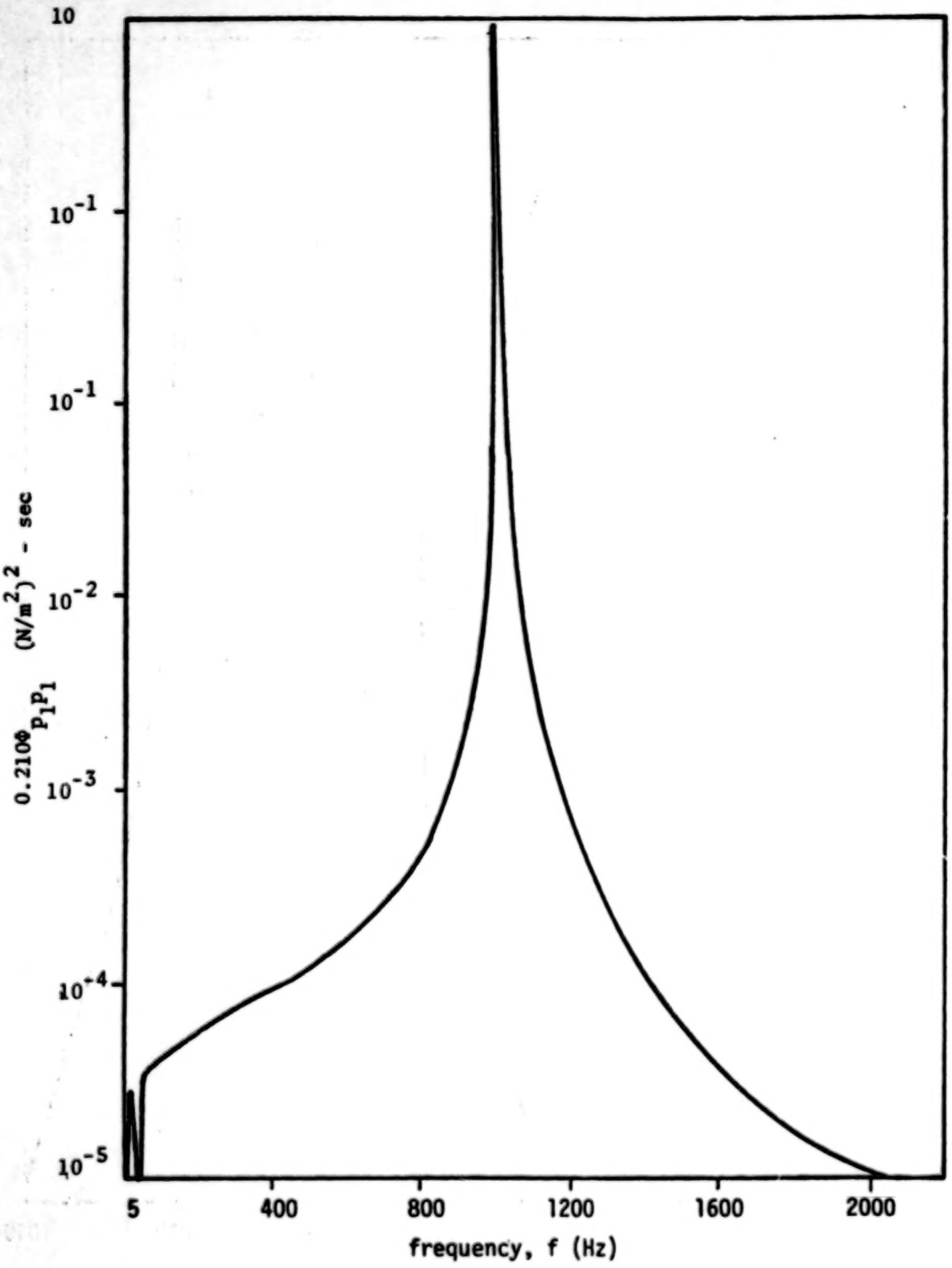

Fig. 27 Spectral Density of P_1

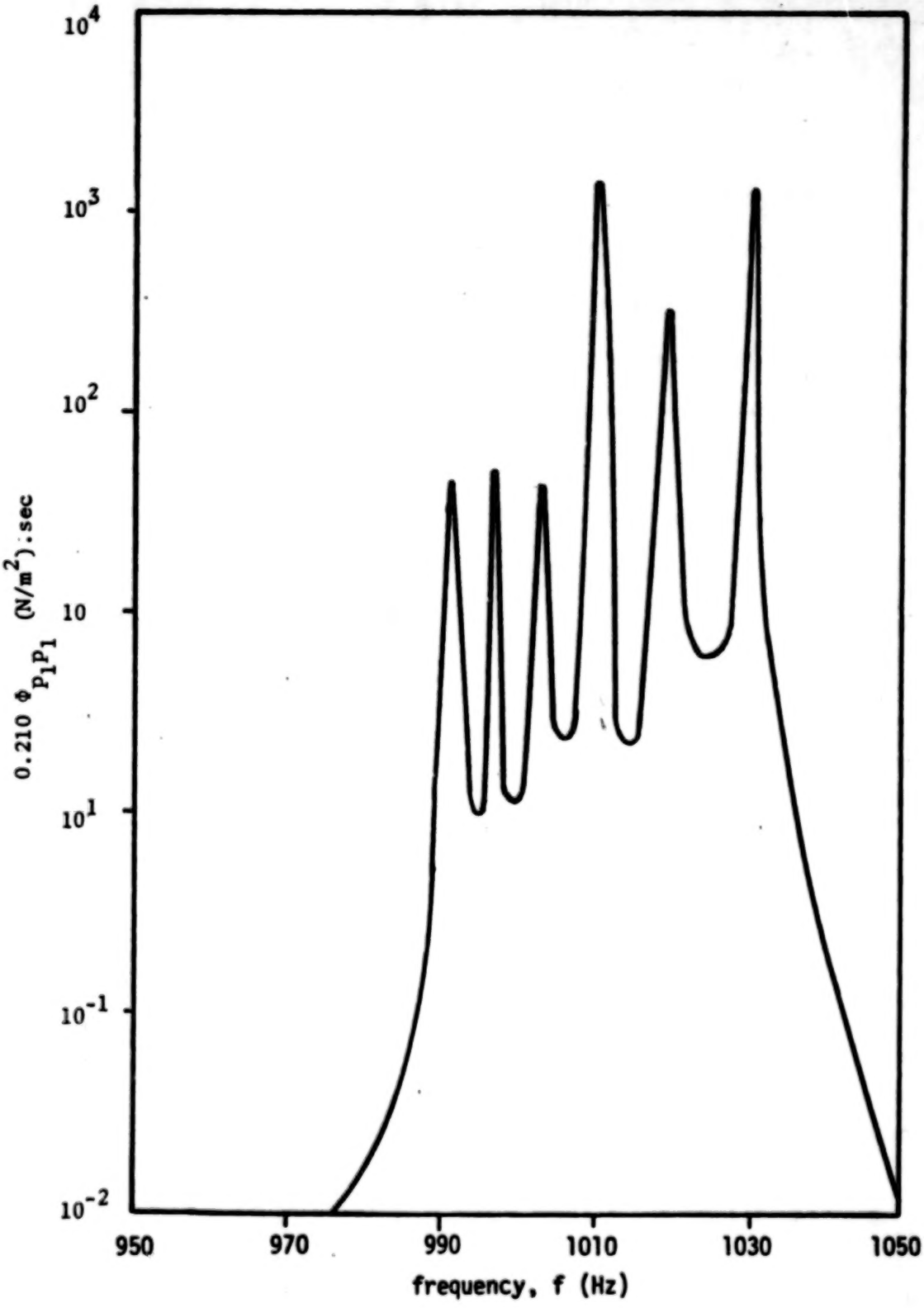

Fig. 28 Spectral Density of P_1 (2nd Peak Region)

VIII. CONCLUSIONS

Based on this investigation, we can conclude that:

(1) It is possible to design a periodic structure which, when excited by turbulent boundary layer pressure fluctuations, would have a narrow-band response. Within this narrow-band region (peak region), the response can be adjusted to satisfy predetermined requirements by changing some structural or flow parameters. Such requirements can be the amplitude, propagation speed, and wave length of the dominant component of a packet of waves constituting the narrow-band response.

(2) It has been found from the parametric study that the membrane thickness and the periodic length of the structural construction significantly affect the location of the peak region, the amplitude, and the wave length of the dominant response. Accordingly, by suitable choice of these two parameters, the periodic structure would have a resonant mode vibrating at a frequency that falls within the energy-containing spectral range of the exciting turbulence pressure field, leading to a favorable interaction.

(3) Structural damping of the membrane or other damping devices such as viscoelastic foundations can be used to adjust the amplitude of the vibration to within a desired range.

(4) As far as the structural response is concerned, the effect of the additional pressure induced by the structural motion above the structure is relatively small. However, this conclusion is based on an analysis where viscosity in the fluid has been neglected. A more accurate representation of the induced pressure can be obtained if the viscous

effects can be included in the governing wave equation. At present, there are no analytical solutions which take viscous effects into account.

(5) The wave propagation approach is most simple and convenient in the analysis of infinitely long periodic structures. However, this advantage diminishes greatly for finite periodic structures and the analysis is very much similar to that of the transfer matrix method.

APPENDIX I

SOME BRIEF COMMENTS ON THE COMPUTER PROGRAMS USED

In this Appendix, no attempt will be made to reproduce the complete computer programs used or to discuss them in detail. However, it is felt useful to comment very briefly on some of the procedures and subroutines which have been helpful in obtaining the numerical results.

(1) In solving the system of simultaneous equations, Eq. (2.33), Eq. (4.45) or (4.58), we have used the I.M.S.L. subroutine LEQT1C.

(2) The eigensystem subroutine package EISPAC was used to obtain the eigenvalues of the matrix $\overline{C}$ in Eq. (3.54).*

(3) The solution of the ill-conditioned system of simultaneous equations, Eq. (3.66), was made possible by use of the U.O.I. library subroutine GAUSZ. This subroutine employes Gauss elimination technique (with complete pivoting).

(4) The inverse of the Vandermonde matrix $\overline{Q}$ in Eq. (3.53) was obtained using the eigensystem subroutine package MINFIT. This subroutine uses a singular value decomposition method to solve a system of equations AX = B. The inverse of matrix A is obtained as a special case in which B is replaced by the identity matrix.

(5) Integration of Eq. (5.6) was carried out using Bode's 5-point integration method [26], namely

$$\int_{x_0}^{x_4} f(x)\,dx = \frac{2h}{45}\,(7f_0 + 32f_1 + 12f_2 + 32f_3 + 7f_4)$$

---

* It is possible to solve the generalized eigenvalue problem of Eq. (3.50) directly by the use of the LZ-algorithm [31] (i.e., without inverting the matrix $\overline{Q}$).

where

$$h = \frac{x_4 - x_0}{4}$$

$$f_j = f(x_0 + jh) \quad ; \quad j = 0,1,2, \ldots, 5 .$$

REFERENCES

1. Kramer, M.O., "The Dolphins' Secret", J. Am. Cos. Naval Engr., 73, 103, 1961.

2. Ash, R.L., "On the Theory of Compliant Wall Drag Reduction in Turbulent Boundary Layers", CR-2387, NASA, April 1974.

3. Fischer, M.C., Weinstein, L.M., Ash, R.L., and Bushnell, D.M., "Compliant Wall-Turbulent Skin-Friction Reduction Research", AIAA 8th Fluid and Plasma Dynamics Conference, Hartford, Connecticut, June 16-18, 1975.

4. Ash, R.L., Bushnell, D.M., Weinstein, L.M., and Balsubramanian, R., "Compliant Wall Surface Motion and Its Effect on the Structure of a Turbulent Boundary Layer". Presented at the Fourth Biennial Symposium on Turbulence in Liquids, University of Missouri-Rolla, September 22-24, 1975.

5. Niles, J. W., "Vibrations of Beams on Many Supports", Proceedings, ASCE, Vol. 82, No. EM 1, 1956, pp. 1-2

6. Lin, Y.K., "Stresses in Continuous Skin Stiffener Panels under Random Loading", Journal of Aerospace Science, Vol. 29, Part 1, 1962, pp. 67.

7. Mercer, C.A., "Response of a Multi-Supported Beam to Random Pressure Field", J. Sound and Vib., Vol. 2, Part 3, 1965, pp. 293.

8. Lin, Y.K., "Free Vibrations of a Continuous Beam on Elastic Supports", Int. J. Mech. Sci., Pergamon Press Ltd., 1962, pp. 409-423.

9. Lin, Y.K., and Donaldson, B.K., "A Brief Survey of Transfer Matrix Techniques with Special Reference to the Analysis of Aircraft Panels", J. Sound and Vib., Vol. 10, Part 1, 1969, pp. 103-143.

10. Vaicaitis, R., Doi, K., and Lin, Y.K., "Spatial Decay in the Response of Damped Periodic Beam", J. of Aircraft, Vol. 9, No. 1, 1972, pp. 91-93.

11. Vaicaitis, R., and Lin, Y.K., "Response of Finite Periodic Beam to Turbulent Boundary-Layer Pressure Excitation", AIAA Journal, Vol. 10, No. 8, 1972, pp. 1020-1024.

12. Lin, Y.K., and McDaniel, T.J., "Dynamics of Beam-Type Periodic Structures", Transactions of the ASME Journal of Engineering for Industry, Paper No. 69-Vibr-17, 1969.

13. Mead, D.J., "Free Wave Propagation in Periodically Supported, Infinite Beams", J. of Sound and Vib., Vol. 11, Part 2, 1970, pp. 131-197.

14. Mead, D.J., and Pujura, K.K., "Space-Harmonic Analysis of Periodically Supported Beams: Response to Convected Random Loading", J. Sound and Vib., Vol. 14, Part 4, 1971, pp. 525-541.

15. Mead, D.J., "Vibration Response and Wave Propagation in Periodic Structures", J. Eng. for Industry, Trans. ASME 93(B), 1971, p. 783.

16. Sen Gupta, G., "On the Relation between the Propagation Constant and the Transfer Matrix Used in the Analysis of Periodically Stiffened Structures", J. Sound and Vib., Vol. 11, Part 4, 1970, pp. 483-484.

17. Sen Gupta, G., "Dynamics of Periodically Stiffened Structures Using a Wave Approach", AFML-TR-71-99, 1971.

18. Brillouin, L., *Wave Propagation in Periodic Structures*, Dover Publications, New York, 1953.

19. Lin, Y.K., Maekawa, S., "Decomposition of Turbulence Forcing Field and Structural Response", AIAA J., vol. 15, no. 5, May 1977, pp. 609-610.

20. Lin, Y.K., *Probabilistic Theory of Structural Dynamics*, McGraw-Hill, New York, 1967.

21. Maestrello, L., Monteith, J.H., Manning, J.C., and Smith, D.L., "Measured Response of a Complex Structure to Supersonic Turbulent Boundary Layers", AIAA 14th Aerospace Science Meeting, Washington, D.C., 1976.

22. Morse, M.P., and Ingard, K.U., *Theoretical Acoustics*, 707 McGraw-Hill Book Company, New York, 1968.

23. Bellman, R., *Introduction to Matrix Analysis*, McGraw-Hill, New York, 1960.

24. Bull, M.K., "Wall Pressure Fluctuations Associated with Subsonic Turbulent Boundary Layer Flow", J. Fluid Mechanics, Vol. 28, Part 4, 1967, pp. 719-754.

25. Schlichting, H., *Boundary Layer Theory*, 6th Edition, McGraw-Hill Book Company, New York, 1966.

26. *Handbook of Mathematical Functions with Formulas, Graphs and Mathematical Tables*, edited by Milton Abramowitz and Irene A. Stegun, Dover Publications, Inc., New York, 1965.

27. Hilton, H. H., "Viscoelastic Analysis", *Engineering Design for Plastics*, Reinhold Publication Company, N.Y., 1964, pp. 199-275.

28. Pister, K.S., and Williams, M.L., "Bending of Plates on a Viscoelastic Foundation", Proc. ASCE, Vol. 86, 1960, pp. 31-44.

29. Ungar, E.E., and Kerwin, E.M., Jr., "Plate Damping Due to Thickness Deformation in Attached Viscoelastic Layers", J. Acoustical Soc. of America, Vol. 36, 1964, pp. 386-392.

30. Bland, D.r., *The Theory of Linear Viscoelasticity*, Pergamon Press, 1960.

31. Kaufman, L., "The LZ-Algorithm to Solve the Generalized Eigenvalue Problem", SIAM Journal on Numerical Analysis, Vol. 11, No. 5, Oct. 1974, pp. 997-1024.

*U.S. GOVERNMENT PRINTING OFFICE: 1977 - 735-078/44

1. Report No.	2. Government Accession No.	3. Recipient's Catalog No.
NASA CR-2909		

4. Title and Subtitle	5. Report Date
Dynamic Response of Some Tentative Compliant Wall Structures to Convected Turbulence Fields	November 1977
	6. Performing Organization Code

7. Author(s)	8. Performing Organization Report No.
H. H. Nijim and Y. K. Lin	
	10. Work Unit No.

9. Performing Organization Name and Address	11. Contract or Grant No.
University of Illinois at Urbana-Champaign Urbana, IL	NSG-1233
	13. Type of Report and Period Covered
12. Sponsoring Agency Name and Address	Contractor Report
National Aeronautics and Space Administration Washington, DC 20546	14. Sponsoring Agency Code

15. Supplementary Notes

Langley Technical Monitor: Jerry N. Hefner
Final Report

16. Abstract

Some tentative compliant wall structures designed for possible skin friction drag reduction are investigated. Among the structural models considered is a ribbed membrane backed by polyurethane or PVS plastisol. This model is simplified as a beam placed on a viscoelastic foundation as well as on a set of evenly spaced supports. The total length of the beam may be either finite or infinite, and the supports may be either rigid or elastic. Another structural model considered is a membrane mounted over a series of pre-tensioned wires, also evenly spaced, and the entire membrane is backed by an air cavity. All these structural models belong to the general class of periodic structures for which a simple mathematical analysis is possible. The forcing pressure field is idealized as a frozen random pattern convected downstream at a characteristic velocity. The results are given in terms of the frequency response functions of the system, the spectral density of the structural motion, and the spectral density of the boundary-layer pressure including the effect of structural motion. These results are used in a parametric study of structural configurations capable of generating favorable wave lengths, wave amplitudes and wave speeds in the structural motion for potential drag reduction.

17. Key Words (Suggested by Author(s))	18. Distribution Statement
Compliant wall structures Viscous drag reduction	Unclassified - Unlimited Subject Category 34

19. Security Classif. (of this report)	20. Security Classif. (of this page)	21. No. of Pages	22. Price*
Unclassified	Unclassified	120	$5.50

*For sale by the National Technical Information Service, Springfield, Virginia 22161

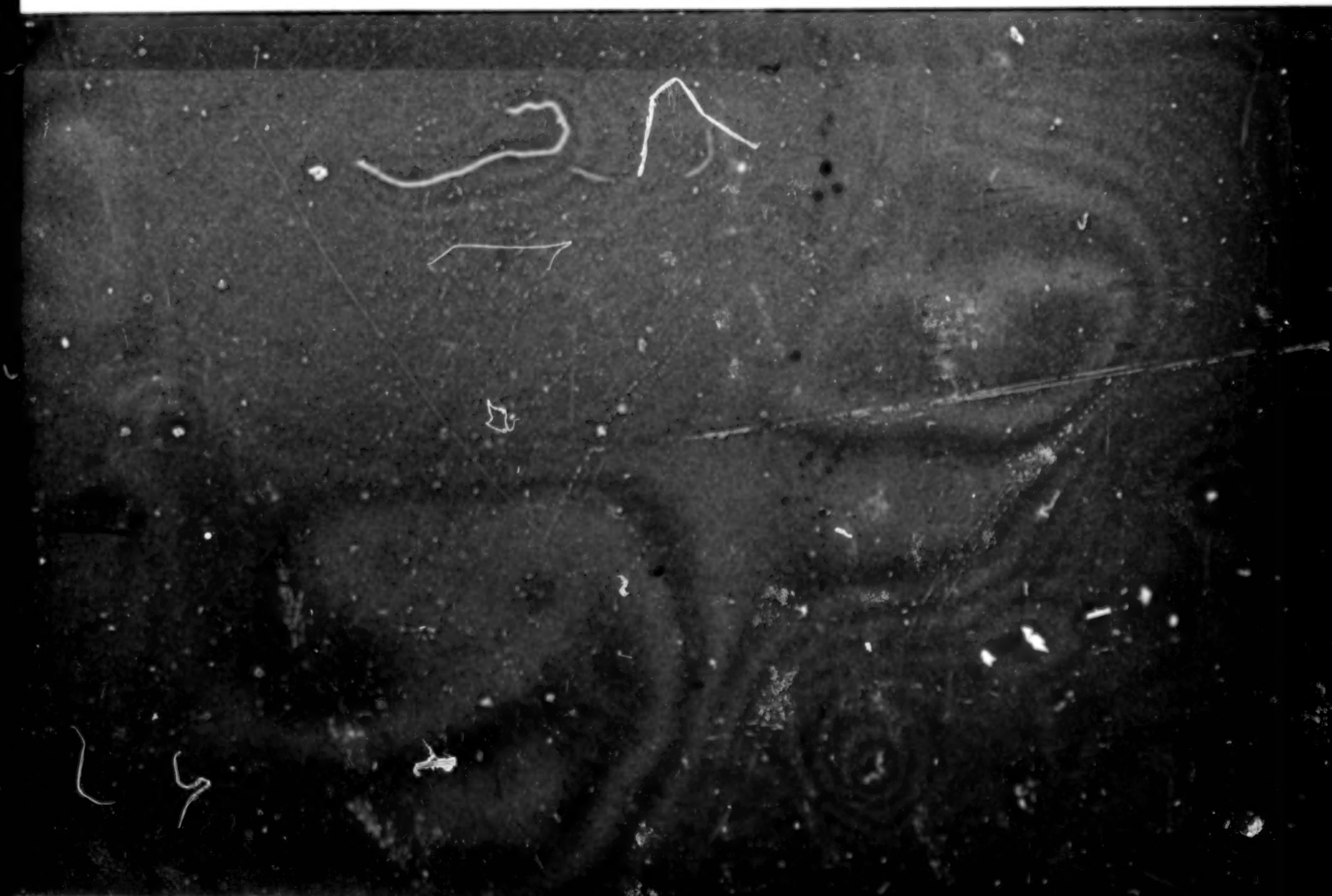

END

4.27.78